AN E.S.R. SPECTROMETER FOR THE STUDY OF TRANSIENT PARAMAGNETIC SPECIES

by

E.W. Firth, B.Sc.

Being a thesis

presented to the University of Keele

for the Degree of Doctor of Philosophy

Department of Physics,
University of Keele,
Keele,
Staffordshire.

November, 1967.

CONTENTS

CHAPTER IV (continued)

CHAPTER V (continued)

Some of the techniques and results described in this thesis were published in J. Sci. Inst. 44, 821 (1967) as a joint paper with D.J.E. Ingram.

ACKNOWLEDGEMENTS

The author would like to express sincere thanks to the following:

Professor D.J.E. Ingram for providing facilities for research in his department and supervising the work; also for many helpful discussions.

Members of the technical staff for much helpful advice and assistance.

Dr. D.C. Lainé and members (past and present) of the E.S.R. research group, Physics Department and the Communication Department.

Miss L.S. Ward for reading and commenting on the proofs of the thesis.

Mr. A.G. Smallman for building the 1Kc/s modulation proton resonance unit.

Mr. M. Pointon and Mr. J.D. Sunderland for assisting with the diagrams.

Mr. M. Cheney for carrying out the photographic work.

Miss K.B. Davies for typing and duplicating the thesis.

The Science Research Council for providing apparatus and maintenance grant.

SYNOPSIS

This thesis is concerned with a description of work carried out in the design, development and use of suitable equipment to be utilised with an Electron Spin Resonance Spectrometer and a Computer of Average Transients in order to record E.S.R. spectra of transient paramagnetic species.

The first part of the thesis contains a basic outline of the theory of E.S.R. and a description and discussion of E.S.R. spectrometers.

There follows a discussion on signal to noise considerations with particular emphasis on the device known as the phase sensitive detector (P.S.D.) with a natural transition to averaging systems which play an important part in a rapid recording spectrometer.

An explanatory review of various methods of recording data on transient paramagnetic species is included, along with the reasons for the development of the particular system utilised by the author.

A description of the apparatus used is included with a detailed description of the design, development and testing of the information processing equipment.

A brief analysis of the E.S.R. spectra of atomic oxygen is given, followed by a description and discussion of the results obtained on the kinetics of their formation and decay processes, in an r.f. discharge, observed as a test sample for an assessment of the equipment.

The concluding chapter discusses the relative merits of the author's system in particular and the advantages and disadvantages of rapid recording systems in general. A final discussion of the possible improvements and alternative versions of the present system is included, along with a technique using an on line computer in conjunction with a fast record slow playback (F.R.S.P.) device to record and present all the relevant data as a "3 dimensional" display.

CHAPTER I

INTRODUCTION

The research project described in this thesis is concerned with the use of a Computer of Average Transients (CAT) in the development of an Electron Spin Resonance (E.S.R.) Spectrometer capable of reproducing the spectra of transient paramagnetic species in the solid, liquid or gaseous phase at any time from a few milliseconds after the commencement of their formation or decay.

The method used is a dynamic system; it does not rely, for example, on "freezing" the decay of the paramagnetic species in a rigid host matrix.

Early dynamic systems relied on following the decay of paramagnetic species by setting the spectrometer on a resonance peak and noting the peak amplitude as a function of time. This method has serious limitations:-

(i) All information on the line shape is lost, unless the experiment is repeated at different field positions.

(ii) The spectrometer must have a rapid response time and thus it is not possible to use a narrow band filter to reduce noise.

Two methods may be used to surmount these difficulties: an adjustable flow system or sampling techniques.

The method of using a flow system is only suitable for samples in the gaseous or liquid phase and is very complex if results are to be obtained over a wide time scale.

The only limitation on the sampling technique is that the paramagnetic species must be repeatedly produced, in transient form, by the periodic application of a suitable stimulus.

The method relies on repetitively generating the paramagnetic species and sampling the output of the E.S.R. spectrometer at a fixed interval, T_D, after the commencement or cessation of the generating stimulus. If the spectrometer is swept through the resonance region slowly compared with the repetition rate, an E.S.R. spectrum of the species as it appears at time T_D will be obtained.

The main disadvantage of this method, as it stands, is that the spectrometer must still possess a short response time and, therefore, the signal-to-noise ratio is poor. This disadvantage may be minimised by the use of averaging techniques.

A digital device known as a Computer of Average Transients forms a very convenient and efficient averaging and display device. The work described in this thesis has been concerned with designing and testing a suitable sampling interface between the E.S.R. spectrometer and an NS513 CAT. Emphasis was placed upon producing equipment which could be easily connected to a standard E.S.R. spectrometer with little modification of the spectrometer itself.

CHAPTER II

ELECTRON SPIN RESONANCE

2.1 Theory of Paramagnetic Resonance

2.1.1 The resonance condition

E.S.R. is concerned with a system in which the energy level configuration is altered by the application of a magnetic field. Resonant absorption is then obtained by exciting transitions, with an external high frequency magnetic field, between the newly formed levels.

In a free radical, in which the free electrons are not coupled to any surrounding nuclei or electrons, the energies of the electrons will be equal. Under zero field conditions the spin vectors, and thus their magnetic moments, will be randomly orientated.

Application of a magnetic field will result in a Zeeman splitting. Electrons will either align with the resolved components of their magnetic moments parallel or antiparallel to the field.

The orientational energy, E, of a magnetic dipole moment $\underline{\mu}$ in a field $\underline{H}$ is given by:-

$$E = -\underline{\mu}.\underline{H} \qquad 2.1$$

The number of possible orientations is limited by quantum considerations.

In the general case of an atom with total angular moment J the quantum number defining the component of J fixed in space can take values $\pm J$, $\pm(J-1)$, $\pm(J-2)$ .....; i.e. there are 2J+1 possible orientations of the total angular momentum. This corresponds, in the simplest case, to 2J+1 equidistant energy levels.

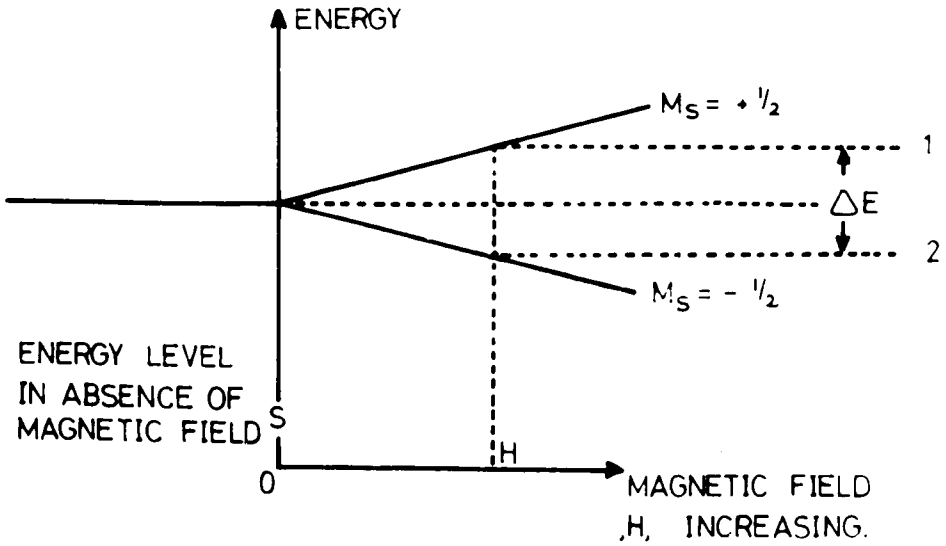

FIG. 2.1. SPLITTING OF ENERGY LEVEL $S=1/2$ UNDER THE INFLUENCE A OF MAGNETIC FIELD.

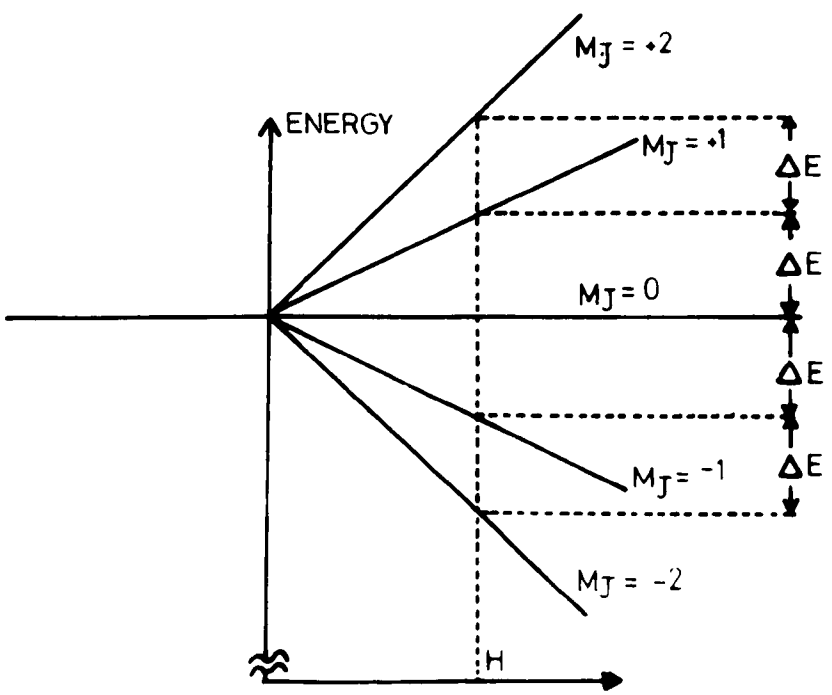

FIG. 2.2. SPLITTING OF J=2 LEVEL UNDER THE INFLUENCE OF A MAGNETIC FIELD.

For a free electron (with $S = \frac{1}{2}$; $l = 0$ $\therefore J = \frac{1}{2}$) there are $2J+1 = 2$ possible orientations under the conditions of L.S coupling that usually apply, i.e. in the case of a free electron the spins line up parallel or antiparallel to the applied magnetic field. Figs. 2.1 and 2.2 show the energy levels of an $S = \frac{1}{2}$ and $J = 2$ state respectively under the influence of a magnetic field.

The Zeeman splitting, ΔE, is given by:-

$$\Delta E = g_J \beta H \qquad 2.2$$

where g_J is the Lande g factor. This is a dimensionless number whose value depends on the mode in which L and S combine to form the total angular momentum J.

If J is mainly due to the orbital angular momentum, L, then $g_J = g_L \simeq 1$, whereas for the case of S being the main contributor to J, $g_J = g_S \simeq 2$. Actually, for a free electron, $g_J = g_S = 2.0023$, the excess 0.0023 being due to the interaction of the electron with its own radiation field.

The factor β, in Equation 2.2, is the Bohr magneton and represents the relationship between units of angular momentum and magnetic moments. $\beta = \frac{eh}{4\pi mc}$ when used with E.M.c.g.s. units. For a population in the upper and lower energy levels of N_1 and N_2 respectively, then N_1/N_2 is given by a Maxwell-Boltzman distribution under thermal equilibrium conditions.

$$\frac{N_1}{N_2} = e^{-\frac{\Delta E}{kT}} \qquad 2.3$$

where k is the Boltzman constant, and T is the absolute temperature.

Transitions between the levels will result if radiation of frequency ν is fed into the system such that:-

$$h\nu = \Delta E \qquad 2.4$$

The probabilities for transitions in the form of stimulated emission (level (1) → (2)) and absorption ((2) → (1)) are equal. The effect will be a net absorption of energy due to the population difference between the two levels.

Thus, from Equations 2.2 and 2.4, we have:-

$$h\nu = g\beta H \qquad 2.5$$

Equation 2.5 is referred to as the resonance condition.

The net absorption would continue until $N_1 = N_2$ when, with no population difference, there would be an equal amount of absorption and stimulated emission resulting in no detectable effect. For an equilibrium to be set up in which there is a steady net absorption there must be some means, other than stimulated emission, by which electrons in level (1) can make the transition to the lower level.

2.1.2 Relaxation processes

The phenomena, other than stimulated emission, by which electrons make the transition from the higher to lower energy level are known as relaxation processes. The rate at which electrons lose energy is described by a relaxation time T which is the time required for the excess energy, over and above thermal equilibrium, to fall to $^1/e$ th of its initial value.

There are two main processes besides spontaneous emission by which relaxation proceeds:-

(i) Generalised spin-lattice relaxation

(ii) Spin-spin interaction.

Any relaxation mechanism whereby spins exchange energy with a surrounding energy reservoir can be included in the generalised definition of the spin lattice relaxation process.

Similarly any process whereby spins exchange energy among themselves will be referred to as spin-spin interaction. Before considering relaxation processes in more detail it is necessary to discuss the behaviour of an individual magnetic dipole.

2.1.3 Behaviour of an individual paramagnet

The classical equation for the torque, $\underline{T}$, on a top with angular momentum $J\hbar$ is:-

$$\underline{T} = \frac{d(\underline{J}\hbar)}{dt} \qquad 2.6$$

The magnetic moment, μ, of an electron is given by Equation 2.7 where γ is the gyromagnetic ratio:-

$$\underline{\mu} = -\gamma \underline{J}\hbar \qquad 2.7$$

The torque on a magnetic moment, μ, placed in a magnetic field, $\underline{H}$, is:-

$$\underline{T} = \underline{\mu} \wedge \underline{H} \qquad 2.8$$

Thus the equation of motion of the magnetic moment vector of an electron in a magnetic field is given by:-

$$\frac{d(\underline{\mu})}{dt} = \gamma \, \underline{H} \wedge \underline{\mu} \qquad 2.9$$

Consider $\underline{H}$ to be of the form of a static magnetic field H_o in the Z direction of a set of laboratory coordinates. The solution of Equation 2.9 is then the precession of constant μ about H_o at a frequency ω_L such that:-

$$\omega_L = \gamma H_o \qquad 2.10$$

The motion of μ is referred to as Larmor precession and ω_L is known as the Larmor frequency; γ, as previously mentioned, is the gyromagnetic ratio.

Consider the addition of a small field, H_1, precessing, perpendicularly to H_o, with an angular frequency ω. The total field $\underline{H}$ in the laboratory frame of reference is given by:

$$\underline{H} = \underbrace{(H_1 \cos \omega t)\underline{i} + (H_1 \sin \omega t)\underline{j}}_{\text{rotating or precessing field}} + \underbrace{H_o \underline{k}}_{\text{static field}} \qquad 2.11$$

Consider the transformation to a new frame of reference rotating about H_o with frequency ω. In this frame of reference

$$\underline{H} = H_1 \underline{i}' + H_o \underline{k}' \qquad 2.12$$

Where the primes indicate reference to the system of rotating coordinates. $\underline{H_1}$ rotates with the new coordinate system and remains constant in amplitude.

Now

$$\left(\frac{d\underline{\mu}}{dt}\right)' = \underline{\mu} \wedge \underline{\omega} + \frac{d\underline{\mu}}{dt} \qquad 2.13$$

Therefore, from Equation 2.9, an equation of motion of $\underline{\mu}$ in the rotating frame is:-

$$(\frac{d\underline{\mu}}{dt})' = (\gamma\underline{H} - \underline{\omega}) \wedge \underline{\mu} \qquad 2.14$$

In order to render Equation 2.14 comparable with Equation 2.9 an effective field $\underline{H}_{eff}$ is defined so that

$$(\frac{d\underline{\mu}}{dt})' = \gamma\underline{H}_{eff} \wedge \underline{\mu} \qquad 2.15$$

i.e. $$\underline{H}_{eff} = \underline{H} - \frac{\omega}{\mu} \qquad 2.16$$

Thus there is a steady effective field $\underline{H}_{eff}$ when the system is observed from the rotating frame.

The result is that $\underline{\mu}$ will precess about $\underline{H}_{eff}$ with a frequency $\underline{\omega}_{eff} = \gamma\underline{H}_{eff}$.

If H_o is varied a condition can be satisfied where $H_o = \frac{\omega}{\mu} = H_{o_{RES}}$ and thus $\underline{H}_{eff} = H_1$; i.e. the effective field is entirely comprised of the rotating field $\underline{H}_1$. This has two important effects:-

(i) The Larmor frequency, ω_L, is now equal to the angular frequency, ω, of the applied rotating field.

(ii) The magnetisation vector, $\underline{\mu}$, will now precess about an axis, perpendicular to the steady field H_o, which is stationary in the rotating frame of reference.

The condition mentioned above is known as resonance and could equally be brought about by maintaining H_o constant and varying ω. In all cases it will be assumed that H_o (or ω) is varied very slowly so that each point in the analysis can be regarded as a steady state response. The result is that the magnetisation vector will precess about H_1 with a frequency $\omega_R = \gamma H_1$. In all paramagnetic resonance experiments $H_o >> H_1$

and so $\omega_L >> \omega_R$, i.e. μ will appear to spiral slowly up and down the Z axis when viewed from the laboratory coordinates.

When μ is in a direction such that it possesses a component in the direction of H_o its energy will be lower than when it is opposed to H_o. The precession at ω_R can be regarded as alternately absorbing and emitting energy. This classical picture is only an approximation to the truth; quantum mechanical considerations show that, in a two level system, the energy taken by the magnetic dipole corresponds to only two discrete values (2J+1 discrete values for a level with total angular momentum J) - intermediate values being forbidden.

Generally for a level with total angular momentum J there are 2J+1 possible orientations each being labelled, from the highest to the lowest, with quantum number m_j where $m_j = +J, J-1, \ldots -J$. Transitions are normally only allowed in which $\Delta m_j = \pm 1$.

2.1.4 Behaviour of the macroscopic system - the Bloch Equations

The above factors can be summarised in a set of equations by describing the system in terms of its macroscopic magnetisation, $\underline{M} = \Sigma \underline{\mu}$. The equations are known as the Bloch Equations, being originally proposed by Bloch to describe the interaction of nuclear paramagnets. Their principles can be equally applied to the behaviour of electrons.

Following the usual procedure, we assume that the steady magnetic field, H_o, is applied along the Z axis of a laboratory frame of reference. Under thermal equilibrium the total magnetisation vector, $\underline{M}$, will lie along the Z axis with a magnitude M_o.

At resonance the total magnetisation, $\underline{M}$, being composed of the sum of individual magnetic moments, $\underline{\mu}$, would be expected to precess about H_1 with a resultant zero net absorption when averaged over several cycles of ω_R. This is equivalent to the case of saturation where the population difference between the two levels has been reduced to zero. In practice it is observed that an absorption does occur; the reason being that the relaxation mechanisms, mentioned previously, provide a means of maintaining the Z component of the net magnetisation, M, close to its thermal equilibrium value, i.e. the population difference is maintained at its thermal equilibrium value as given by the Maxwell-Boltzman distribution (Equation 2.3).

The net magnetisation can remain at its approximately equilibrium value because the relaxation mechanisms are sufficiently strong so that only relatively few individual magnetic moments, μ, complete the slow precession at frequency ω_R about H_1, the majority relaxing back to their thermal equilibrium value.

Bloch proposed that the relaxation was of exponential form and assigned relaxation times, analogous to time constants, of T_1 and T_2 for spin-lattice and spin-spin relaxation respectively.

M_z tends towards its thermal equilibrium value in the absence of an external r.f. field by loss of energy to some reservoir external to the spin system and this is referred to as spin-lattice relaxation. In the presence of a perpendicular r.f. field, H_1, the process is one of competition between H_1 and the spin lattice relaxation; but, in order to

avoid any saturation effects, the spin-lattice relaxation must have almost complete dominance.

The rate of decay of M_1 in a direction perpendicular to H_o is described by the relaxation time T_2 and does not involve a transfer of energy to a reservoir. A possible mechanism for T_2 could arise from the dephasing effect that a nearby spin has on another due to slightly different precession frequencies, ω_L, produced by the different magnetic fields produced by one spin at the site of another. This is referred to as spin-spin relaxation and does not involve the decay of the individual μ_x and μ_y components (T_1 is responsible for this) but only their dephasing so that the resultant M_x and M_y are reduced as the dephasing increases in severity.

The relaxation of M_z can thus be described by:-

$$\frac{dM_z}{dt} = \frac{M_o - M_z}{T_1} \qquad 2.17$$

and with a perpendicular field H_1:-

$$\frac{dM_z}{dt} = \gamma(H \wedge M)_z + \frac{M_o - M_z}{T_1} \qquad 2.18$$

For relaxation in the transverse direction:-

$$\frac{dM_x}{dt} = \gamma(H \wedge M)_x - \frac{M_x}{T_2} \qquad 2.19$$

$$\frac{dM_y}{dt} = \gamma(H \wedge M)_y - \frac{M_y}{T_2} \qquad 2.20$$

Equations 2.18, 2.19 and 2.20 are the Bloch Equations.

2.1.5 Steady state solution of the Bloch Equations

In resonance experiments γH_1 ($= \omega_R$) is chosen $\ll \frac{1}{T_1}$ or $\frac{1}{T_2}$; $T_1 > T_2$ and so this condition can be replaced by $\gamma H_1 \ll \frac{1}{T_1}$. Under this condition relaxation processes cause M_z to relax back to M_o in a time much shorter than the period of a precession of M about H_1 and thus it may be assumed that M_z remains very close to its thermal equilibrium position. Implicit in the derivation of the steady state solution to Bloch's Equations is the assumption that the passage through resonance is much shorter than $\frac{1}{\gamma H_1}$.

The static susceptibility, χ_o, is defined by:-

$$M_o = \chi_o H_o \simeq M_z \qquad 2.21$$

The steady state solution to the Bloch equations is (3,4,5)

$$M_x = \frac{\chi_o \gamma H_{o_{RES}} \gamma (H_{o_{RES}} - H_o) T_2^2 H_1}{1 + \gamma^2 (H_o - H_{o_{RES}})^2 T_2^2} \qquad 2.22$$

$$M_y = \frac{\chi_o \gamma H_{o_{RES}} T_2 H_1}{1 + \gamma^2 (H_o - H_{o_{RES}})^2 T_2^2} \qquad 2.23$$

If M_x' is the perpendicular magnetisation in the rotating frame then:-

$$M_x' = M_x \cos \omega t + M_y \sin \omega t \qquad 2.24$$

where M_x and M_y are the transverse magnetisations in the laboratory coordinate system.

The high frequency field, H_1, generally encountered in magnetic resonance is linearly polarised:- $H_1 = H_x^L$.

H_x^L can be considered as being composed of two, counterotating circularly polarised, components.

$$\text{i.e.} \quad H_x^L = H_1^L \cos \omega t = H_1 \cos \omega t + jH_1 \sin \omega t + H_1 \cos(-\omega t) + jH_1 \sin(-\omega t) \qquad 2.25$$

$$\therefore \quad H_x^L = 2H_1 \cos \omega t$$

$$\therefore \quad H_1^L = 2H_1$$

Now both M_x and M_y are proportional to H_1 and therefore proportional to H_1^L.

Thus, M_x can be rewritten as:-

$$M_x = (\chi' \cos \omega t + \chi'' \sin \omega t)H_1^L \qquad 2.26$$

Substituting into equations 2.22 and 2.23 respectively:

$$\chi' = \frac{\chi_o}{2} \gamma H_{o_{RES}} \frac{\gamma(H_{o_{RES}} - H_o)T_2^2}{1 + (H_o - H_{o_{RES}})^2\gamma^2T_2^2} \qquad 2.27$$

$$\chi'' = \frac{\chi_o}{2} \gamma H_{o_{RES}} \frac{T_2}{1 + (H_o - H_{o_{RES}})^2\gamma^2T_2^2} \qquad 2.28$$

The dynamic, or complex, susceptibility χ is then defined as:-

$$\chi = \chi' - j\chi'' \qquad 2.29$$

This definition accounts for the inability of the magnetisation to follow, instantaneously, the high frequency component of the applied field; there will be a phase lag, θ, given by

$$\theta = \text{arc tan } \frac{\chi''}{\chi'}$$

associated with it.

The energy absorbed from the transverse field is:-

$$H_x^L \frac{dM_x}{dt} = H_1^L \frac{d(M_x \cos \omega t + M_y \sin \omega t)}{dt}$$

$$= H_1^L (\chi'' \cos^2 \omega t - \chi' \sin \omega t \cos \omega t) \qquad 2.30$$

The power absorbed, P, can be evaluated by integrating over a complete cycle of the high frequency field and dividing by its period $\frac{2\pi}{\omega}$

Thus

$$P = H_1^L \frac{\omega}{2\pi} \int_0^{\frac{2\pi}{\omega}} H_x^L \frac{dM_x}{dt} = (H_1^L)^2 \chi'' \frac{\pi \omega}{2\pi}$$

$$= \frac{(H_1^L)^2 \chi'' \omega}{2} \qquad 2.31$$

where it is seen that only the imaginery part of the susceptibility is responsible for power absorption. The real portion, χ', of the dynamic susceptibility describes the dispersion introduced in the sample.

Substituting into Equation 2.28 gives

$$P = \frac{(H_1^L)^2 \omega}{2} \frac{\chi_o}{2} \frac{\gamma H_{o_{RES}} T_2}{1 + (H_o - H_{o_{RES}})^2 \gamma^2 T_2^2} \qquad 2.32$$

i.e. the power absorbed is a maximum at $H_o = H_{o_{RES}}$.

Paramagnetic resonance experiments usually provide a measure of the power absorbed as H_o is slowly swept through the region $H_{o_{RES}}$ and thus an estimate of χ''.

2.2 Linewidths of Paramagnetic Resonance Spectra

Several factors may contribute to the width of a paramagnetic absorption line. The mechanisms involved may be broadly divided into two processes:-

(i) Homogeneous broadening

(ii) Inhomogeneous broadening

Homogeneous broadening is caused by mechanisms in the spin system which broaden the response of the individual spins and thus broaden the overall response of the system. The width $\Delta E = g\beta\Delta H$ of a homogeneously broadened line is related to the lifetime, τ, of the spins in a particular state by Heisenberg's Uncertainty Principle.

$$\Delta E.\tau \sim \hbar = \frac{h}{2\pi} \qquad \text{where h is Planck's constant.}$$

The phenomena of inhomogeneous broadening does not broaden the absorption of the individual spins themselves, but distributes the resonant frequencies of the various spins over a certain range. Thus the macroscopic effect is an overall broadening of the resonance absorption, but the lifetimes of individual spins is not reduced by this mechanism. Thus the width of an inhomogeneously broadened line and the lifetimes of the spins are not related by the Uncertainty Principle.

The various factors which can contribute to the width of the resonance line of solids and gases are briefly discussed below.

2.2.1 Homogeneous broadening processes

(i) Linewidth due to spontaneous emission

In both solids and gases there is a finite probability that an electron in one state will undergo a spontaneous transition to another state. The contribution to the linewidth of such a process can be shown to vary as the cube of the frequency. It has a value of about 10^{-4} c/s in the microwave region and is thus negligible compared with that due to other mechanisms.

(ii) Spin-lattice relaxation

In the process of spin-lattice relaxation, energy is exchanged between the spin system and the lattice vibrations (phonons). Possible mechanisms have been suggested by Waller and Kronig.

Waller described a process whereby the magnetic dipoles of the spins interacted with the surrounding magnetic field which is modulated by the lattice vibrations.

An alternative explanation by Kronig suggests that the interaction occurs due to a modulation of the crystalline electric field by lattice vibrations.

(iii) Spin-spin relaxation

Spin-spin interaction is a result of the fact that the magnetic dipole of a spin will influence the field experienced by its neighbours. It has been shown, during the discussion of the Bloch Equations, that the magnetic dipole moment vector of a spin in a steady magnetic field, H_o, can be regarded as a top precessing about the direction of H_o with a frequency γH_o. The dipole thus produces a steady component in the

direction of the applied field and a rotating component in the plane perpendicular to the axis of precession. This gives rise to two effects: a time independent effect in the direction of the applied magnetic field producing an incremental field at neighbouring spins and a time dependent effect, at the precession frequency, which can couple to neighbouring spins producing transitions and thus providing another means of relaxation. A theoretical expression for the second moment, $\langle \Delta\nu^2 \rangle$, of a line due to this dipole-dipole interaction has been derived by Van Vleck (3).

In liquids and gases, where the molecules are moving rapidly with respect to one another, the effect of the coupling between dipoles may be largely nullified because the interactions between them will average out to zero. Thus this broadening mechanism is largely removed resulting in a "motional narrowing".

The field at a distance r from a dipole of moment μ is proportional to $\frac{\mu}{r^3}$ and thus the interaction decreases rapidly with r. In gases the mean separation between dipoles is large and thus there is very little spin-spin interaction.

(iv) Saturation broadening

For resonant absorption to continue, under equilibrium conditions, a population difference between the upper and lower level must be maintained. When the resonance condition is satisfied, the incident microwave power induces upward transitions at a greater rate than downward transitions because of the greater population in the lower level. Thus, if the relaxation mechanisms are not sufficient to maintain

the thermal equilibrium value of the population difference, Δn, its value will be reduced. The result of this will be a reduction in the net absorption, particularly at the centre of the resonance peak, where the stimulated transition rate is a maximum, and to a lesser extent in the wings of the line. The resultant effect will give a lineshape which is broader than the actual resonance curve.

Saturation broadening occurs more readily for gaseous than for solid samples due to the lower density of atoms or molecules in the former; thus, for a given microwave power, there is a greater power incident upon each atom or molecule involved in the resonance. An indication of the degree of saturation is given by the value of the saturation factor defined as $(1 + \gamma^2 H_1^2 T_1 T_2)^{-1}$ which becomes significantly less than unity as the system approaches saturation.

(v) Pressure broadening

The width of the resonant absorption of paramagnetic gases is very dependent on the pressure of the gas. This phenomena is a consequence of collision processes; the higher the pressure the shorter the time between collisions of gaseous atoms or molecules. Thus a relaxation, induced by a collision, is more likely to occur at higher pressures. The broadening produced by this process is directly proportional to the gas pressure and forms a very major contribution to the total linewidth.

Pressure broadening can be reduced by examining the sample at low pressures but this gives rise to a low sample density resulting in low absorption and a greater likelihood of producing the saturation effects discussed in paragraph (iv).

Pressure broadening becomes an important factor at pressures ~ 0.1 torr and above.

(vi) Wall collisions

Another line broadening mechanism, restricted to gases, occurs at low pressures when the mean free path, of the gas molecules or atoms, is of the order of the resonant cavity dimensions. Pressure broadening at these pressures is no longer important but relaxation can occur when the molecules or atoms collide with the cavity walls, thus giving rise to a line broadening.

(vii) Doppler broadening

Unlike solid samples the atoms or molecules in a gas have non zero velocities in random directions. The frequency of the applied alternating field will appear higher or lower to an individual molecule depending on whether it is moving with a component of velocity in the same direction or opposed to that of the radiation. Thus there will be spread of frequencies over which the resonant condition is satisfied, i.e. a further broadening will occur. At room temperature typical molecular velocities are 10^4 - 10^5 cms/sec resulting in line broadening of a few kc/s.

2.2.2 Inhomogeneous broadening processes

(i) Modulation broadening

Many E.S.R. spectrometers utilise a high frequency field modulation which gives rise to sidebands separated from the main resonance curve by the order of the modulation frequency. The sidebands may or may not be resolved depending on the width of the main resonance and the

modulation frequency. For non resolved sidebands the only effect will be a line broadening. The broadening can be reduced by lowering the modulation frequency but this may have an adverse effect on the spectrometer sensitivity. In general a compromise is made between sensitivity and resolution on a superheterodyne spectrometer is used. Modulation broadening is a property of the E.S.R. spectrometer itself and does not contribute towards the actual linewidth of the sample.

(ii) Magnet inhomogeneity

The steady magnetic field applied to the paramagnetic sample must be homogeneous over the sample volume if an additional source of broadening is to be avoided.

Any variation of magnetic field over the sample will result in the resonance condition being satisfied at different magnet input currents at different parts of the sample. The resultant resonant absorption curve will be an overlap of several absorption curves as the magnet passes through the region of resonance.

Magnet homogeneity is optimised by using highly polished pole faces adjusted to be accurately plane parallel. The edge effect is minimised by the addition of adjustable shims on the pole edges.

2.3 Electron Spin Resonance Spectrometers

2.3.1 Choice of frequency

The resonance condition, $h\nu = g\beta H_o$, indicates that ν and H_o are interdependent. It can be shown (3) that the rate of absorption of energy at resonance is proportional to the population difference Δn.

Since $\Delta n \propto e^{h\nu/kT}$ it can be seen that the rate of absorption of energy increases as ν increases.

For optimum sensitivity it is thus desirable to use as high a frequency, ν, as possible but this is mainly limited by the high magnetic fields that would be required. Conventional electromagnets can supply fields of the required homogeneity up to 15 kilogauss corresponding to frequencies ~ 45 Gc/s, i.e. in the microwave region. Radar and communications research has been responsible for the development of components and techniques in the X band (9Gc/s) and Q band (~ 35Gc/s) regions and thus the majority of spectrometers are designed to operate in one or other of these frequency ranges.

With the recent advent of superconducting magnets, capable of providing fields in excess of 50kGauss, spectrometers operating in the 75Gc/s (4mm wavelength) and 150 Gc/s (2mm) regions have been developed.

2.3.2 Basic requirements for a spectrometer

The basic requirements for apparatus capable of detecting paramagnetic resonance are:-

(i) A coherent source of electromagnetic radiation, frequency ν, to produce transitions.

(ii) A steady magnetic field, H_o, which can be applied to the sample.

(iii) A specimen holder where the electromagnetic radiation and steady magnetic field can interact with the sample.

(iv) A system capable of detecting, displaying and/or recording any resultant absorption.

It is possible to pass through the resonance condition (Equation 2.5) by varying either ν or H_o. In practice it is far easier to vary H_o than ν linearly with time over wide ranges.

(i) The microwave source

The microwave power necessary to stimulate transitions is usually obtained from a reflex klystron which is able to deliver radiation which is essentially monochromatic, largely because it incorporates a high Q factor cavity. The microwave power and frequency are maintained to a high degree of constancy by the use of stabilised power supplies.

(ii) The steady magnetic field

For conventional spectrometers working in either X or Q band regions, a stable and homogeneous magnetic field is provided by an electromagnet engineered to a high degree of accuracy. The magnet windings are fed by very high stability current supplies; provision is usually made for a slowly varying ramp voltage to be impressed on the error voltage in the supply so that the output current and thus the magnetic field can be swept through the resonance value.

(iii) Sample container

In order to achieve as large a value of the microwave magnetic field as possible, a resonant cavity is used. The sample is placed in a position of maximum magnetic field, but not so that it disturbs the electric field. The losses in microwave cavities can be made vanishingly small resulting in very high Q factors and thus a high concentration of radiation at the sample. The cavity is placed between the poles of the electromagnet in

such a way that the microwave magnetic field and steady magnetic field are perpendicular. The klystron and cavity are the only narrowband microwave components in the system, all the other components being comparatively wideband.

(iv) Detection system

Detection in an E.S.R. spectrometer is usually carried out by using the rectifying action between a tungsten wire and a slab of silicon, although backward, hot carrier and Schottky microwave detectors which have lower noise figures are coming into more general use (6).

The E wave of the microwave power, to be detected, is coupled via a probe to one end of the point contact junction, the other end of the junction being electrically connected to the waveguide wall.

There are two main regions in the operating characteristics for a crystal detector:-

(a) For power levels $< 10^{-5}$ watts, the rectified crystal current is proportional to the incident microwave power. This is known as the square law region.

(b) At power levels greater than 10^{-4} watts, the crystal current is proportional to the square root of the incident microwave power.

Two other properties of microwave crystals must be considered in the design of a practical spectrometer:

(1) Conversion loss $L = \frac{\Delta P_{IN}}{\Delta P_{OUT}}$

L is a measure of the efficiency of detection. Unfortunately L is dependent on the incident power being very high (very inefficient)

$\sim \frac{1}{500P}$ (2) for values of $P < 10^{-5}$ watts. At powers above 10^{-4} watts, i.e. in the linear region, the value of L falls to an approximately constant value of L ~ 3.

(2) Crystal noise. In the consideration of crystal noise, its dependence on frequency and incident microwave power are of great importance.

Apart from the basic Johnson, or thermal, noise there is an excess noise dependent on the crystal current and thus dependent on the incident microwave power. The excess noise increases as the square of the crystal current. The optimum working point for a crystal detector must maintain a compromise between inefficiency due to a high value of L and a large amount of noise due to the excess noise generated in the crystal. The optimum working point occurs at a crystal current of ~ 0.5mA.

The noise spectrum of a crystal is by no means white; apart from the white Johnson noise the excess noise exhibits a $^{1}/f$ dependent spectrum.

Thus the noise power, P_{noise}, for a crystal can be expressed as (6)

$$P_{noise} = (kT + \frac{CI^2}{\nu})\Delta\nu \qquad 2.33$$

where C is a constant, I = crystal current and ν = output frequency observed over a bandwidth $\Delta\nu$. The term kT is the expression for the Johnson noise. The term $\frac{CI^2}{\nu}$ expresses the excess crystal noise and is only weakly temperature dependent.

Thus, it can be seen that, the optimum performance can be obtained from a detector crystal when detection is carried out at a high frequency and with a bias current of ~ 0.5mA flowing through the detector.

2.3.3 Desirable features of a spectrometer

The desirable features to be incorporated in a practical E.S.R. spectrometer are discussed in the following sections:-

(i) High sensitivity: The sensitivity of a spectrometer can be related to the minimum number of paramagnetic centres that can be detected by the spectrometer which in turn can be related to the static susceptibility χ_o; χ_o is related to χ'' and χ' by Equations 2.27 and 2.28. The sensitivity of an absorption spectrometer (i.e. a device which detects and measures χ'') is usually quoted in terms of χ''_{min} where χ''_{min} is the smallest value of χ'', the imaginery part of the dynamic susceptibility (see Equation 2.29), which can be detected. χ''_{min} is generally related to the noise within the system. Obviously it is desirable to be able to detect as small a value of χ''_{min} as possible and thus the sensitivity of a spectrometer is of paramount importance. This is especially true in the study of transient paramagnetic species where it may be difficult to generate large paramagnetic concentrations and during their decay χ'' is always decreasing. An expression for the sensitivity of an E.S.R. spectrometer is discussed in a later section in this chapter.

(ii) Good stability: A factor closely connected with the sensitivity of a spectrometer is the long term stability. In order to achieve a high sensitivity, techniques to reduce the noise to a minimum are used. All such methods rely on reducing the bandwidth of the system and this, in turn, means that the response time of the system is increased, resulting in a much slower field sweep through a resonance signal being necessary if an accurate reproduction of the lineshape is to be achieved.

If any low frequency noise in the form of drift exists in the spectrometer then, with the use of longer sweep times, it will increase in importance and thus effectively reduce the sensitivity. It is thus important that any long term drift is minimised(12).

(iii) Separation of absorption and dispersion modes: As shown in Equation 2.29, the dynamic susceptibility χ consists of two components; a real part χ' responsible for a phase change of the absorbed microwaves at resonance; and χ'', an imaginery part, which describes the absorption of microwave power, by the sample, at resonance. χ' and χ'' are related to one another by the Kronig-Kramers equations and thus χ' may be deduced from χ'' and vice-versa. In any measurement, it is important that either pure absorption or pure dispersion is being detected and not a mixture of both, especially when lineshape is being studied.

(iv) Resolving power: An E.S.R. spectrum may consist of many narrow closed spaced lines. In any analysis of samples in which such spectra occur it is important that the spectrometer is capable of resolving the spectra. There are two main factors which determine the resolving power; the magnet homogeneity and the extent of any modulation broadening. These factors have been discussed in the section on inhomogeneous broadening (Section 2.2.2).

2.4 Practical E.S.R. Spectrometers

A development from a simple D.C. detection E.S.R. spectrometer up to the 100 Kc/s field modulation used by the author will be discussed. An account of the latest techniques is given.

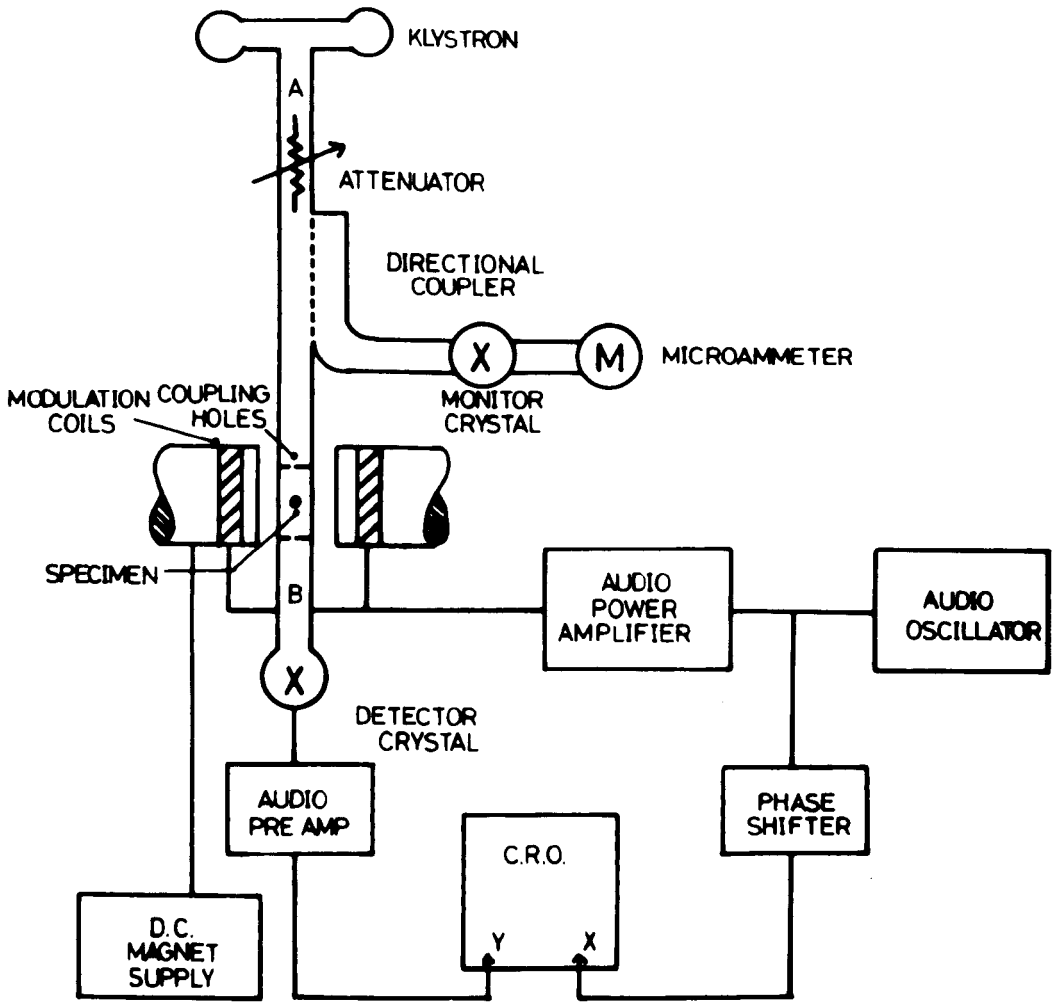

FIG. 2.3. SIMPLE CRYSTAL VIDEO TRANSMISSION CAVITY E.S.R. SPECTROMETER.

2.4.1 Transmission cavity spectrometer

One of the simplest forms an E.S.R. spectrometer can take is shown in Fig. 2.3.

There are several shortcomings in such a system which combine to render its sensitivity low. The major disadvantage lies in the fact that it is not possible to vary the microwave powers at the crystal and sample independently. To obtain optimum sensitivity it is desirable to apply a large microwave power to the sample, but this would probably result in the detector crystal receiving a non-optimum bias resulting in a high excess noise. The use of a "bucking system" overcomes this difficulty. Referring to Fig. 2.3, microwave power is bled out of the system, using a directional coupler, at point A. The power is then fed through an attenuator and phase shifter and back into the system, using a directional coupler situated at point B. Thus the power arriving at the detector crystal is a mixture of the net power transmitted through the resonant cavity and the power from the "bucking-arm". Adjustment of the amplitude and phase of the bucking power enables the bias at the crystal to be set at its optimum working point regardless of the sample power, providing the klystron is capable of supplying the total power required.

Even with the addition of the bucking system into the spectrometer shown in Fig. 2.3, there still remains the disadvantage that a video system requires a large bandwidth to ensure that a lineshape is reproduced with reasonable fidelity. The required bandwidth could be reduced by drastically lowering the field modulation frequency and recording the spectrometer output on a pen recorder but at these low frequencies the $1/f$ noise from the crystal is very severe.

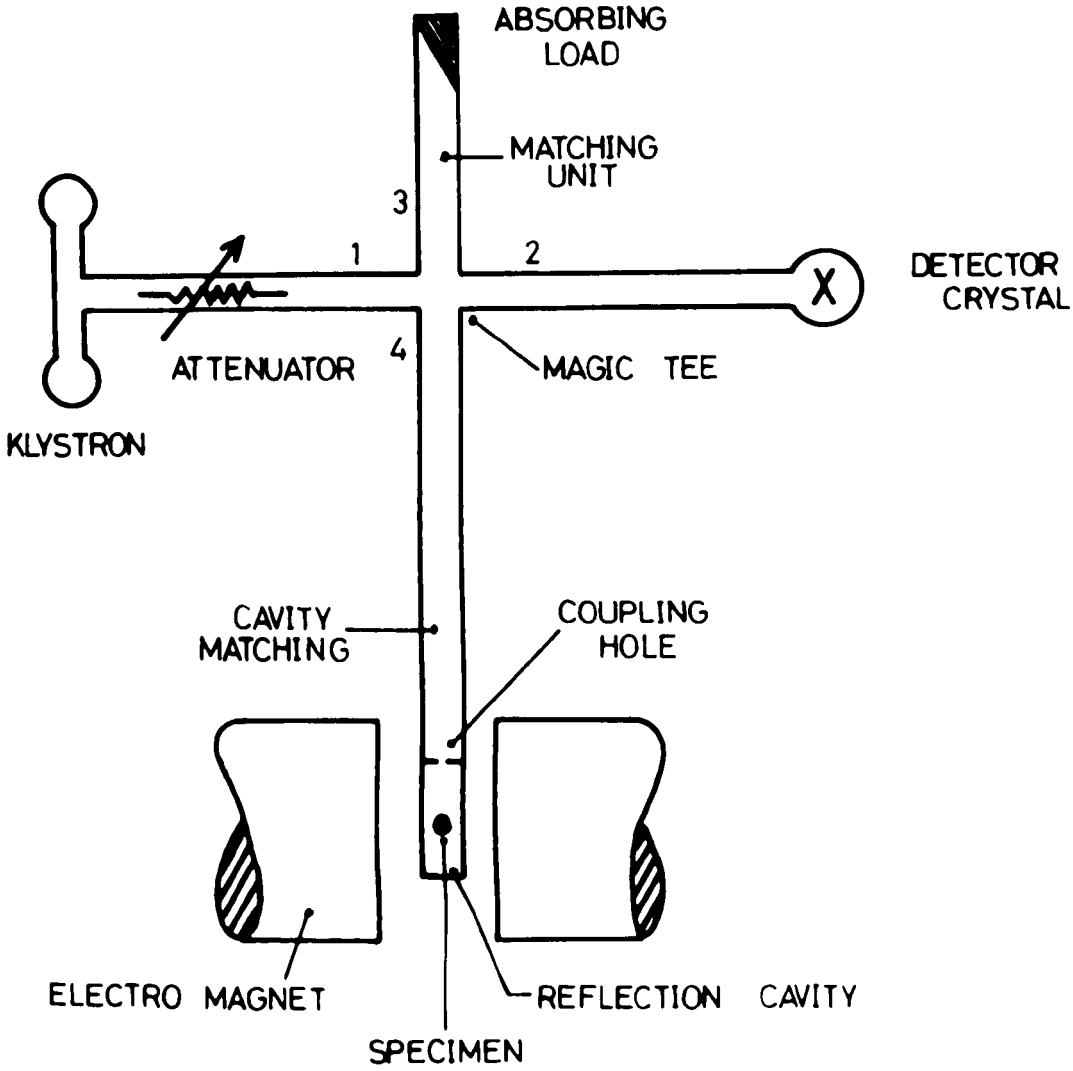

FIG. 2. 4. BASIC REFLECTION CAVITY AND BRIDGE SPECTROMETER.

2.4.2 The reflection cavity spectrometer

An alternative means of attaining independence of sample and crystal power is by the use of a bridge system used in conjunction with a reflection cavity. The basic system is shown in Fig. 2.4. Power coupled into arm 1 of the 'magic tee' is divided equally between arms 3 and 4 if they are matched. Any unbalance in the matching between arms 3 and 4 results in power being fed to arms 1 and 2. When the reflection cavity is correctly matched to the waveguide no power is reflected from arm 4 and thus if arm 3 is adjusted for zero reflection, there will be no microwave power incident on the crystal detector in arm 2. The bridge is then balanced. In practice the bridge is not operated at perfect balance because the detector crystal would then operate in the region of zero power and thus with a very high value of conversion loss L. The deliberate introduction of a small amount of mismatch in arm 3 ensures that the crystal can be biased to its optimum working point without disturbing the matching and power level of the resonant cavity. When the resonant condition is satisfied, power is absorbed by the sample resulting in the matching of the cavity in arm 4 being disturbed. Power reflected from the cavity disturbs the state of balance of the bridge and thus there is a change in the power level at the detector crystal. The advantage of the bridge system is that resonance is observed as a relatively large increase in the detected microwave power whereas the basic transmission system results in a small decrease in a large detected power.

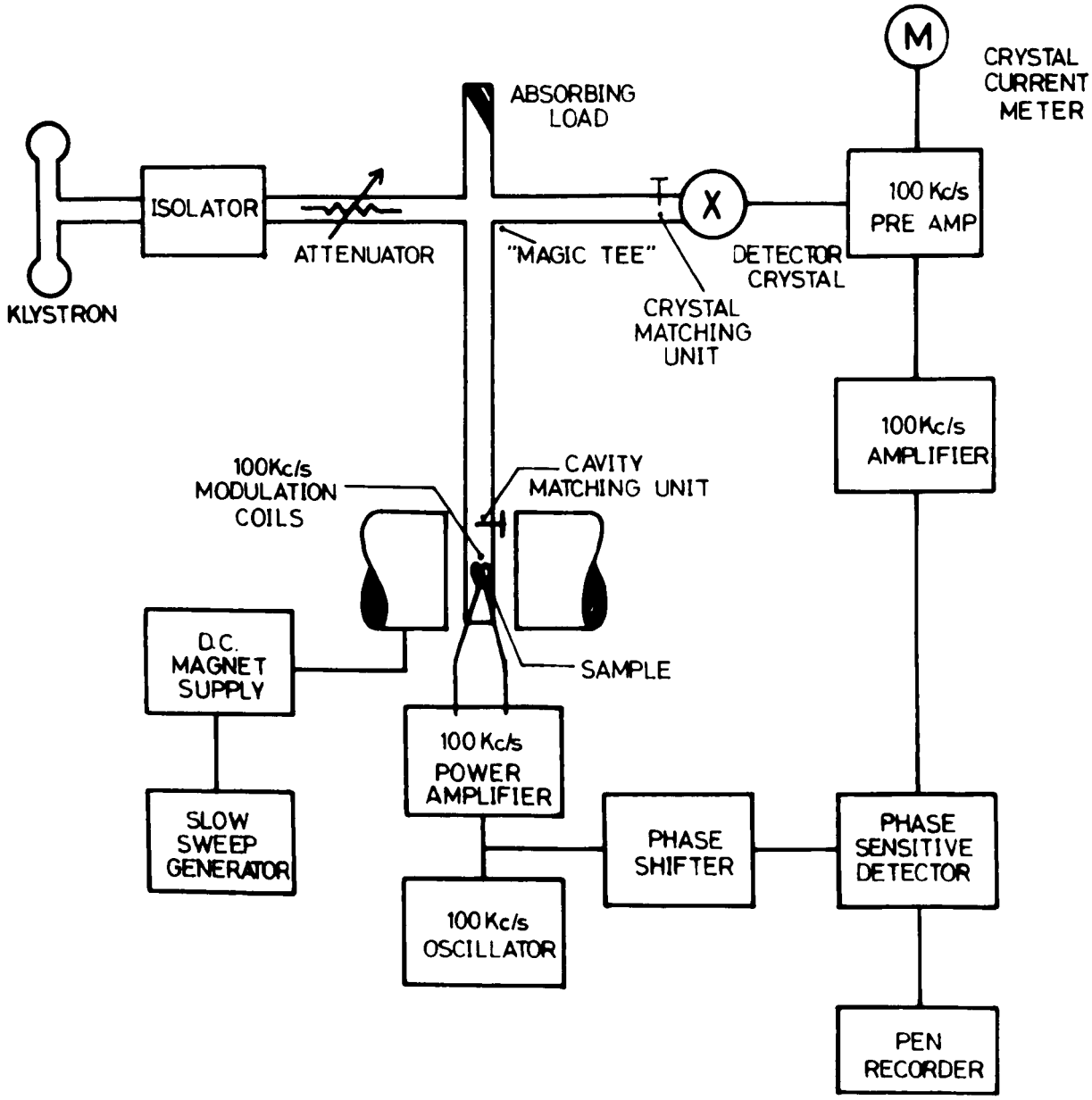

FIG. 2.5. BLOCK DIAGRAM OF A BASIC 100 Kc/s FIELD MODULATION SPECTROMETER.

2.4.3 The high-frequency field modulation spectrometer

The basic bridge and reflection cavity system described in Section 2.4.2 still suffers similar disadvantages to the transmission system regarding the large detection bandwidth required and the high excess crystal noise encountered by working at low frequencies.

The high-frequency field modulation spectrometer depicted in Fig. 2.5 overcomes the bandwidth problem and, by utilising a high detection frequency, minimises the $^{1}/f$ noise from the crystal. The field modulation is applied using a coil around the sample. A narrow detection bandwidth is achieved by the use of a phase-sensitive detector (P.S.D.); this device is discussed in detail in Chapter III.

By modulating the steady magnetic field with a small high frequency component the slope of the absorption is sampled. Considering the line shape function g(H): when the field is modulated with a component $H_m \sin \omega_m t$:-

$$g(H) = g(H_o + H_m \sin \omega_m t)$$

Expanding as a Taylor series:-

$$g(H) = g(H_o) + g'(H_o)H_m \sin \omega_m t + \tfrac{1}{2}g''(H_o)H_m^2 \sin^2 \omega_m t + \ldots\ldots \quad 2.34$$

When H_m is very small Equation 2.34 approximates to:-

$$g(H) = g(H_o) + g'(H_o)H_m \sin \omega_m t \quad 2.35$$

where a prime indicates the order of the derivative of a function. The A.C. component of g(H) is obtained by passing the detector crystal output through a narrow band amplifier tuned to the modulation frequency,

$\omega_m/2\pi$, and thus the output is proportional to the first derivative, $g'(H_o)$, of the lineshape function, $g(H_o)$, the D.C. component involving $g(H_o)$ in Equation 2.35 being removed.

Increasing the amplitude, H_m, of the high frequency modulations will result in a larger output but distortion will result due to higher order terms in the Taylor series being no longer negligible. In the study of weak absorption, large amplitude modulation can be utilised to improve the sensitivity; although the resultant derivative will be distorted, the position of the absorption maximum will be accurately recorded as the zero crossing point of the first derivative. The use of a P.S.D. besides reducing the system bandwidth to that of the output recording circuitry, also results in a true derivative being recorded; the detected signal at ω_m undergoing a phase change of 180^o as passage from the positive to negative slope of the absorption line occurs.

Narrowband high frequency detection techniques result in a large reduction in detected crystal noise. The optimum frequency for many crystal detectors is in the 30Mc/s region but the modulation broadening occurring in a field modulation spectrometer results in a compromise by using a modulation frequency of ~ 100kc/s. However, Buckmaster and Dering (11,12) have shown that with modern crystal detectors there is little advantage in using detection frequencies >0.2Mc/s.

2.4.4 Superheterodyne detection

Detection at an optimum frequency without the disadvantage of modulation broadening can be carried out by using superheterodyne detection. The power from an additional local oscillator klystron set at a frequency

different from that of the signal klystron by a constant frequency (intermediate frequency) is mixed with the signal power just before the detection crystal. The power at the detection frequency is thus modulated at the intermediate frequency (I.F.). Superheterodyne detection is very sensitive, in principle, but places stringent demands on the stability of the microwave bridge components. The bridge must be critically adjusted to avoid saturation of the I.F. amplifier following the detector crystal. Hyde (8) has shown that for low cavity powers (< 1mW) the performance of a 100kc/s field modulation spectrometer and superheterodyne spectrometer are comparable. At greater powers microphonics contribute the limiting noise of the superheterodyne because of the difficulty in maintaining a stable coupling to avoid saturation of the I.F. amplifier. At high I.F. levels there is also the possibility of non linear mixing of I.F. with low frequency crystal noise resulting in an additional noise source.

The simplicity of the h.f. field modulation system results in its widespread use except where exceptionally high resolution is required; under these conditions the added complexity of a superheterodyne system must be tolerated.

Recent data obtained by Buckmaster and Dering (9,11) has shown that it is possible to approach the theoretical spectrometer sensitivity for an ideal detector at detection frequencies of ~ 100kc/s using homodyne and superheterodyne techniques.

The homodyne technique was originally applied to E.S.R. spectrometers by Feher (10) using barretter detection instead of crystal detection. The homodyne technique utilises two detectors and a balanced mixer and the klystron noise is largely cancelled as a result; the biasing power for the crystals is fed via a bucking arm to one arm of the balanced mixer and it is thus possible to use the spectrometer with the microwave bridge balanced. Any unbalance off resonance will give rise to additive A.M. klystron noise at the detector crystals.

The combination of balanced mixer and superheterodyne techniques is embodied in a recent design by Buckmaster and Dering (11), of an E.S.R. spectrometer featuring superheterodyne demodulation using a single klystron as the source of both the local oscillator and sample cavity microwave power. The instability usually associated with superheterodyne systems is overcome by the use of triple synchronous demodulations at the microwave, intermediate and field modulation frequencies using a balanced mixer and two phase sensitive detectors working at the I.F. and field modulation frequencies. By phase locking the klystron (12) to a high stability crystal oscillator and simultaneously following the resonant frequency of the sample cavity, the resultant frequency is virtually independent of the random fluctuations in microwave bridge balance and drift in the resonant cavity frequency. The use of an I.F. of 100kc/s means that, with modern detector crystals, $^{1}/f$ noise is negligible (11,12). A low frequency field modulation can be used, to avoid modulation broadening, without a loss in sensitivity because detection has already taken place at the optimum 100kc/s I.F. Buckmaster and Dering (12)

recommend that the choice of field modulation frequency should be above 500c/s in order to avoid cavity microphonics but at these frequencies modulation broadening is undetectable.

2.4.5 Sensitivity of a balanced bridge reflection cavity spectrometer

The following discussion is based on a treatment of the subject by Ingram (2). The sensitivity of an E.S.R. spectrometer can be conveniently considered by first examining the parameters which contribute to give an output signal at resonance.

Bleaney and Stevens (13) have shown that the paramagnetic absorption occurring at resonance is equivalent to a change in Q factor of the resonant cavity system. In this context the term "cavity system" refers to the sample cavity and the waveguide to which it is coupled. The Q factor of a reflection cavity system can be considered in terms of electrical analogues, as possessing two parts (10): an unloaded Q, Q_o, defined by losses due to the cavity alone and an external Q factor, Q_x, specified in terms of power leakage out of the cavity.

$$Q_o = \frac{\omega L}{r} \qquad 2.36$$

$$Q_x = \frac{\omega L}{R_o n^2} \qquad 2.37$$

A loaded Q, Q_L, is then described which combines the losses from the cavity alone and the power leakage

$$Q_L = \frac{\omega L}{R_o n^2 + r} \qquad 2.38$$

R_o is the characteristic impedance of the waveguide, n is the equivalent "turns ratio" of an equivalent coupling transformer between the waveguide

and cavity and is determined by the size of the coupling hole into the cavity, r is the resistive loss of the cavity walls plus any loss due to the sample. Feher defines a coupling coefficient,

$$\beta = \frac{R_o n^2}{r} = \frac{Q_o}{Q_x} \qquad 2.39$$

If $\beta > 1$ the cavity is described as overcoupled and for $\beta < 1$ the cavity is undercoupled. With $\beta = 1$ the cavity is critically coupled and matched to the waveguide impedance and under these conditions $Q_o = 2Q_L = 2Q_x$. Under this condition no reflection of power occurs, all the power being absorbed in the cavity. $\beta = 1$ is the condition necessary for the balance of the microwave bridge, in a reflection cavity spectrometer.

Wilmshurst, Gambling and Ingram (14) indicate that it can be assumed that the detector crystal is working in a linear region because, in practice, the resonance signal at the detector is small compared with its biasing power. Under these conditions Feher (10) shows that the optimum coupling to the cavity occurs at $\beta = 1$, i.e. under matched conditions.

The mean power, P, absorbed in unit volume of a paramagnetic sample is:

$$P = \tfrac{1}{2}\omega H_1^2 \chi''(H) \qquad 2.40$$

where ω = angular frequency of incident r.f. field,

H_1 = amplitude of r.f. magnetic field-

$\chi''(H)$ = imaginery part of dynamic susceptibility.

The Q factor of a cavity is given by:-

$$Q = \omega \frac{\text{Energy stored in cavity}}{\text{Average power dissipated in cavity}}$$

Thus, off resonance,

$$Q = Q_o = \frac{\omega \frac{1}{8\pi} \int_{V_c} H_1^2 \, dV_c}{P_1} \qquad 2.41$$

At resonance:

$$Q = \frac{\omega \frac{1}{8\pi} \int_{V_c} H_1^2 dV_c}{P_1 + \frac{1}{2}\omega \int_{V_s} H_1^2 \chi'' dV_s} \qquad 2.42$$

where P_1 is the power dissipated by losses in the cavity. V_c and V_s are the cavity and sample volumes respectively.

Then

$$Q = \frac{1}{\frac{1}{Q_o}\left[1 + \frac{4\pi \int_{V_s} H_1^2 \chi'' dV_s}{\int_{V_c} H_1^2 \, dV_c}\right]} \qquad 2.43$$

Assuming that the power absorbed by the sample at resonance << P_1 then:

$$Q \simeq Q_o \left[1 - \frac{4\pi\chi'' \int_{V_s} H_1^2 dV_s}{\int_{V_c} H_1^2 dV_c} Q_o \right] \qquad 2.44$$

Thus the change in $Q = \Delta Q = Q - Q_o$

$$\therefore \quad \Delta Q = Q_o^2 \, 4\pi\chi'' \, \eta \qquad 2.45$$

where

$$\eta = \frac{\int_{V_s} H_1^2 dV_s}{\int_{V_c} H_1^2 dV_c}$$

is known as the "filling factor" and is a parameter which describes how well the sample fills the cavity in terms of the microwave magnetic field distribution in the cavity.

The change in Q, ΔQ, occurring at resonance can be related to the change in microwave voltage, ΔV, at the detector to obtain (10,14)

$$\Delta V = V\pi\chi'' \eta Q_o \qquad 2.46$$

where V is the microwave voltage injected from the klystron into the microwave bridge. Equation 2.46 takes account of the fact that only half the incident power reaches the cavity and only half of the power reflected from the cavity reaches the detector crystal; the division of power that occurs with a "magic tee" is a disadvantage because the sensitivity is related to the power at the sample. The use of a 3 port circulator (15),

a non-reciprocal microwave component, in place of the "magic tee" overcomes this division and loss of power available at the sample; but the results of an investigation by Buckmaster and Dering (11) have indicated that it is impossible to maintain a high degree of bridge balance over long periods with such a device.

An expression for the ultimate sensitivity of a balanced bridge spectrometer can be obtained by initially considering a perfect detector, which exhibits thermal noise alone, matched to the characteristic impedance of the waveguide. The assumption is then made that the minimum detectable value of ΔV, ΔV_{min}, equals the r.m.s. value of the thermal noise voltage $V_{n.r.m.s.}$. $V_{n.r.m.s.}$ is given by the expression:-

$$V^2_{n.r.m.s.} = 4kTR_oB \qquad 2.47$$

originally derived by Nyquist (16).

Equating ΔV_{min} and $V_{n.r.m.s}$ (Equations 2.46 and 2.47) gives:-

$$\chi''_{min\ ideal} = \frac{2}{\pi\eta Q_o} \frac{(kTR_oB)^{\frac{1}{2}}}{V} \qquad 2.48$$

$\chi''_{min\ ideal}$ may be expressed in terms of the incident power $P = \frac{V^2}{4R_o}$ for a matched cavity; thus:

$$\chi''_{min\ ideal} = \frac{1}{\eta\pi Q_o}\left(\frac{kTB}{P}\right)^{\frac{1}{2}} \qquad 2.49$$

Equation 2.49 does not take the excess crystal noise and the noise of the detection equipment into account. An expression for the minimum value of χ'' that will be detected with practical equipment, $\chi''_{min\ prac.}$ is given by:-

$$\chi''_{min\ prac} = \frac{1}{\eta\pi Q_o}\left(\frac{FkTB}{P}\right)^{\frac{1}{2}} \qquad 2.50$$

where F is a degradation factor or noise figure of the detection equipment. F describes how far short of the theoretical ideal the performance of an item of electrical equipment falls in terms of noise.

Examination of Equation 2.50 indicates that χ''_{min} can be minimised in a system by an increase in the Q factor of the sample cavity. Q factors greater than 5,000 are difficult to produce especially when the damping effects of the sample and modulation coils are included.

An increase in microwave power, P, will give a lower value of χ''_{min} but care must be taken to avoid saturation effects, discussed in Section 2.2.1.(iv), which will lower the ultimate sensitivity.

There is very little control of the filling factor, η, for a particular cavity; increasing the sample volume, V_s, will undoubtedly lead to interference with the distribution of the E.M. waves in the cavity resulting in a lowering of Q_o.

There are three parameters, system bandwidth, B, absolute temperature, T, and noise factor, F, which, if reduced, will improve the ultimate sensitivity of a given system.

The bandwidth, B, of the system may be reduced to exceedingly low values by the use of a P.S.D. as a final detector (Chapter III). Any lowering of B entails sweeping through a resonance line more slowly in order to avoid distortion of the lineshape. Any slow drift in bridge balance, klystron frequency and cavity frequency will be more critical

and the spectrometer may not hold its value of χ''_{min} for a sufficiently long period to allow a sweep through a spectrum to be completed.

The temperature at which measurements are carried out can be reduced but it must be noted that the temperature, T, in Equation 2.50 refers to the operating temperature of the detection system. Cooling the crystal would present considerable practical difficulties. Cooling the sample will give rise to a greater population difference, between energy levels, resulting in a larger absorption but this does not involve a reduction in χ''_{min} for the spectrometer and may appreciably alter the characteristics of the E.S.R. spectrum of the sample under consideration.

The reduction of F, the total noise factor of the system, involves a consideration of the parameters which contribute to the overall noise of the system and are discussed below.

2.4.6 Noise in the detection system

The contributions to the noise in the detection system of an E.S.R. spectrometer arise from four main sources:

(i) Crystal detector

(ii) Klystron

(iii) Microwave components

(iv) Amplifier noise.

(i) Crystal noise has already been discussed in a previous section (2.3.2.(iv)). The design of E.S.R. spectrometers is largely influenced by the crystal noise. With modern crystal detectors and the use of methods (11) to minimise any excess noise, present techniques aim at minimising klystron and microwave component noise.

(ii) and (iii) Klystron and microwave component noise can be conveniently discussed together as their effects are strongly interelated. High frequency F.M. and A.M. noise is very small compared with other noise sources; but drift in klystron frequency, cavity resonant frequency and microwave bridge balance (11) not only mar long term stability but also cause klystron F.M. noise to be discriminated, for example, by an off tune sample cavity to give a high degree of A.M. noise. Bridge balance is exceedingly important in a balanced mixer system and Buckmaster and Dering (11) have shown that the maximum degree of bridge balance obtainable is proportional to the difference between the cavity and klystron frequencies; when the klystron and cavity frequencies are equal, the spectral width of the klystron output is then the determining factor in the balancing of the bridge. It is for these reasons that Buckmaster and Dering (11) use simultaneous phase locking of the microwave frequency to a high stability, crystal controlled, 1Mc/s oscillator, to reduce the spectral width of the klystron, and frequency locking of the klystron to the resonant frequency of the cavity.

Microphonics form another combined source of noise from the klystron and microwave components; this can be minimised by using a final detection frequency >500c/s (11).

(iv) Amplifier noise is used to describe the overall noise contribution from the electronics of the detection system. The low level preamplifier following the detector crystal forms the largest contribution; but by careful design and impedance matching noise figures of 1dB can be achieved (17).

Gambling and Wilmshurst (18) utilised the very low noise properties of an ammonia maser; the expected improvement was not achieved because of the ease with which the preamplifier saturated due to F.M. noise discriminated by the sample cavity. A recent analysis by Buckmaster and Dering (7) has indicated that the use of parametric or maser preamplifiers is only justified for samples which saturate at exceedingly low power levels (~ 1μW) or if a microwave source with low spectral purity (high F.M. noise) is used. Buckmaster and Dering (7) were able to show that, when the noise due to discrimination of klystron F.M. noise becomes the dominant term in the total noise figure, F, of the system, the equation for the ultimate sensitivity becomes:

$$\chi''_{min} \sim \frac{1}{4\pi\eta}\left(\frac{\sigma B}{3}\right)^{\frac{1}{2}} \qquad 2.51$$

where σ is the standard deviation of the klystron F.M. noise.

REFERENCES

(a) General

1. Ingram, D.J.E., "Spectroscopy at Radio and Microwave Frequencies" (2nd Edition), (Butterworths London 1967).

2. Ingram, D.J.E., "Free Radicals as studied by Electron Spin Resonance" (Butterworths London 1958).

3. Pake, G.E., "Paramagnetic Resonance" (Benjamin Inc., New York 1962).

4. Siegman, A.E., "Microwave Solid-State Masers" (McGraw-Hill Book Co. 1964).

5. Slichter, C.P., "Principles of Magnetic Resonance" (Harper and Row 1964).

6. Townes, C.H. and Schawlow, A.L., "Microwave Spectroscopy" (McGraw-Hill Book Co. 1955).

(b) Specific References

7. Buckmaster, H.A. and Dering, J.C., J. Sci. Inst. 44, 430 (1967).

8. Hyde, J.S., "Evaluation of an E.P.R. Superheterodyne Spectrometer", (Varian Associates 7th Annual NMR-EPR Workshop (1963)).

9. Buckmaster, H.A. and Dering, J.C., Canad. J. Phys. 43, 1088 (1965).

10. Feher, G., Bell Syst. Tech. J. 36, 449 (1957).

11. Buckmaster, H.A. and Dering, J.C., Canad. J. Phys. 45, 107 (1967).

12. Buckmaster, H.A. and Dering, J.C., J. Sci. Inst. 43, 554 (1966).

13. Bleaney, B. and Stevens, K.W.H., Rep. Prog. Phys. 16, 108 (1953).

14. Wilmshurst, T.H., Gambling, W.A. and Ingram, D.J.E., J. Electron. Control. 13, 339 (1962).

15. Faulkner, E.A., J. Sci. Inst. 39, 135 (1962).

16. Nyquist, H., Phys. Rev. 32, 110 (1928).

17. Wilmshurst, T.H., J. Sci. Inst. 44, 403 (1967).

18. Gambling, W.A. and Wilmshurst, T.H., Proc. 3rd Int. Conf. on Quantum Electronics 401 (1964) (Ed. P. Grivet and N. Bloembergen; Dunod, (Paris)).

CHAPTER III

SIGNAL-TO-NOISE RATIO CONSIDERATIONS

3.1 Noise Considerations in a Measuring System

One of the most important parameters concerned with the noise of a system is its bandwidth. A system with a large bandwidth presents a large "window" through which noise can enter.

Nyquist (1) showed that Johnson (2) or thermal noise voltage, V_n, in a resistor R ohms in equilibrium at a temperature $T^{o}A$ measured over a bandwidth B is given by:

$$\langle V_n^2 \rangle = 4kTRB \qquad 3.1$$

where k = Boltzman's constant,

$\langle V_n^2 \rangle$ = root mean square (r.m.s.) value of the noise voltage.

The spectrum of Johnson noise is 'white', i.e. it is independent of frequency. Such independence of noise on frequency does not extend to all sources of noise. Flicker noise of the type encountered in microwave detector crystals (3), already discussed in Chapter 2.3.2(iv), has a power spectrum with an f^{-1} dependence.

Generally, therefore, two factors must be considered in minimising noise in a system:-

(i) Bandwidth

(ii) Frequency of operation or detection.

For example, in considering an E.S.R. spectrometer a major contribution to the overall noise is from the detector crystal. In order to minimise

this noise the microwave power falling on the crystal detector is usually modulated at a high frequency, f_m, the choice of which is discussed in Chapter II. The output from the crystal detector must be amplified and presented in a form usable by a device such as a pen-recorder, meter or oscilloscope; i.e. the variation in the amplitude of f_m must be converted to a variation in D.C. level. In carrying out this "second detection" the bandwidth of the amplifier and "second detector" is very important.

Consider simple detection as shown in Figure 3.1. The signal to be detected is passed through an amplifier of bandwidth B_A; the output of the amplifier is passed to the detector, the output of which is connected to a low pass filter and D.C. recorder of combined bandwidth B_D. Robinson (4) has shown that for a low signal-to-noise ratio at the amplifier input under either square-law or linear detection the "effective noise bandwidth" B_n for such a system is:

$$B_n = (2B_A B_D)^{\frac{1}{2}} \qquad 3.2$$

subject to the condition $B_A >> B_D$ which will always be satisfied in practice. The terminology "effective noise bandwidth" is used to describe B_n because the noise at the output of the system is consistent with this value for B_n when substitution is made into Equation 3.1. The signal bandwidth of the system depicted in Figure 3.1 is limited to B_D and, thus, for this system the condition $B_n > B_D$ holds making the signal-to-noise ratio characteristics very poor.

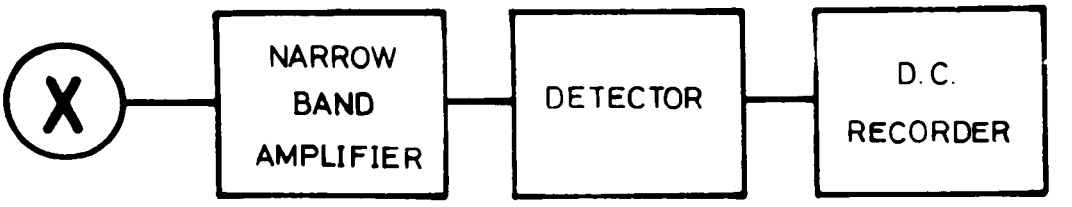

FIG.3.1. SIMPLE DETECTION.

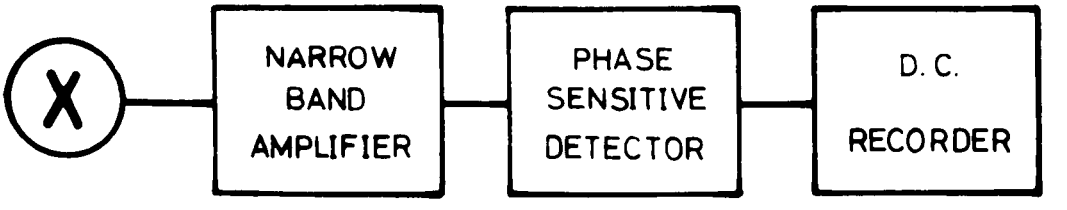

FIG.3.2. DETECTION USING PHASE SENSITIVE DETECTOR

From an experimental view the idea would be $B_n < B_D$ but this would imply that it was possible to discriminate directly between signal and noise. The best condition encountered in practice is $B_n \sim B_D$ and this is provided by a device known variously as a phase sensitive detector (P.S.D.), lock in amplifier or synchronous detector.

3.2 The Phase Sensitive Detector

The phase sensitive detector (P.S.D.) is essentially a device whose gain is proportional to a reference voltage (see Fig. 3.2.). Suppose that the input signal V_S is of the form:

$$V_S = S \sin(2\pi f_m t + \phi) \qquad 3.3$$

where f_m is the frequency of the signal.

Consider the case when the reference voltage, V_R, is of the form:

$$V_R = R \sin 2\pi f_m t \qquad 3.4$$

Then the output, V_{OUT}, of the P.S.D. will be:-

$$V_{OUT} = RS \sin 2\pi f_m t \sin(2\pi f_m t + \phi) \qquad 3.5$$

After passing through a low pass filter of bandwidth ΔF, much less than the bandwidth, B_A, of the input noise and with a cut off frequency $f_c = \frac{1}{T}$, then the resulting D.C. output V_{DC} is given by:-

$$V_{DC} = \frac{1}{T} \int_{\tau}^{T+\tau} RS \sin 2\pi f_m t \sin(2\pi f_m t + \phi) dt$$

$$= \frac{RS}{T} \int_{\tau}^{T+\tau} (\sin^2 2\pi f_m t \cos\phi + \sin 2\pi f_m t \cos 2\pi f_m t \sin\phi) dt \qquad 3.6$$

For T very large w.r.t. $1/f_m$, i.e. for a very low frequency cut off filter $f_c << f_m$

$$V_{DC} = \frac{RS}{2} \cos \phi \qquad 3.7$$

If ϕ is zero, i.e. the signal and reference are in phase, then the output is a maximum with positive polarity. If $\phi = \pi$ the output has the same maximum value but is of negative polarity. With $\phi = \pi/2$ or $3\pi/2$ the output is zero.

Van der Ziel (5) has pointed out that the value of the output is proportional to the peak amplitude of the signal providing the reference peak amplitude is constant. Thus the P.S.D. is a peak reading device and not an R.M.S. instrument like a simple detector.

With an input to the P.S.D. at a frequency $f_m \pm F$, there will be an output at frequency F.

For an input r.m.s. noise voltage N_{rms} the output noise power spectrum W(F) at a frequency F is the result of input noise spectra of both $w(f_m+F)$ and $w(f_m-F)$.

$$\therefore \quad W(F) = R^2_{rms} N^2_{rms} (f_m \pm F) = R^2_{rms} \{w(f_m+F) + w(f_m-F)\} \qquad 3.8$$

For white noise input $w(f_s+F) = w(f_s-F) = w$.

and $\therefore \quad W(F) = W = 2R^2_{rms} w$.

$$\text{Signal output power} = V^2_{DC} = \frac{R^2S^2}{4} = R^2_{rms} S^2_{rms} \qquad 3.9$$

Thus output S/N power ratio in a bandwidth B_D

$$= R^2_{rms} S^2_{rms} \frac{1}{W.B_D} = \frac{S^2_{rms}}{2wB_D} \qquad 3.10$$

Assuming that no noise is generated internally in the P.S.D. but only in the process of mixing, then apparent signal/noise input power ratio, I, = actual signal/noise output power ratio, O.

$$I = \frac{S^2_{rms}}{wB_{eff}}$$

where B_{eff} is the effective noise bandwidth.

Thus

$$B_{eff} = 2B_D \qquad 3.11$$

which is considerably lower than the factor $(2B_DB_A)^{\frac{1}{2}}$ for simple detection and is independent of any input circuit bandwidth providing $B_D \ll B_A$. This small effective bandwidth is retained independently of f_m and any change in f_m, equally, has no effect providing the experimental modulation and reference are derived from the same oscillator. The amplitude stability of the reference is of major importance because of the dependence of the output, V_{DC}, on the amplitude, R, of the reference. For this reason the reference is usually derived from a limiter fed from the reference oscillator in order to eliminate a possible source of noise.

A common form of P.S.D. (4) utilises a square wave reference voltage V_R, where V_R takes the values:-

$$V_R = +1 \quad \text{when} \quad \cos 2\pi f_m t > 0$$

and $\qquad 3.12$

$$V_R = -1 \quad \text{when} \quad \cos 2\pi f_m t < 0$$

This type of reference is utilised because it is easier to produce devices whose gain can be switched between zero and some fixed value.

The switching characteristics of diodes (both thermionic and semiconductor) valves and transistors (unipolar and bipolar) can be used. In practice the square wave reference voltage is used to change the effective gain of the P.S.D. between + 1 and - 1 and vice-versa once during each cycle. The reference voltage, V_R, can be expressed in terms of a Fourier series (6):

$$V_R(t) = 2 \sum_{n=1}^{\infty} \frac{\sin(\pi h/2)}{\pi h/2} \sin 2\pi n f_m t \qquad 3.13$$

For a signal input $V_S = S \sin(2 f_m t + \phi)$, the output of the P.S.D. $V_R(t)\ V_S(t)$ is given by:

$$V_R(t)\ V_S(t) = 2S \sin(2\pi f_m t + \phi) \{\frac{2}{\pi} \sin 2\pi f_m t - \frac{2}{3\pi} \cos 2\pi 3 f_m t + \frac{2}{5\pi} \cos 2\pi 5 f_m t - .....\} \qquad 3.14$$

After passing through a low pass filter with a cut off frequency $f_c << f_m$ the output voltage V_{DC} is given by:-

$$V_{DC} = \frac{2}{\pi} S \cos \phi \qquad 3.15$$

With either type of P.S.D. the input signal, V_S, usually consists of a signal of frequency f_m whose amplitude, S, is a slowly varying function of time S(t) and thus S(t) will be faithfully reproduced at the output providing the highest frequency component, f_s, of S(t) is much less than B_D, the bandwidth of the output filter and D.C. recording circuitry.

The "switching type" of P.S.D., originally described by Dicke (7), performs well providing that the signal input, $V_S(t)$ does not contain any odd harmonics of the fundamental f_m; otherwise phase sensitive detector action will occur between these harmonics and the odd harmonics occurring

in the square wave reference to give outputs after filtering. This disadvantage is usually overcome by passing the signal through a narrow-band amplifier, whose response is centred at f_m, prior to applying it to the P.S.D.; this action has the added advantage that noise outside the bandwidth of this amplifier is removed and thus there is less likelihood of noise outside this bandwidth saturating the various components of the P.S.D. and inhibiting its action.

When analysis is carried out at several different frequencies a tunable narrowband amplifier may prove inconvenient and, in this instance a "product type" P.S.D. using a sinusoidal reference, as described by Holland (8) is desirable; otherwise the "switching" type of P.S.D. is perfectly suitable (9,10,11,12,33). P.S.D.s of the latter type used in conjunction with a narrowband amplifier are usually employed in an E.S.R. spectrometer.

The signal to noise ratio (S/N) improvement, G, occurring in a P.S.D. is:-

$$G = \frac{\frac{S_o^2}{N_o^2}}{\frac{S_i^2}{N_i^2}} = \frac{S_o^2}{S_i^2} \cdot \frac{N_i^2}{N_o^2} \qquad 3.16$$

where S_o, N_o are the output signal and noise voltages and S_i and N_i are the corresponding input parameters.

Considering simple low pass RC filters with time constants T_i and T_o at the input and output respectively then the transfer functions are given by:

$$A_{i_o}^2(\omega) = \frac{1}{1 + \omega^2 T_{i_o}^2} \qquad 3.17$$

Thus, for white noise at the input:-

$$\frac{N_i^2}{N_o^2} = \frac{\int_o^\infty A_i^2(\omega)d\omega}{\int_o^\infty A_o^2(\omega)d\omega} = \frac{T_o}{T_i} \qquad 3.18$$

$$\frac{S_o^2}{S_i^2} = \frac{4}{\pi^2}\frac{S^2}{S^2} = \frac{4}{\pi^2} \qquad 3.19$$

from equation 3.15 with $\phi = 0^o$.

Thus

$$G = \frac{4}{\pi^2}\frac{T_o}{T_i} \qquad 3.20$$

Equation 3.20 is in good agreement with the expression

$$G' = \frac{1}{F_d} = \frac{2}{\pi^2}\frac{T_o}{T_i} \qquad 3.21$$

obtained by Aubrun and Veillet (13) in their analysis of a P.S.D. The difference of a factor of 2 is due to the fact that Aubrun and Veillet's treatment considers an output derived during only half a cycle of the reference voltage, i.e. for a time $\frac{1}{2f_m}$ in each cycle.

3.3 Further Improvement in Signal-to-Noise Ratio using Summation or Averaging Techniques

An E.S.R. spectrometer is particularly susceptible to low frequency noise. The main reasons are:

(a) f^{-1} noise from microwave detector crystal

(b) Power output fluctuations of klystron

(c) Gain variations of amplifier

(d) Microphonics which give rise to a variation in the balance of the microwave bridge

(e) "Pickup" - interaction between input and output other than through the spectrometer. Unfortunately the level of pickup does not remain constant but is dependent on the position of personnel in the vicinity of the spectrometer.

It has been pointed out that f^{-1} noise from the crystal can be reduced either by high frequency field modulation or superheterodyne detection but even after such precautions a large number of sources of low frequency remain.

The lowest frequency, f_L, which will prove significant is determined by the time, T_S, spent in sweeping through a spectrum. An approximate relationship is $f_L \sim \frac{1}{10T_S}$. The highest signal frequency, f_H, which will be passes is dependent on the output time constant T_o. The effective bandwidth, B_E, resulting from a low pass RC filter of time constant T_o is (4) :-

$$B_E = \frac{1}{4T_o}$$

In order to pass a signal without distortion of the line shape it is usual to use an effective bandwidth

$$B_E = \frac{5}{T_S} \rightarrow \frac{6}{T_S}$$

Thus $T_S \sim 20 \rightarrow 30\ T_o$.

In order to avoid low frequency noise the value of T_S can be reduced thus raising f_L. However this requires that T_o must be reduced if line shape distortion is to be avoided. Thus the value of B_E must be increased. The sensitivity of an E.S.R. spectrometer (Chapter 2.4.5) is given by Wilmshurst, Gambling and Ingram (14) as:-

$$\chi''_{min} = \frac{1}{\pi\eta Q_o}\left(\frac{FkTB_E}{P}\right)^{\frac{1}{2}} \qquad 3.21$$

Thus for a given spectrometer and sample:-

$$\chi''_{min} \propto (FB_E)^{\frac{1}{2}} \propto \left(\frac{F}{T_S}\right)^{\frac{1}{2}} \qquad 3.22$$

$$\text{Noise factor } F = \frac{\text{input S/N}}{\text{output S/N}} = \frac{S_i^2}{S_o^2} \cdot \frac{N_o^2}{N_i^2} \qquad 3.23$$

$$\text{Input noise power} = kTB_E R \propto N_i^2 \qquad 3.24$$

and $S_o = gS_i$ where g is the "gain" of the amplifier and detection system.

Thus

$$F = \frac{1}{g^2} \frac{N_o^2}{kTB_E R} = \frac{K^2 P_o}{B_E} \qquad 3.25$$

where K is a constant and P_o is the output noise power.

Thus

$$\chi''_{min} \propto P_o = \int_{f_L}^{f_L+B_E} w(f)df \qquad 3.26$$

where w(f) is the power density spectrum defined by:-

$$w(f) = \frac{dP}{df} \qquad 3.27$$

Consider n sweeps through a spectrum, each of duration T_S/n. This will result in n noisy traces of the signal.

From equation 3.26

$$\frac{\chi''_{min}(T_S/n)}{\chi''_{min}(T_S)} = \frac{\int_{nf_L}^{n(f_L+B_E)} w(f)df}{\int_{f_L}^{(f_L+B_E)} w(f)df} = \frac{S/N(T_S)}{S/N(T_S/n)} \qquad 3.28$$

where $S/N(T_S)$ and $S/N(T_S/n)$ are the voltage signal to noise ratios for sweeps of duration T_S and T_S/n respectively.

Equation 3.28 will be applied to two examples.

(i) White noise $\therefore$ w(f) = constant = w

$$\therefore \frac{S/N(T_S)}{S/N(T_S/n)} = n^{\frac{1}{2}} \qquad 3.29$$

(ii) $^1/f$ noise $\therefore$ w(f) = w/f

$$\therefore \frac{S/N(T_S)}{S/N(T_S/n)} = \frac{\left[\log f\right]_{nf_L}^{nf_L+nB_E}}{\left[\log f\right]_{f_L}^{f_L+B_E}}$$

$$= \frac{\log\frac{n(f_L+B_E)}{nf_L}}{\log\frac{f_L+B_E}{f_L}} = 1 \qquad 3.30$$

If now the n traces are placed in correct register and summed, the signal voltage, which is coherent, will add in direct proportion to n, whereas the noise voltage, being incoherent, will add in the proportion $n^{\frac{1}{2}}$. Thus:-

$$\frac{\text{S/N for 1 sweep of duration T}}{\text{S/N for n sweeps of duration T}} = \frac{1}{n^{\frac{1}{2}}} \qquad 3.31$$

R.R. Ernst (15) has shown that Equation 3.31 holds well for $f^{-\lambda}$ noise where $0 \leq \lambda \leq 1$.

Considering the case of white noise and f^{-1} noise respectively:-

(i) for white noise, combining Equations 3.29 and 3.31 gives:-

G = gain in signal to noise ratio for a given experimental time T_S

$$= \frac{\text{S/N for n sweeps of duration } T_S/n}{\text{S/N for 1 sweep of duration } T_S} = 1 \qquad 3.32$$

i.e. Equation 3.32 indicates that the "lost" signal to noise ratio has been regained.

(ii) for f^{-1} noise (using Equations 3.30 and 3.31)

$$G = n^{\frac{1}{2}} \qquad 3.33$$

i.e. Equation 3.33 indicates that there is an improvement in signal to noise ratio by summing.

In both Equations 3.32 and 3.33 the same total experimental time is utilized in performing the single sweep and n sweep experiments. The noise spectrum encountered from an E.S.R. spectrometer will be a mixture of "white" and $1/f$ noise and thus $1 \leq G \leq n^{\frac{1}{2}}$.

3.4 Summing and Averaging Techniques

The value of G will be the same whether n traces are added or averaged. The problem of placing the n scans of the complete signal into correct register and summing or averaging them can be tackled in many ways. The various methods can be broadly subdivided into two main categories:-

(1) Analogue techniques

(2) Digital techniques

3.4.1 Analogue techniques

The simplest method of utilizing the analogue technique, in principle, would be to register and sum (or average) graphically or numerically but, obviously, such a method would prove slow and tedious.

Automatic analogue systems have been constructed relying on one of the following cumulative memory techniques:-

(a) Photographic techniques (16,17).

(b) Recycled delay lines (18) - acoustic delay lines are usually employed.

(c) Magnetic or electrostatic drum or tape storage (20,21 and 22). Techniques (b) and (c) have been combined by Beurle (19).

(d) Electrostatic storage tubes (23,24,25,26).

(e) Condenser store - the most important device utilizing this technique is the Boxcar Integrator (6,27,28,29) and its use will be described in Chapter IV.

3.4.2 Digital techniques

The digital method of averaging relies on converting the analogue signal into digital form. This operation is carried out by using either an analogue-to-digital converter (A.D.C.) or by a comparison technique. A number of counts proportional to the analogue signal are stored in a digital memory store usually of the ferrite core variety. When the averaging or summation has been carried out for a sufficient number of scans the memory is "read" by reconverting the number of counts into an analogue signal.

The performance of a digital system far outpasses that of an analogue system in both stability and dynamic range. The dynamic range of a system is defined as the ratio of the maximum to minimum signal amplitudes which can be accurately stored in the system and is usually expressed in decibels. It is possible to obtain dynamic ranges in excess of 100dB for a digital system as compared with 40dB for a good analogue system.

3.5 The Computer of Average Transients

A device known as a digital memory oscilloscope, multichannel analyser, time averaging computer (TAC) or computer of average transients (hereinafter abbreviated to CAT) utilises digital techniques and can be used to sum or average n scans in correct register.

The principle of operation of the CAT can be explained by direct comparison with an oscilloscope. The CAT contains time base circuits; the X direction, however, is divided into N memory 'channels' of a finite

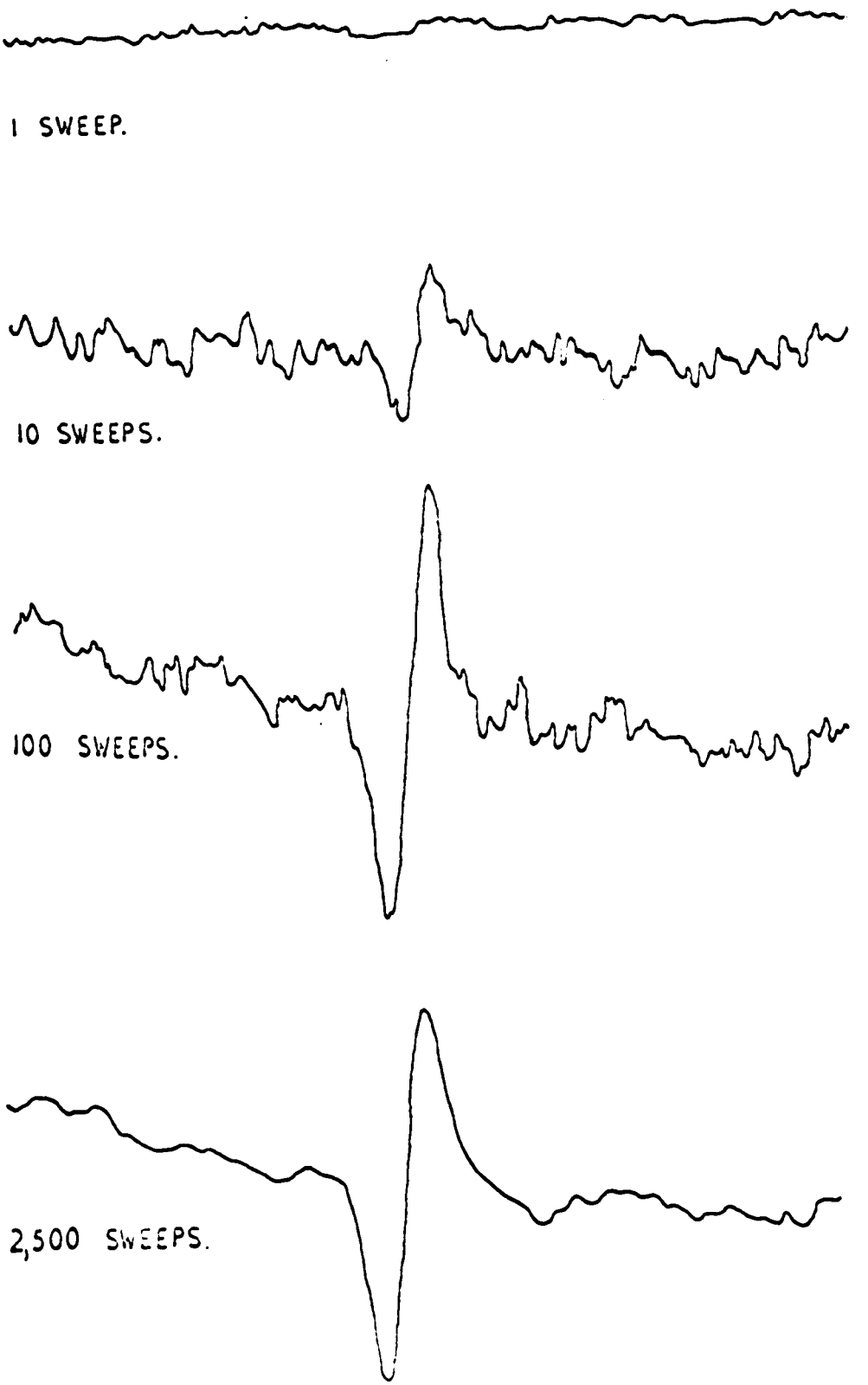

FIG. 3. 3. INCREASE IN SIGNAL-TO-NOISE RATIO WITH NUMBER OF SUPERPOSITIONS.

'width'. At the start of a timebase sweep, of total duration T_S, the first channel opens for a period T_S/N and any voltage at the Y input during this period is converted into digital form and stored in a part of the ferrite core memory set aside for that particular channel. At the end of the first period T_S/N, the first channel closes and the second channel opens for the same duration and a similar process occurs. This sequence is repeated until all N channels have opened and closed in succession. With the second and any subsequent sweeps the same successive opening and closing of the channels occurs. Any Y input present, when a given channel is open, is converted into digital form and combined in some way with the digital signal already stored in the part of the memory relevant to the particular channel. The method of combining an existing stored signal with an incoming signal varies with the type of CAT.

The "totalising" or summation type of CAT stores in each channel a number of counts proportional to the signal at the Y input when the relevant channel is open. When this channel next opens a number of counts, again proportional to the signal at that time, is added to the counts already stored in that channel. This process continues, the number of counts in each channel steadily increasing. Thus the stored amplitude in any one channel is a function of the number of sweeps as well as the actual signal amplitude. The conversion of analogue signal to digital data is carried out by an analogue to digital converter (A.D.C.); this device gives an output frequency which is linearly related to the amplitude of the input voltage. The A.D.C. must be capable of processing

FIG. 3.4.

ENHANCEMENT OF A STATIC SPECTRUM (g = 2) WITH A WAVEFORM COMPARISON CAT

(i) Single sweep

(ii) Four sweeps

(iii) Sixteen sweeps

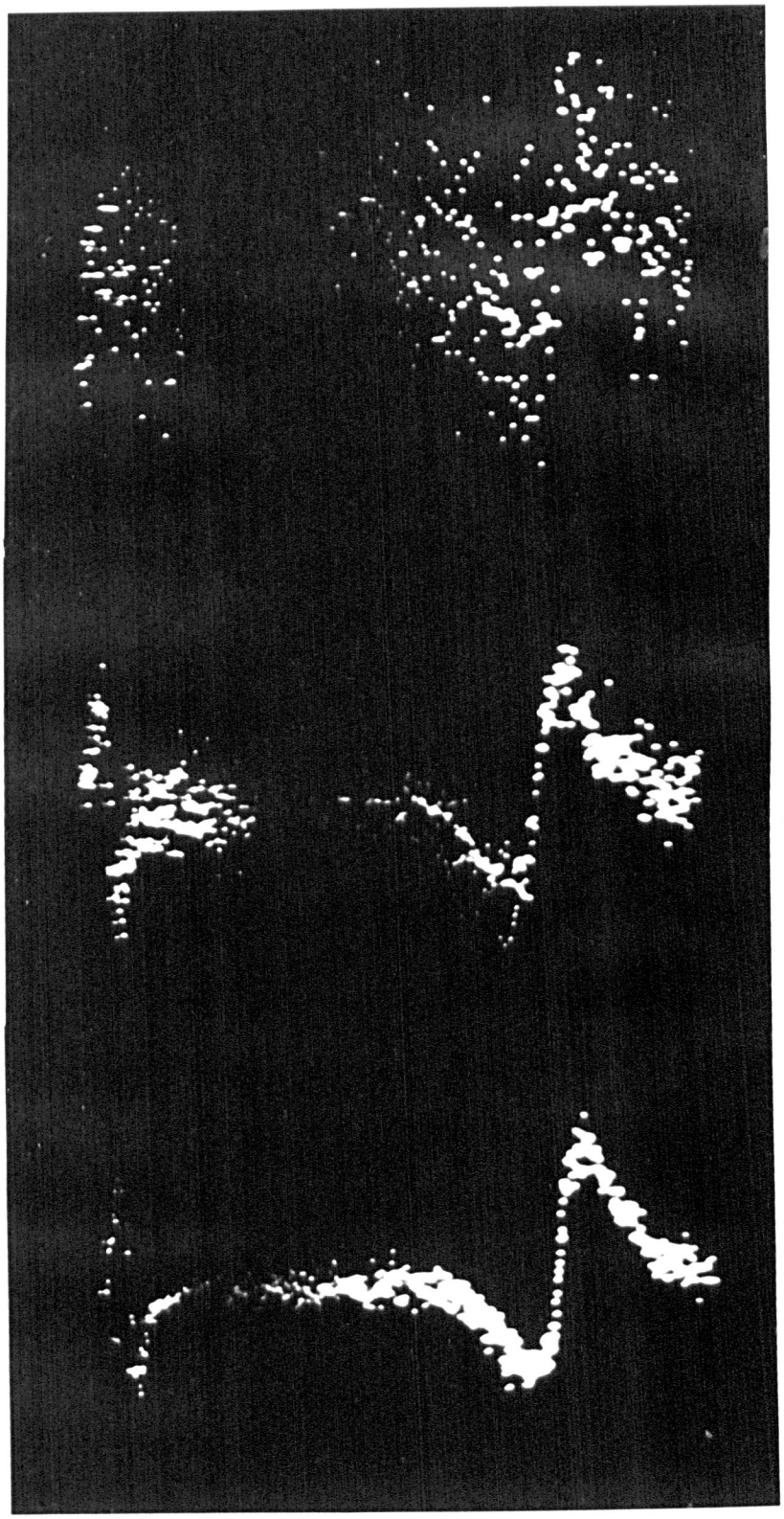
(i)
(ii)
(iii)

both negative and positive voltages and, therefore, it operates about a centre frequency, corresponding to zero volts, which increases for a positive input and decreases for a negative voltage. Thus even for zero input a number of counts, corresponding to the centre frequency, will be given out by the A.D.C. and thus the "totalising" CAT is subect to a "rising baseline".

The "waveform comparison" or averaging CAT makes comparisons, at the rate of C/sec, between the signal already stored in a given channel and the signal being presented to it each time the channel is opened. The signal stored is only modified by increasing or decreasing it by one count depending on whether W successive comparisons have all been greater or smaller than the signal already stored. The value of W, known as the "weighting factor" can be selected by the operator. As W is increased, so the probability of random noise altering the stored signal is reduced; it will be shown in Chapter IV that W can be usefully compared to a time constant in an analogue system. When all the channels in the waveform comparison type of CAT have been opened a reasonable number of times, the number of stored counts is a function of the average value of the signal only and not the number of scans. Thus there is no dependence of signal height stored in a given channel on the number of times the channel has been opened and this will form an important consideration in the use of a CAT for rapid recording studies.

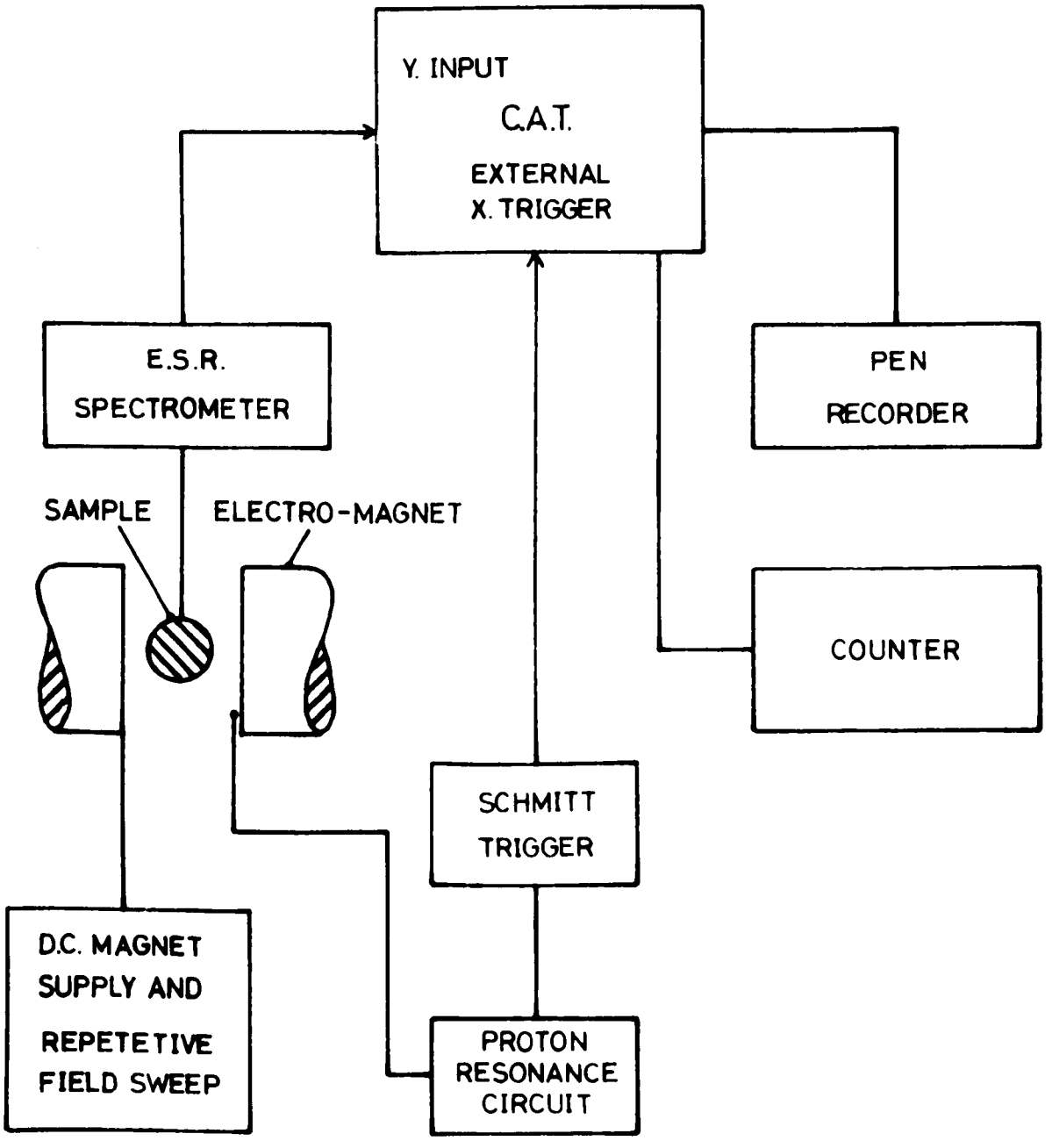

FIG.3.5. BLOCK DIAGRAM OF EXPERIMENTAL ENHANCEMENT SYSTEM USING A C.A.T.

3.6 Enhancement of Static Signals

When employing a CAT to enhance a static E.S.R. spectrum the different channels and memory circuits of the CAT are correlated with successive field sweep increments of the external magnetic field. The applied magnetic field is therefore made to sweep repetitively through the E.S.R. spectrum and the resulting absorption signal of the spectrum is fed, together with its associated noise to the different channels of the CAT; each channel storing the signal corresponding to a given small field increment. After n sweeps through the E.S.R. spectrum the signal to noise improvement will be $\frac{n}{\sqrt{n}} = \sqrt{n}$ as shown by R.R. Ernst (15) and expressed in Equation 3.31. A variety of workers have used this technique to enhance the signal-to-noise ratios of an electron spin resonance spectrometer (29,30,31) and in similar systems by other authors (32).

Examples of enhanced spectra of two different free radicals (g=2) obtained from a totalising CAT and a waveform comparison CAT are shown in Figs. 3.3 and 3.4 respectively, and a block diagram of the experimental set up used to record the spectra is shown in Fig. 3.5; the counter being used to display the number of field sweeps accomplished during an experiment.

REFERENCES

1. Nyquist, H., Phys. Rev. 32, 110 (1928).

2. Johnson, J.B., Phys. Rev. 32, 97 (1928).

3. Townes, C.H. and Schawlow, A.L., "Microwave Spectroscopy" (McGraw-Hill 1955).

4. Robinson, F.N.H., "Noise in Electrical Circuits" (Oxford University Press 1962).

5. Van der Ziel, A., "Noise" (Chapman and Hall, London 1955).

6. Schwartz, M., "Information Transmission, Modulation and Noise" (McGraw-Hill 1959).

7. Dicke, R.H., Rev. Sci. Inst. 17, 268 (1946).

8. Holland, L.R., Rev. Sci. Inst. 37, 1202 (1966).

9. Schafer, C.R., Electronics 27, 189 (1954).

10. Moore, R.D., Electronics 35, 40 (1962).

11. Williams, P., J. Sci. Inst. 42, 474 (1965).

12. Faulkner, E.A. and Harding, D.W., J. Sci. Inst. 43, 97 (1966).

13. Aubrun, J.N, and Veillet, P., C.R. Acad. Sci. (Paris) 256, 1696 (1963).

14. Wilmshurst, T.H., Gambling, W.A. and Ingram, D.J.E., J. Electron. Control 13, 339 (1962).

15. Ernst, R.R., Rev. Sci. Inst. 36, 1689 (1965).

16. Block, F. and Garber, D.H., Phys. Rev. 76, 585 (1949).

17. Ross, I.M. and Johnson, F.B.,Nature 167, 286 (1951).

18. An Wang, and Way Dang Woo, J. App. Phys. 21, 49 (1950).

19. Beurle, J., Communication Theory p.231, (Edited Jackson, London(1953)).

20. Suryan, G., Phys. Rev. 80, 119 (1950).

21. Paul, R.J., M.Sc. Thesis, University of Birmingham (1962).

22. Morleigh, S., J. Brit. I.R.E. 21, 211 (1961).

23. Harrington, J.V., J. App. Phys. 21, 1048 (1950).

24. Jensen, A.S., R.C.A. Review 16, 197 (1955).

25. Gibbons, D.J., Elect. Eng. 33, 630 (1961).

26. Paul, R.J., British Communications and Electronics 11, 28 (1962).

27. Blume, R.J., Rev. Sci. Inst. 32, 1016 (1961).

28. Holcomb, D.F. and Norberg, R.E., Phys. Rev. 98, 1074 (1955).

29. Parker, A.J., Ph.D. Thesis, University of Birmingham (1965).

30. Allen, L.C. and Johnson, Le R.F., J. Am. Chem. Soc. 85, 2668 (1963).

31. Klein, M.P. and Barton, G.W., Rev. Sci. Inst. 34, 754 (1964).

32. Jardetzkey, O. and Wade, N.G. and Fischer, J.J., Nature 197, 183 (1963).

33. Ryan, D.P., Rev. Sci. Inst. 37, 486 (1966).

CHAPTER IV

METHODS OF RECORDING TRANSIENT E.S.R. SPECTRA

4.1 Introduction

The majority of E.S.R. studies are carried out on stable or quasistable paramagnetic species. Most initial attempts at recording transient paramagnetic species tended to rely on essentially stopping the rapid decay by freezing the specimen in a chemically inert host and examining the substance using a conventional steady state spectrometer. Besides the obvious complications inherent in such a system there is the added disadvantage that complex physical interactions may occur between the host and specimen.

4.2 Flow Systems

A conventional spectrometer can also be used to study gaseous or liquid short lived species, particularly when the transient species are the result of an admixture of two stable reagents, i.e. a reaction of the type: $A + B \rightarrow C \rightarrow D$ where A, B and D are non paramagnetic reagents, C is the short lived paramagnetic product of the reaction of A with B and D is the non paramagnetic product to which C eventually decays.

A and B are mixed by passing them through jets into a mixing chamber where the reaction is initiated. The reaction continues while passing down an outlet tube and thus the state of decay of C is dependent on the reagent flow rates and their position along the tube. Therefore an examination of C at various stages of its decay can be carried out using

a conventional spectrometer by varying either the reagent flow rate and/or the position along the tube at which any measurement is made. This technique is particularly useful when applied to non reversible reactions.

Both "freezing" and "flow" methods have limitations; the first in the lack of precise kinetic data it can reveal, the second in the fact that observations must occur over a finite volume of sample. In a flow system uniform mixing is difficult to achieve and large quantities of reagent are required to obtain a result.

4.3 Peak Observation

Many attempts at a direct observation of the kinetics of a decay have relied on setting the magnetic field on a value corresponding to a peak of the E.S.R. spectrum. The decay of the species can then be observed directly as a change in the output of the spectrometer. Fessenden (1) utilised this method along with more sophisticated techniques mentioned below for increasing the signal-to-noise ratio of the system. With a peak observation method it is impractical to detect changes in lineshape.

A spectrometer used for peak observation must be extremely stable; and the response time, T_R, very short in order that the spectrometer can follow rapid decays. The need for a short response time means that a conventional spectrometer is no longer suitable. Unfortunately a reduction in response time implies an increase in the effective bandwidth of the spectrometer, B_E, as mentioned in Chapter III. The minimum detectable value of the imaginery component of the complex susceptibility χ''_{min} is

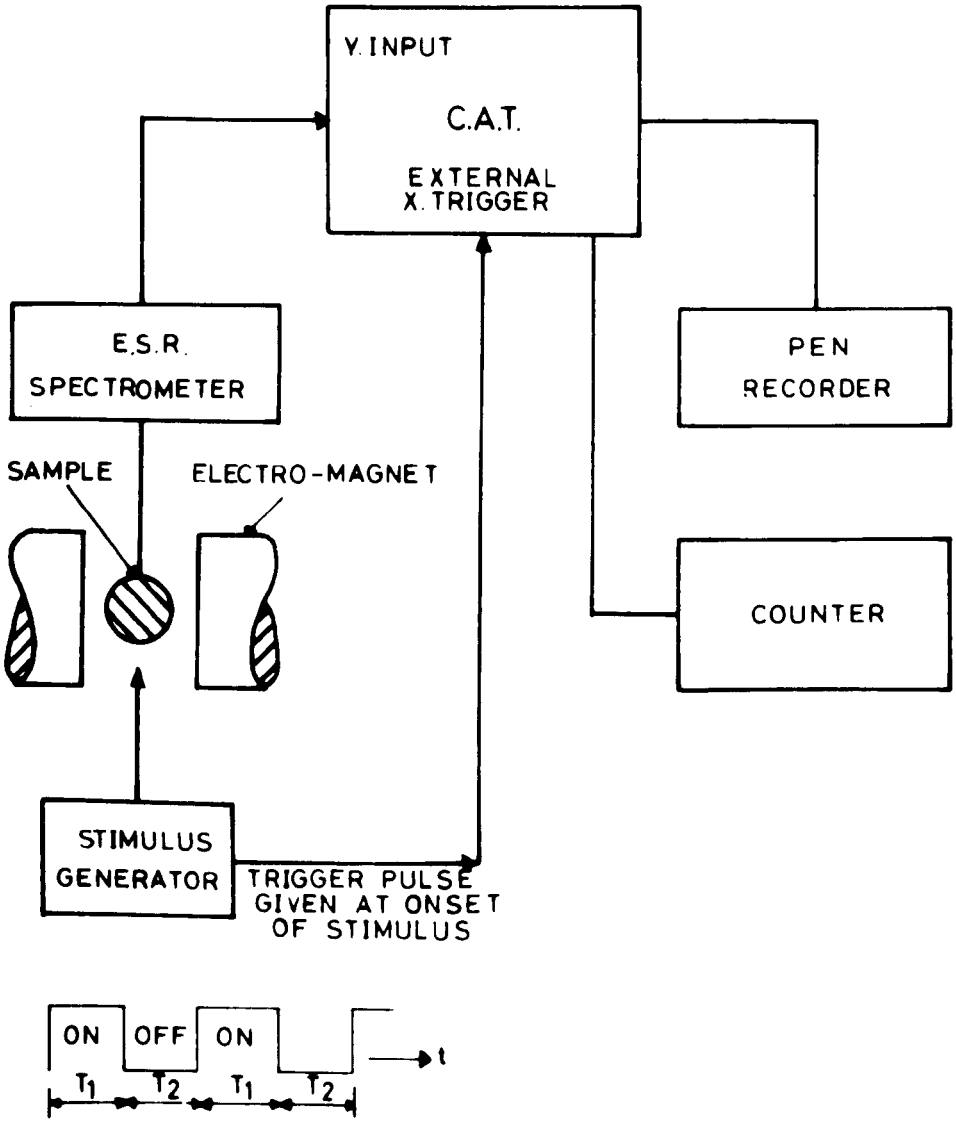

FIG. 4. 1.

BLOCK DIAGRAM OF EXPERIMENTAL PEAK OBSERVATION SUPERPOSITION SYSTEM USING C.A.T.

proportional to $(B_L)^{\frac{1}{2}}$. Thus a reduction in response time will result in a loss of sensitivity. For example: a decrease in response time from 1 second to 1 msec. will result in a decrease in sensitivity by a factor of $(1000)^{\frac{1}{2}} \approx 30$.

It is essential that the lost sensitivity is, at least, regained and preferably enhanced.

A rapid recording spectrometer is, in general, required to deal with lower signal levels than those encountered in steady state analysis; once the decay process has been initiated, the spectrometer output will decrease during the decay with a consequent reduction in signal-to-noise ratio.

4.4 Use of CAT in a Peak Observation Superposition System

The digital averaging device (CAT) previously mentioned would seem to present an ideal solution to the problem. The lost sensitivity resulting from the necessary increase in spectrometer bandwidth, could be regained by repetitively stimulating a suitable sample into its transient paramagnetic state and correlating each channel with a particular time during the sample's decay. In effect several decay curves of the peak amplitude are superimposed. This type of system is referred to as a superposition system (2,3) and a schematic diagram of a hypothetical system is shown in Fig. 4.1. Referring to Fig. 4.1, $T_1 >> T_F$ (the formation time of the species); $T_2 >> T_L$ (the decay time or lifetime of the species). Such a system, in common with all later systems described in this thesis, is limited to use with samples which undergo reversible reactions during

their decay, i.e. samples which can be made to generate the transient paramagnetic species by the application of a suitable stimulus. The range of sample lifetimes are severely limited in such a system mainly by the computer's maximum usable sweep speed; this maximum speed is governed by the rate at which each channel of the CAT can accept information.

A great advantage of the peak observation (P.O.) superposition system is that there is little wastage of information, the information from the whole of the decay being utilised. Nevertheless the minimum lifetimes which can be reasonably accurately recorded with such a system is in the region of 100 msecs although one of the latest CATs (4) is capable of reducing this figure to ~15msecs.

4.5 Use of the Superposition Technique to Record Whole Spectra

The work described in this thesis is concerned with the development of apparatus to enable a CAT to be used in conjunction with an E.S.R. spectrometer to record the whole of a transient spectrum at various times during its decay.

One of the first systems considered was a superposition technique whereby the magnetic field is swept through the whole spectrum in a time much shorter than the sample's lifetime. The decay occurring during this rapid sweep can thus be neglected. The time at which the field sweep commenced, after the cessation of each stimulus, is adjusted so that the appearance of the signal at various times during its decay may be examined. Several scans, at one particular delay time, T_D, are superimposed by the CAT thus enhancing the signal-to-noise ratio.

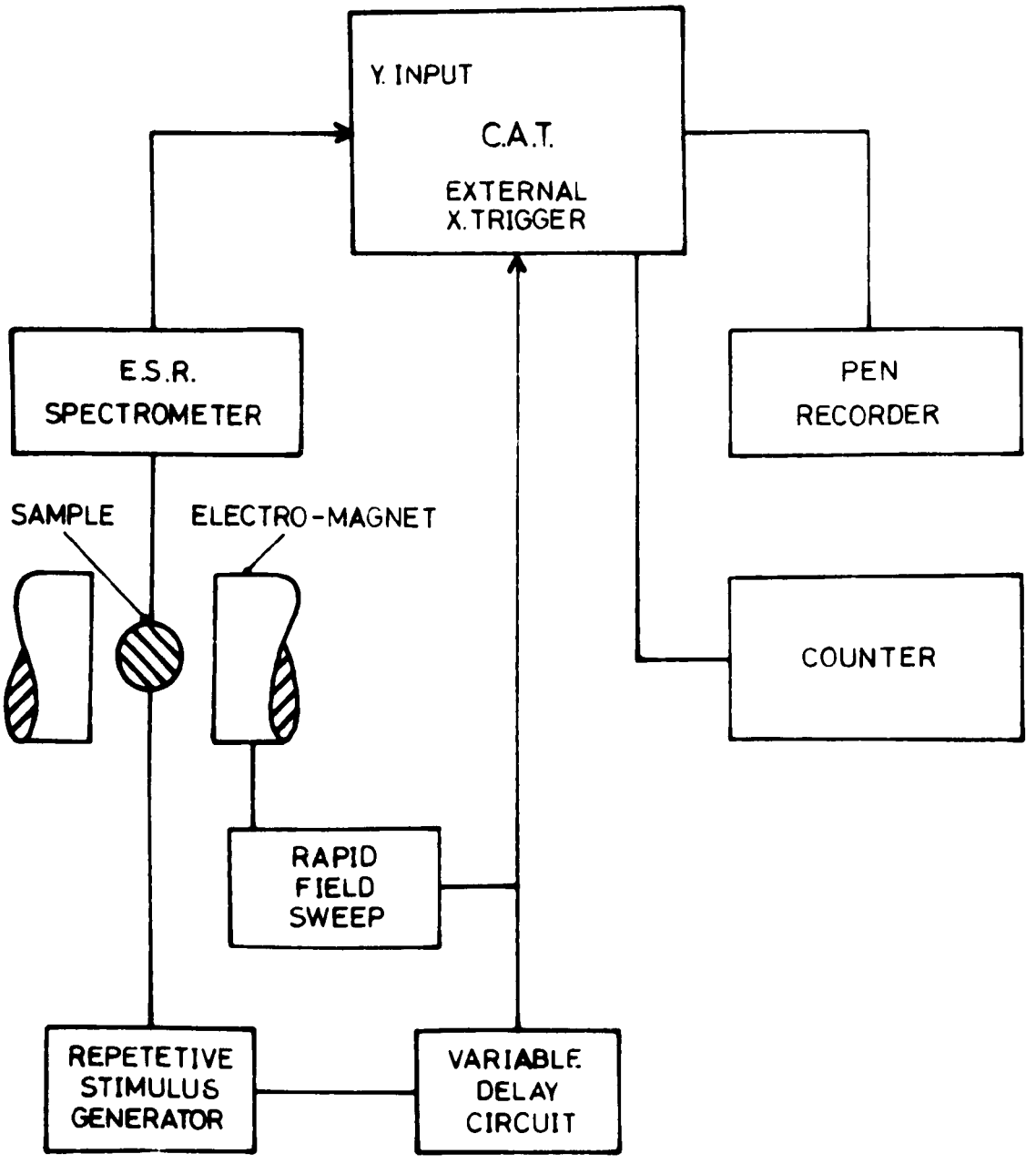

FIG. 4. 2. HYPOTHETICAL SUPERPOSITION SYSTEM TO RECORD COMPLETE TRANSIENT E.S.R. SPECTRUM

A hypothetical circuit for a superposition system is illustrated in Fig. 4.2 by way of explanation.

Unfortunately there are many interdependent limitations of such a system:-

(1) The field sweep through the spectrum must be accomplished in a time $T_S < \frac{T_L}{100}$ (T_L, the lifetime of the sample, is defined as the time required for the paramagnetic concentration to fall to $^1/e$ of its in initial value).

It is impossible to sweep a large magnet at a sufficiently high rate with any degree of accuracy for all but the longest lifetimes.

(2) Even if a sufficiently fast field sweep could be accomplished, the shortest usable sweep time in a CAT would impose the next limitation.

(3) The response time, T_R, of the spectrometer must be further decreased from the values required for a peak observation spectrometer in order that distortionless reproduction of the E.S.R. lineshape is allowed.

A rapid recording superposition spectrometer would be limited to minimum sample lifetimes of seconds and considerable signal-to-noise ratio enhancement would be required to order to regain the lost sensitivity.

4.6 Use of Sampling and Averaging Techniques

In order to render the examination of short lived transient free radicals, in fairly low concentrations, feasible using presently available techniques, it is essential that observation be possible using conventional field sweep speeds. The idea of recording the whole spectrum during each

decay process must be discarded. A sampling technique must be utilised in conjunction with an averaging device.

The development of the techniques used for sampled data systems will be described from their initial use in general peak observation systems through to their specialised use in an E.S.R. peak observation spectrometer. The extension of these principles to an E.S.R. spectrometer capable of recording a complete transient spectrum will then be discussed.

The reasons for using sampling and averaging techniques are discussed below.

It has already been established that the response time of the spectrometer must be reduced to a sufficiently low value to enable the decay of the peak of a transient signal to be followed and this requirement is a necessity because the decay time of the species is an intrinsic property of the sample. However the further reduction in the response time, necessary in order that the whole signal is displayed, is a function of the sweep-rate through the signal. If the whole signal is to be displayed during a time small compared with the decay time of the sample then the sweep time, T_S, << decay time of the sample, T_L, resulting in a further decrease in response time so that $T_R << T_S$. However, if T_S is increased until $T_S >> T_L$ the response time required will be approximately that required to follow the decay time because in time T_L, the field sweep only moves through an exceedingly small region of the spectrum with the result that any change in spectrometer output is virtually due to the decay of the sample alone. Under these conditions, however, only a small

part of the decay information is relevant, i.e. the spectrum as it appears at a given time, T_D, after the onset of its decay is required and the relevant information is "picked out" using sampling techniques, the slow field sweep gradually covering the whole region of the spectrum.

Sampling techniques can be conveniently combined with averaging techniques in order to regain the initial lost sensitivity entailed by the original reduction in T_R. The use of sampling enables the whole of a transient spectrum to be recorded and can be considered as increasing the "effective bandwidth" of the recording apparatus.

4.7 Disadvantages of Sampling and Averaging Systems

The use of sampling techniques results in a large wastage of information because, as the name suggests, only certain selected pieces of information are used, the remainder of the information being rejected. As a result the required information will take a long time to accumulate. The wastage of information can be overcome by duplication of sampling and averaging apparatus, but this would prove costly and complicated.

The use of averaging techniques also restricts the type of sample which can be examined to those which undergo a reversible reaction in the production of the transient species, i.e. reactions of the type:

$$X \underset{}{\overset{\text{STIMULUS}}{\rightleftharpoons}} Y$$

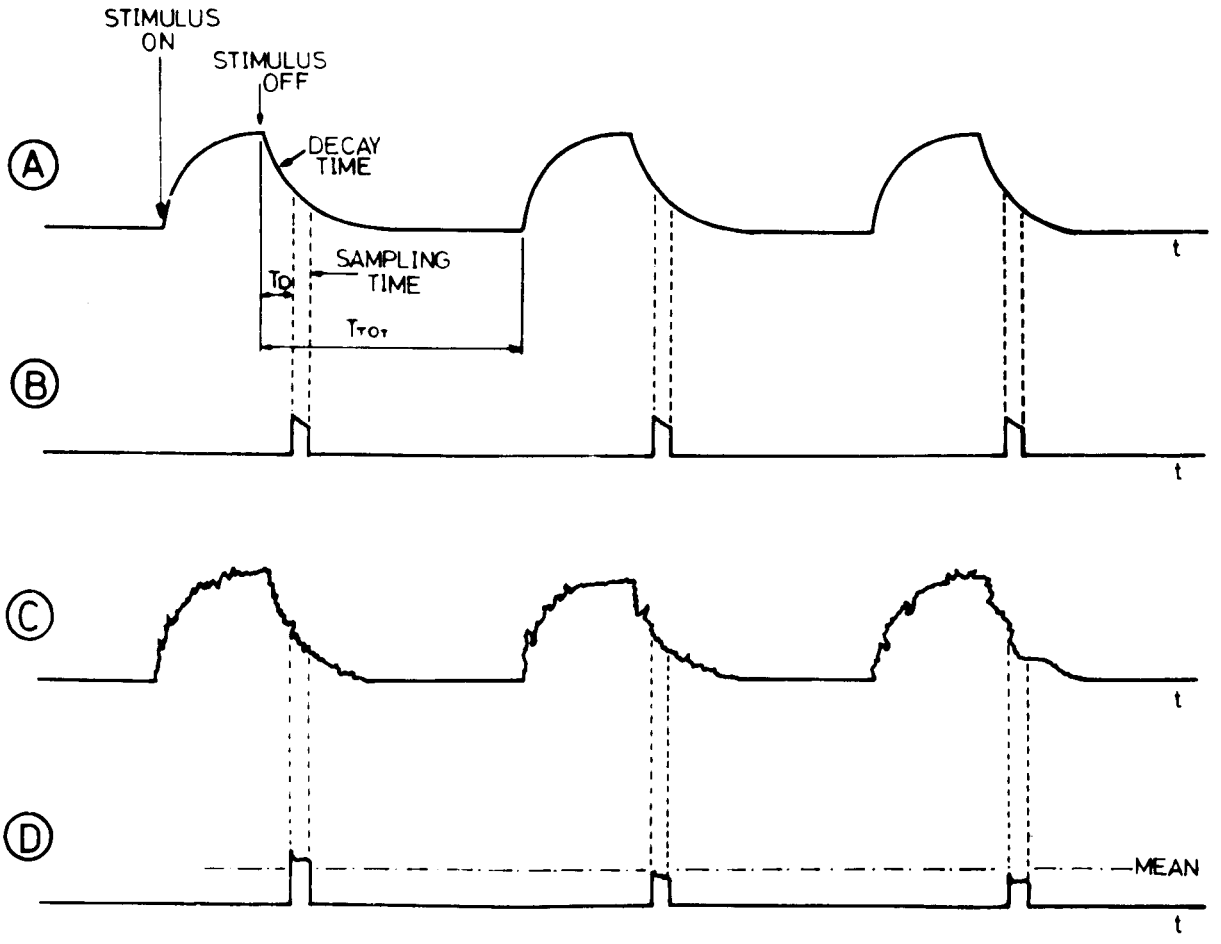

FIG. 4.3. ILLUSTRATION OF PRINCIPLES OF SAMPLING AND AVERAGING

(A) Repetitive formation and decay signal without noise

(B) Sampled portions taken at same point on each decay curve

(C) "Noisy" version of (A)

(D) Resulting "noisy" samplings

4.8 Principle of Sampling and Averaging

The principle of sampling is illustrated in Fig. 4.3. Diagrams A and B show the repetitive sampling of a noiseless signal; C and D extend the idea to sampling and averaging of a repetitive noisy signal.

The signal is produced repetitively by stimulating at regular intervals. After a certain time, T_D, has elapsed following the removal of the stimulus, a gate, which is placed between the signal output and the recording apparatus, is opened for a short time in order to allow the signal to pass.

If the samples are applied to an averaging system the result will be the mean value of the samples. For n samples there will be an improvement in the signal-to-noise ratio of $n^{\frac{1}{2}}$ over the signal-to-noise ratio for one sample.

If now the time, T_D, by which the sampling pulse is delayed from the time of cessation of the stimulus, is slowly swept from $T_D = 0$ to $T_{TOT} > T_L$, then the whole of the decay curve will be presented at the output of the averaging device. For a given stimulus repetition rate $\frac{1}{T_R}$ (where T_R is the time between successive stimuli) and a given time, T_S, to sweep T_D from zero to T_{TOT}, then the total number of samples, $n = \frac{T_S}{T_R}$.
If each sampling pulse is of duration ξ then the effective sweep time, T_E, spent covering the signal is given by:-

$$T_E = n\xi = \frac{T_S}{T_R}\,\xi \qquad 4.1$$

The averaging of the samples is usually carried out by an RC filter of time constant T_o. T_o must be sufficiently small compared with T_E so that

the decay curve is produced without distortion. However, T_o must be large enough to average out the noise. Thus the amount of noise governs, to a large extent, the total sweep time, T_{TOT}, for a given experiment.

The sampling technique permits a fast repetitive signal occurring in a time T_L to be displayed in a time T_S. This technique is used, with or without averaging, in devices known as sampling oscilloscopes (6,7,8) which permit fast repetitive waveforms to be displayed on a slow timebase oscilloscope or on a pen recorder.

Sampling and averaging are essentially techniques which exchange bandwidth for time without losing waveform fidelity; they have been used in peak observation systems by many workers. Robinson and Yogi (9) utilised digital averaging techniques, similar to those described for steady state enhancement, to average the sampled output from a 1 μsec risetime infra red detector.

Fessenden (1) observed the formation and decay of the peak of the E.S.R. signal from ethyl radicals produced in liquid ethane by radiolysis with 2.8MeV electrons. The P.O. spectrometer used by Fessenden employed sampling and analogue averaging.

4.9 Sampling and Averaging Used to Display Entire Spectrum

Parker (2,3) and Bennett (19) extended the ideas of sampling and analogue averaging to spectrometers capable of recording a complete transient E.S.R. spectrum, and not just the peak, at a particular value of T_D. The systems differ from a P.O. spectrometer in that T_D is not changed during a particular experiment whereas the magnetic field is slowly swept through

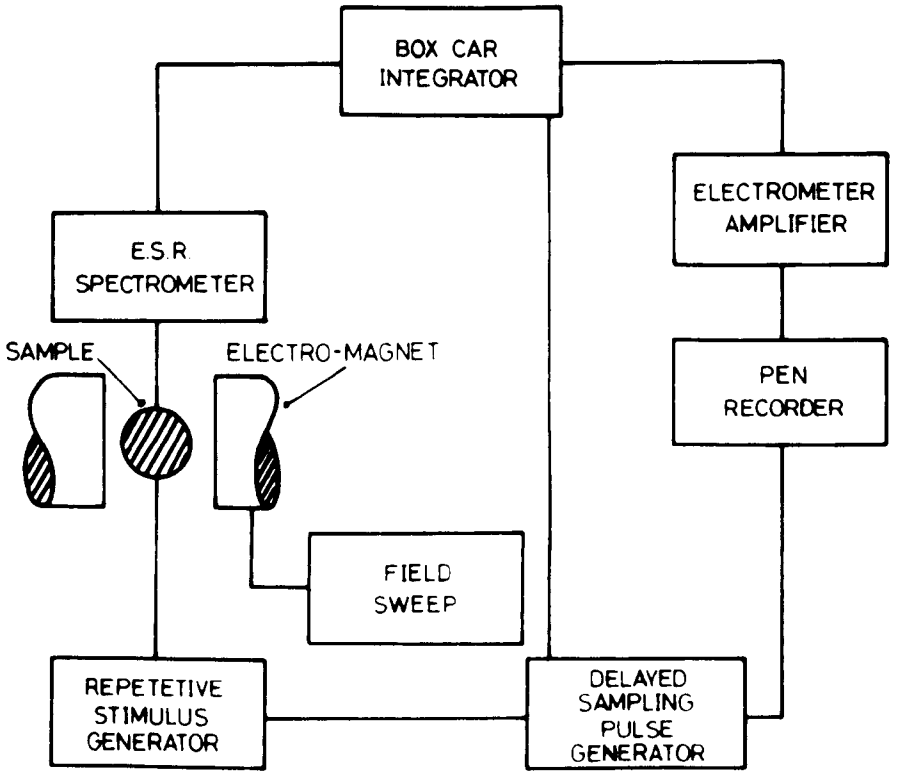

FIG. 4. 4. BLOCK DIAGRAM OF SAMPLING AND ANALOGUE AVERAGING SYSTEM FOR RECORDING THE COMPLETE SPECTRUM OF A TRANSIENT PARAMAGNETIC SPECIMEN

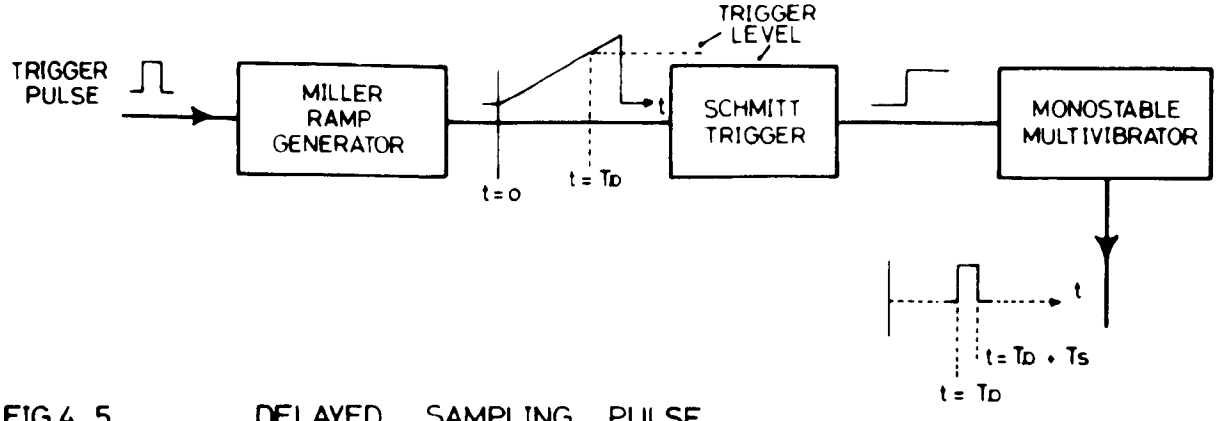

FIG. 4. 5. DELAYED SAMPLING PULSE GENERATOR USED WITH ANALOGUE AVERAGING DEVICE.

the region in which the spectrum occurs. This is the reverse of a P.O. spectrometer in which the magnetic field is maintained constant and the value of T_D is swept slowly. The same conditions regarding the choice of T_o, T_S, and ξ apply to the complete spectrum (C.S.) spectrometer as to the P.O. spectrometer. Thus instead of obtaining all the kinetic information of one element of the spectrum during a particular experiment one obtains a recording of the complete spectrum at a time T_D during its decay.

In both the P.O. and C.S. spectrometers $\xi << T_L$ to obtain a good time resolution of the decay.

Information on the kinetics of the whole spectrum can be obtained by performing experiments for various values of T_D.

4.10 Description of a Complete Spectrum Spectrometer using Analogue Averaging

A schematic diagram of a C.S. spectrometer as used by Parker and the author to observe the decay of oxygen atoms is shown in Fig. 4.4.

4.10.1 Sample and stimulus

The sample consisted of oxygen gas which was dissociated into atomic oxygen by a 13 Mc/s r.f. discharge. The r.f. constituted the stimulus; upon its removal the oxygen atoms recombined into their molecular state.

4.10.2 Repetitive stimulus generator

The r.f. oscillator is gated using a relay multivibrator; the discharge being successively applied for one second and then removed for one second to allow adequate times for formation and decay, respectively,

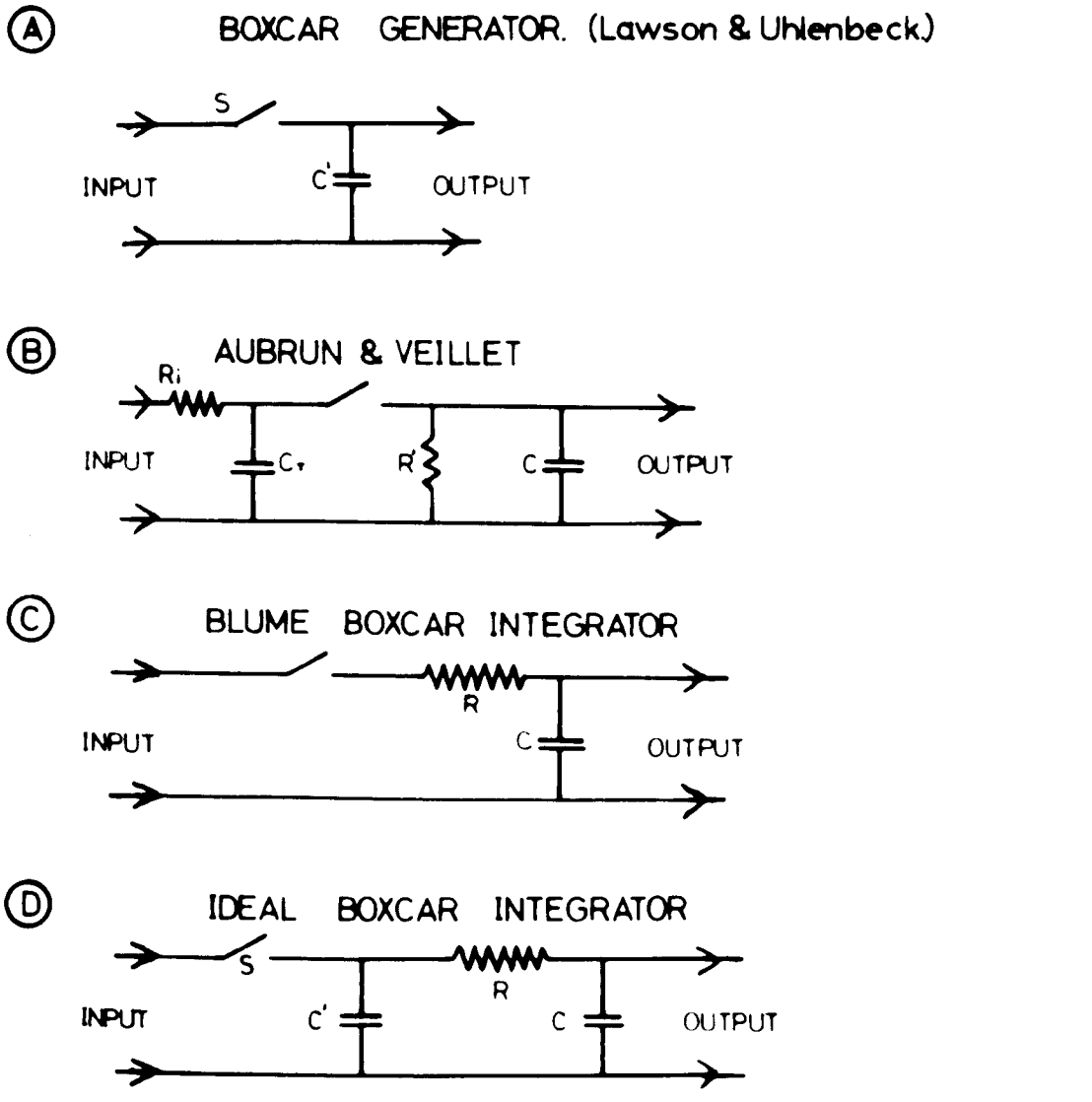

FIG. 4. 6. BOXCAR CIRCUITS.

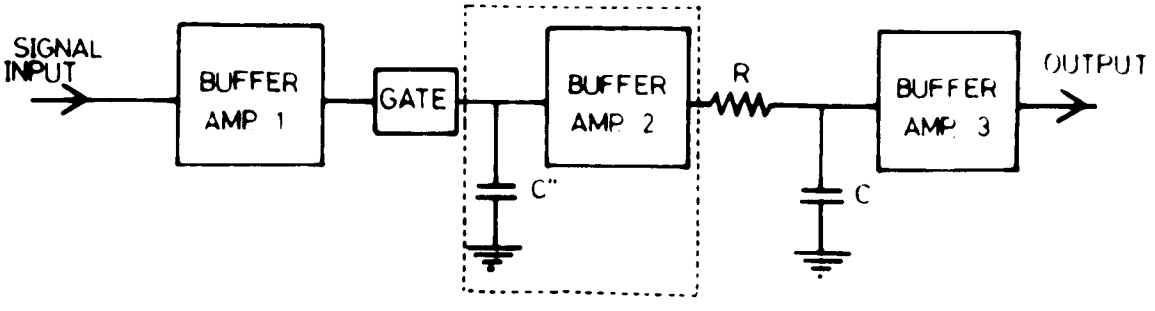

FIG. 4. 8. PRACTICAL CIRCUIT OF IDEAL BOXCAR INTEGRATOR.

of the oxygen atoms. Another set of relay contacts is used to generate a trigger pulse at the cessation of the stimulus.

4.10.3 Delayed sampling pulse generator

The pulse given at the cessation of the stimulus triggers a Miller ramp generator, the output of which is fed to a Schmitt trigger circuit. Thus by varying the slope of the ramp and the trigger level of the Schmitt circuit it is possible to vary the delay between the input pulse and the time at which the Schmitt trigger changes its state. The change of state in the Schmitt circuit triggers a monostable multivibrator to provide a sampling pulse of a standard 50 μsec width which renders it suitable for sample lifetimes down to 5 msecs. The sampling pulse is used to open the gate between the E.S.R. spectrometer output and the averaging circuitry.

A block diagram of the delayed sampling pulse generator described above is shown in Fig. 4.5.; a delay stability of ±1% has been quoted for this circuit (2).

4.10.4 Averaging circuitry

Both the sampling and averaging were carried out by a device known as the Boxcar Integrator. In order to indicate the improvement in signal-to-noise ratio obtained by sampling and averaging an analysis of the various versions of the Boxcar Integrator will be carried out. Finally an improved version of the Blume Boxcar utilised by Parker will be described.

Fig. 4.6 indicates schematically the various types of Boxcar integrator in ascending order of merit. S is an electronic gate which only

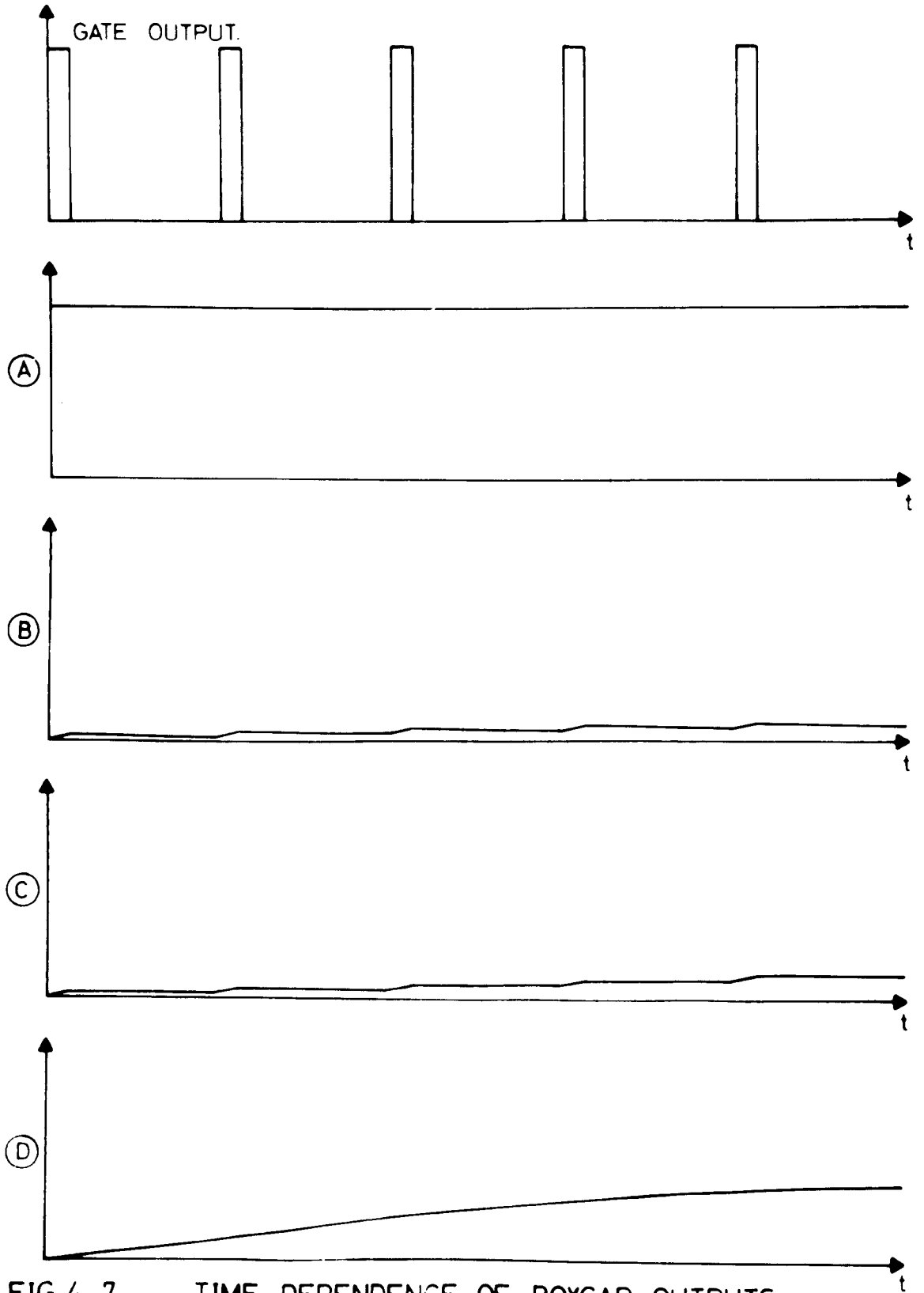

FIG.4. 7. TIME DEPENDENCE OF BOXCAR OUTPUTS FOR DEVICES SHOWN IN FIG.4. 6.

allows signal passage when a sampling pulse is applied. The output of the devices, as a function of time, is indicated in Fig. 4.7. for a constant input voltage.

(A) Boxcar Generator

The Boxcar generator, as described by Lawson and Uhlenbeck (10) is a sampling circuit only. C' forms a "hold" capacitor which clamps the output voltage between the sampling periods. The gate is assumed to be fed from a zero impedance source. The output for a varying signal input will be in the form of a step curve with flat tops. It is by virtue of its output that the boxcar is so named. The output is assumed to feed into an infinite impedance device. Practical devices approach the ideal input and output conditions as closely as possible.

(B) Aubrun and Veillet Integrator

Aubrun and Veillet (11) have made an analysis of the change between input and output signal-to-noise ratio for a system with periodically varying gain. The specialised case of sampling and averaging for such a system is considered. The system is assumed to have zero gain excepting the period when the sampling pulse is present. For the duration of the sampling pulse it will be assumed that the device has a gain of unity and its operation can be understood by referring to Fig. 4.6B.

Aubrun and Veillet found that subject to certain conditions, namely:-

(i) $R_iC_i \ll T_R \ll RC\ (= T_o)$ where T_R is the repetition period of the sampling pulse; R_iC_i and RC are the input and output time constants respectively.

(ii) The sampling pulse width $\xi \ll T_R$; then the improvement in signal-to-noise power ratio

$$G = \frac{\text{S/N power ratio at output}}{\text{S/N power ratio at input}} = \frac{2T_o}{T_R} \qquad 4.2$$

Aubrun and Veillet (12,13) have verified their theory experimentally by obtaining an enhancement for the nuclear resonance of Fe^{57}.

(C) Blume Circuit

A major disadvantage of Aubrun and Veillet's circuit is that the magnitude of the output signal is dependent on the sampling repetition rate T_R. This disadvantage is overcome in Blume's boxcar circuit (14). Both the Blume circuit and the Ideal Boxcar, discussed below, can be considered as sophisticated versions of the boxcar generator.

Lawson and Uhlenbeck (10) have shown that the spectral power density of the noise at the output $W_o(f)$ is related to that at the input $W_i(f)$ by the expression

$$W_o(f) = \frac{2 \sin^2\phi}{\phi^2} T_R \overline{\{(V - V_S)^2\}} \qquad 4.3$$

where $\phi = \pi f T_R$ with f being the signal frequency and T_R the sampling repetition period. V_S and V are the signal voltage and signal and noise voltages respectively.

The term $\frac{\sin^2\phi}{\phi^2}$ represents the noise introduced by switching.

The output is obtained by sampling signal and noise at the input and thus:

$$\sigma_o^2 = \text{variance of noise at O/P}$$

$$= \sigma_i^2 = \text{variance of noise at I/P} = \overline{(V - V_S)^2} \qquad 4.4$$

$$\text{Now } \sigma_i^2 = W_i(f)B \qquad 4.5$$

where B is the bandwidth of the input circuitry.

Thus

$$W_o(f) = \frac{2\sin^2\phi}{\phi^2} T_R W_i(f) B \qquad 4.6$$

It is reasonable to assume that the highest frequency component passed by the system, $f_{max} << \frac{1}{T_R}$ because $f_{max} \sim \frac{1}{4T_o}$ and $T_o >> T_R$; assuming the same conditions apply to the Blume circuit as those of Aubrun and Veillet's circuit. Thus $\phi << \pi$ and $\frac{\sin\phi}{\phi}$ in this region of interest of f will be unity.

Thus

$$W_o(f)_{f_{max}} = 2 T_R W_i(f)B \qquad 4.7$$

$\therefore$ Noise power at the output $= w_o(f)_{f_{max}} f_{max}$

$$= 2 T_R B f_{max} W_i(f) \qquad 4.8$$

Thus for a given system the gain in signal to noise power ratio

$$G = \frac{V_S^2}{W_i(f)B2T_R f_{max}} \Bigg| \frac{V_S^2}{W_i(f)B} = \frac{1}{2T_R f_{max}} \qquad 4.9$$

Now $f_{max} \sim \frac{1}{4T_o}$ (3,15) and thus Equation 4.9 becomes:-

$$G = \frac{2T_o}{T_R} \qquad 4.10$$

which is in exact agreement with the expression obtained by Aubrun and Veillet (11) for their sampling circuit. Thus the enhancement obtained by the Blume circuit is no improvement on the Aubrun and Veillet system. However, the condition that $T_R << T_o$ is no longer necessary and the output,

subject to certain conditions, is independent of T_R. The averaging and "holding" properties of the Blume circuit have been used by a variety of workers in the measurement of spin lattice relaxation times in N.M.R. (16). An integrator with similar properties to the Blume circuit, using analogue computing techniques, has been described by Reichert and Townsend (17). A digital version of the Blume boxcar integrator is used by Ware and Mansfield (18) for N.M.R. studies. Parker (2) has described an effective time-constant,

$$T_A = \frac{T_o T_R}{\xi} \qquad 4.11$$

for the Blume circuit. T_A applies to the signal alone. The noise bandwidth is defined by the value of T_o and is thus larger than the signal bandwidth by a factor $\frac{T_R}{\xi}$. The factor $\frac{T_R}{\xi}$ can be regarded as an "inefficiency factor" because it places a high value of minimum sweep time for a given system. $\frac{T_R}{\xi}$ is, of necessity, > 1 and thus a serious limitation is placed on the Blume circuit. The effective time constant, T_A, is a direct result of the fact that, for a given total sweep time, T_{TOT}, the effective sweep time,

$$T_E = n\xi \qquad 4.12$$

where the total number of samples, n, taken during a sweep through the signal is given by

$$n = \frac{T_{TOT}}{T_R} \qquad 4.13$$

$\therefore$ from Equations 4.12 and 4.13:-

$$T_E = \frac{T_{TOT}}{T_R}\,\xi \qquad 4.14$$

The inefficiency of the Blume Boxcar integrator is a serious shortcoming which led the author to consider possible ways of overcoming it. An improved design is suggested and analysed below which, theory indicates, should overcome the "inefficiency factor". This device is referred to as:-

(1) The Ideal Boxcar Integrator

Ideally it is required that T_o applies to both signal and noise and this is accomplished in the Ideal Boxcar Integrator suggested by the author. A schematic diagram of the Ideal Boxcar Integrator is shown in Fig. 4.6.D and its output for a constant input voltage is compared with that of other analogue integrating devices in Fig. 4.7. A proposed form of a practical version in shown in Fig. 4.8.; the buffer amplifiers are assumed to possess extremely high input impedance, neglible output impedance and a voltage gain of unity. With reference to Fig. 4.6.D, the capacitor $C' >> C$ so that the fall in the voltage across C' as it comes into electrical equilibrium with C is negligible. In practice C' can be simulated using a buffer amplifier and capacitor as illustrated by C'' and buffer amplifier (2) in Fig. 4.8.

The output time constant, T_o, is operating in the charging mode throughout the whole period of the experiment and the signal time constant is now reduced to T_o.

For a given set of experimental conditions, in changing from the Blume to the Ideal circuit, either:-

(i) the original time constant, T_o, can be retained and the experimental sweep time reduced by a factor ξ/T_R, or

(ii) the time constant, T_o, can be increased by a factor of T_R/ξ and the original sweep time, T_S, retained. In either case no signal distortion will result although the first condition will result in a much shorter experimental time and the second in an improvement in signal to noise ratio.

The signal to noise power ratio gain, G_I, under identical experimental conditions, is given by:-

$$G_I = G_B \frac{T_R}{\xi} = \frac{T_o}{\xi} \qquad 4.15$$

The expressions for G_I and G_B assume that a signal at the input is transferred to the output with no change in shape or amplitude. G_I could not be made infinitely large in a practical system because the effective sweep time $T_E = n\xi$ still applies in as much as a certain number of samples are required to define the signal with sufficient resolution. A practical limit will be placed on ξ by the finite time required to charge capacitor C'' in Fig. 4.8. Unfortunately the experiments with the C.S. Spectrometer using a Boxcar Integrator were completed long before the advantage of the Ideal Boxcar were realised. However recent preliminary experiments by the author indicate that the expected improvement is achieved. The ideas behind the theory of operation also have a certain relevance to the C.S. Spectrometer which is the subject of this thesis.

4.10.5 Monitoring and Recording of Integrator Output

In order to achieve the long holding times obtainable with a Blume or Ideal Boxcar Integrator it is essential that any measuring equipment connected to the integrator output places the minimum of loading on the storage capacitors. In the event of any appreciable loading occurring the

Blume circuit will tend towards the properties of the Aubrun and Veillet circuit.

In the apparatus described, as used by Parker (2,3), a Vibron electrometer type 33B with an input resistance of $10^{13}\Omega$ was used; the net leakage resistance across the holding capacitor is ~ $10^{11}\Omega$ being mainly contributed to by the back resistance of the gating diodes. With the 0.01μf integrating capacitor used, the holding time, as defined by Blume (14) is $\frac{10^{11}.10^{-8}}{10^{2}}$ seconds = 10 seconds, which is more than adequate for a value of T_R = 2 seconds.

Recordings of the transient spectra of decaying atomic oxygen have been obtained up to delays of 600msec., each spectrum took 32 minutes to record and was slightly distorted owing to the large value of T_o required. Undoubtedly the distortion could have been reduced if an Ideal boxcar had been used. There are two main disadvantages of the system both attributed, in some way, to the long time constants and high resistances involved:-

(i) The apparatus is very prone to drift and requires a considerable "settling period" before a recording can be attempted.

(ii) A spectrum is recorded in a single long field sweep. Any drift in the spectrometer or external transient electrical interference occurring during a recording will disturb the stability of the Boxcar Integrator thus rendering the recording completely unusable.

The disadvantages, mentioned above, make the equipment very critical in initial adjustment and slow in producing usable results.

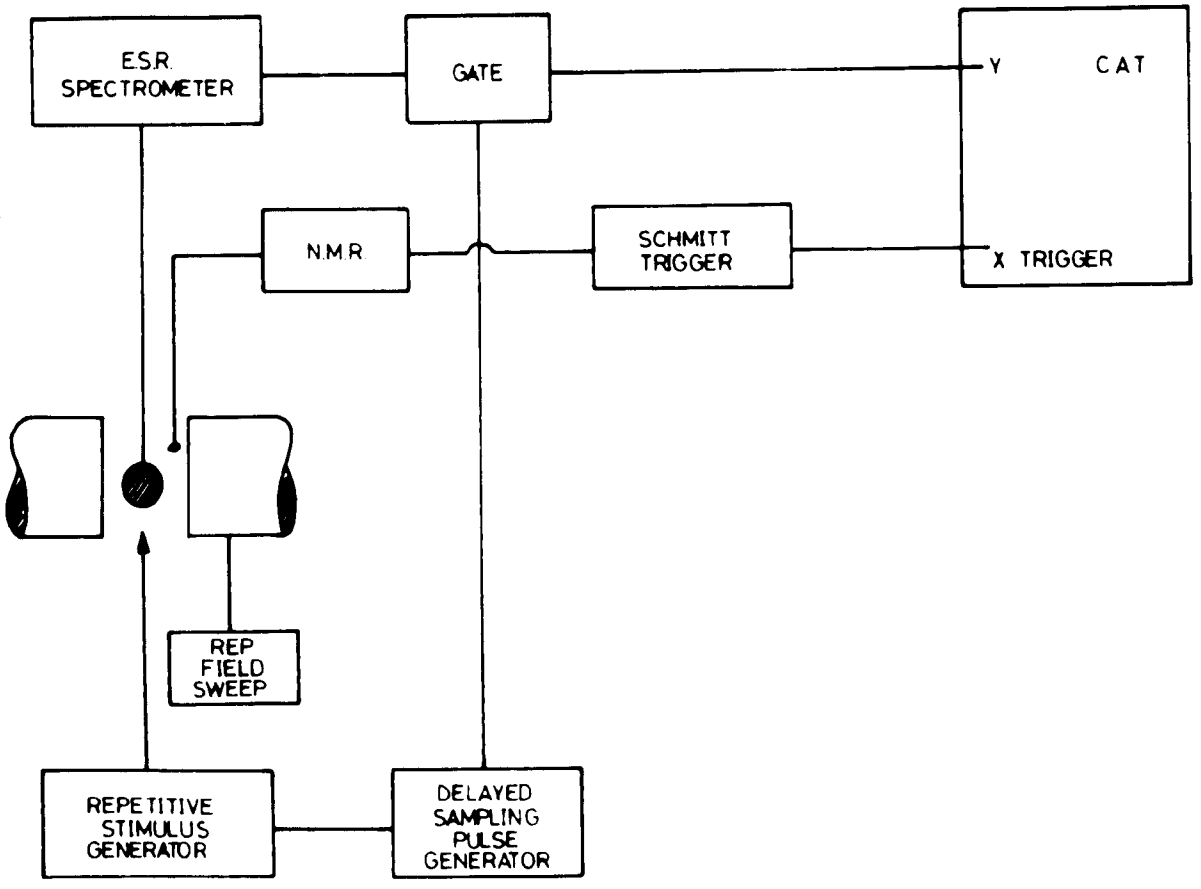

FIG. 4. 9. INITIAL C.S.S. USING SAMPLING AND DIGITAL AVERAGING.

4.11 Use of a CAT in a Complete Spectrum System

From previous discussions a CAT would appear to present a better alternative as a means of averaging and storing. However it must be used in conjunction with a sampling technique in order to overcome the bandwidth difficulties which have already been discussed.

A block diagram of the initial version of a C.S. spectrometer using sampling and digital averaging, constructed and used by the author, is shown in Fig. 4.9. A description of the principles of operation will be given in the following sections, including certain modifications incorporated in the final version on which experimental work was carried out. Detailed design and development data for individual parts of the system are described in Chapter V and a description of the results obtained from transient spectra are reported in Chapter VI.

4.11.1 Principle of the method

The method used is basically as follows. The magnetic field is repetitively swept slowly through the region in which the spectrum of the transient species occurs; and the field sweep is synchronised with the time base of the CAT. The memory channels in the CAT open sequentially so that each channel is always open for exactly the same small field increment during each sweep. At the same time, the sample under investigation is repeatedly stimulated to reproduce its initial state containing the unpaired electrons. The stimulus repetition rate, $^{1}/T_{R}$, is of such a value that the paramagnetic species can decay to approximately zero concentration in between successive stimuli but is greater than the field sweep repetition rate $^{1}/T_{F}$. Thus the concentration of the paramagnetic species

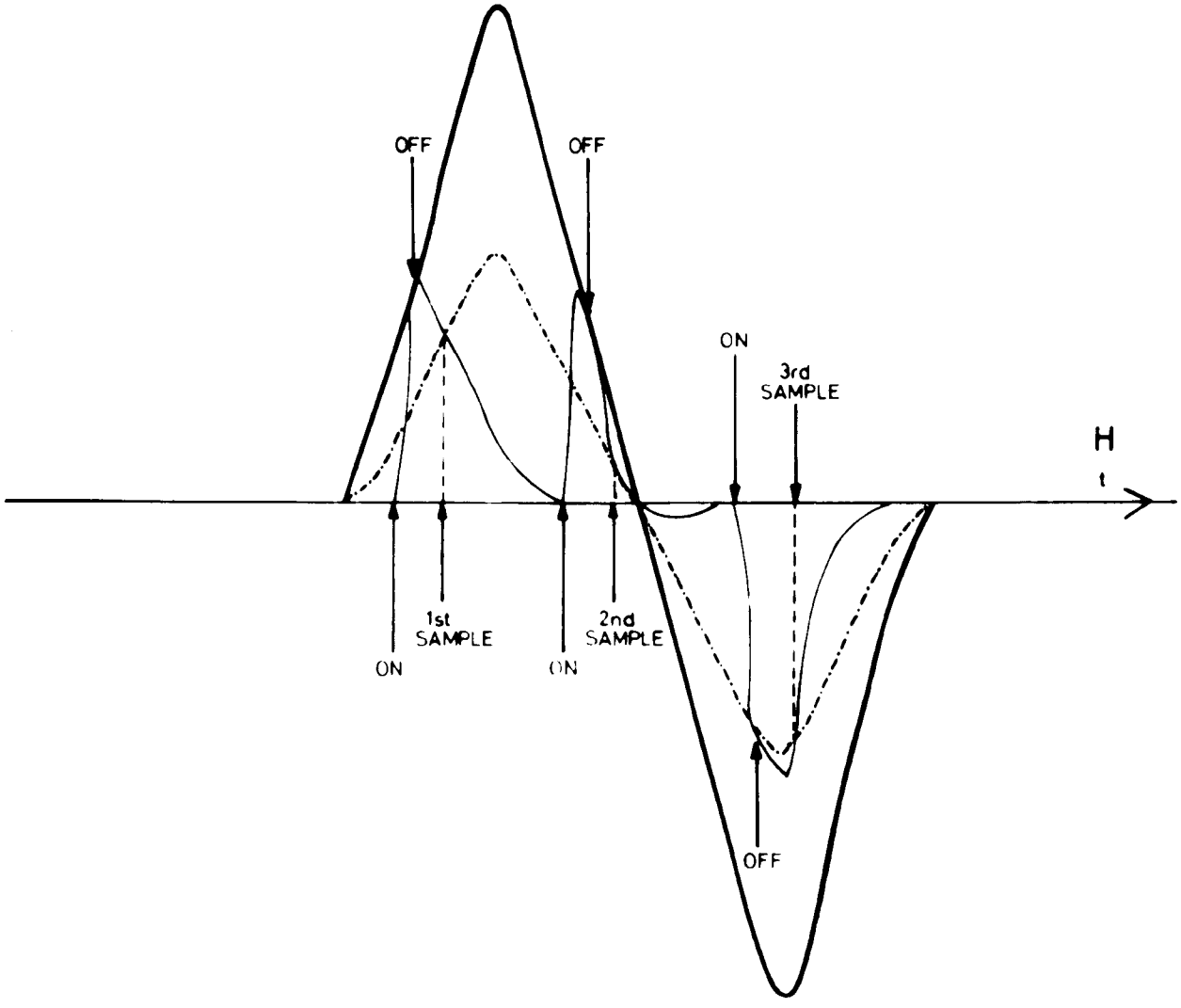

FIG. 4. 10. TYPICAL APPEARANCE OF AN E.S.R. SPECTROMETER OUTPUT WITH A TRANSIENT PARAMAGNETIC SAMPLE.

builds up to a maximum during the stimulus and then at the cessation of each stimulus it decays away, and is reformed on the reapplication of the next stimulus. The typical appearance of the output of a spectrometer with a transient paramagnetic sample undergoing three stimuli during a single field sweep is shown as the thin line trace in Fig. 4.10; the thick line showing the whole spectrum at t = 0, the dotted spectrum shows the appearance at the sampling time.

At the cessation of each stimulus a sampling circuit is triggered; this causes a sampling pulse, of duration T_s, to be generated after a time T_D has elapsed from the stimulus cessation. This sampling pulse opens a D.C. coupled linear analogue gate for the period T_s. The gate is placed between the spectrometer output and the input of the CAT and thus allows the signal present at the output of the spectrometer, at the time at which the sampling pulse occurs, to be sampled for the duration T_s and stored in the CAT memory.

Thus, as the magnetic field is slowly swept certain parts of the spectrum are sampled and these selected signals are presented to the CAT as pulses of width T_s; the height of each pulse being equal to the amplitude of the signal, at the time and at the magnetic field at which the sampling occurred. Due to the fact that samples are only taken at a time T_D after the cessation of the stimulus, the sampled amplitudes will only be representative of the signal as it appears at time T_D after the commencement of its decay. During a single field sweep only very few channels receive information but the sampling is in no way field dependent;

i.e. $T_F \neq nT_R$ (where n is an integer) and thus it is reasonable to assume that after many field sweeps each region of the signal will have been sampled approximately the same number of times and stored in its corresponding channel in the CAT.

An unlucky choice of stimulus repetition rate, such that $T_F = nT_R$, can result in the same channels being sampled during each sweep but this is immediately obvious and a fine adjustment can easily be effected, in T_R, to overcome this trouble.

Ideally

$$T_F = \frac{NkT_R}{N+k} \qquad 4.16$$

where k is an integer and N is the number of channels in the CAT. If in the first sweep channels n_1, n_2, n_3 .... n_n accept sampled information then, if the above equation (4.16) holds, during the 2nd sweep channels $n_1 + 1$, $n_2 + 1$, $n_3 + 1$ .... $n_n + 1$ will accept information and during the n^{th} sweep channels $n_1 + (n-1)$, $n_2 + (n-1)$, $n_3 + (n-1)$ .... $n_n + (n-1)$ will accept information. It is possible to choose a condition satisfying Equation 4.16 in practice by careful observation and fine adjustment of T_R.

The value of T_D can be chosen so as to register the appearance of the signal at any desired time during its decay

4.11.2 Choice of sampling time, T_s

There are two main factors which govern the value of the sampling time, T_s:-

(i) T_s must be chosen to be much less than the lifetime of the sample so that no appreciable decay occurs during the sampling period, T_s.

(ii) T_S must be much less than T_D so that a good time resolution is obtained.

4.11.3 The digital averaging device

A CAT presents an ideal choice of digital averaging device; the facilities included in it ease the problems of synchronisation of the field and memory channels, and the ultimate display of the final signal.

The 'waveform comparison' or averaging type of CAT, as described in Chapter 3.5, is more suitable for the sampling apparatus described above because of the independence of signal height stored and the number of samples received by each channel.

4.11.4 Input coupling to CAT

Four possible modes of coupling the D.C. coupled analogue gate to the input of the CAT will be discussed in ascending order of merit.

(a) Gate directly coupled to CAT

During the whole averaging process, with the apparatus depicted in Fig. 4.9, the memory channels are being successively opened and closed in synchronism with the repetitive magnetic field. If the gate between the spectrometer output and the CAT is closed, then only the noise associated with the input-impedance will appear at the input of the channels; but when the gate is open the E.S.R. signal, together with its associated noise, will be fed to the input of the channels. It follows that if any given channel is itself opened, by the field sweep, for a larger number of times with the gate closed than when it is open, the averaging process described above will tend to reduce the stored signal to zero, the noise of the channel input itself quickly averaging out any signal that does become stored.

FIG. 4.11.

SIGNAL FROM A STABLE FREE RADICAL SHOWING THE DEPENDENCE OF THE STORED SIGNAL AS THE RATIO BETWEEN ON TIME, T_S, AND OFF TIME, T_D, OF THE GATE.

(i) $T_S : T_D$ (1 : 10)

(ii) $T_S = T_D$

(iii) $T_S : T_D$ (10 : 1)

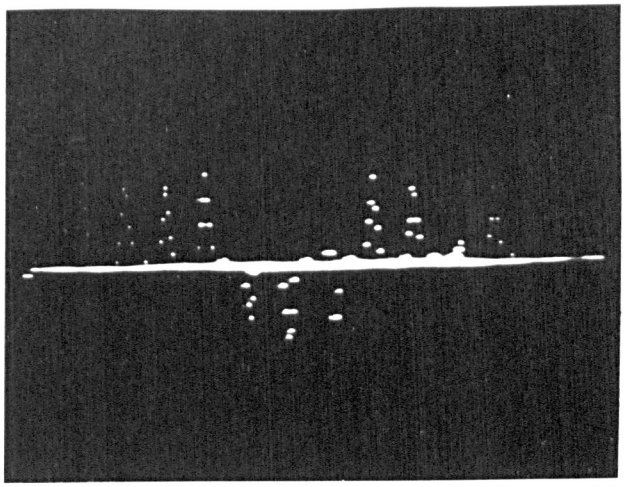

(i)

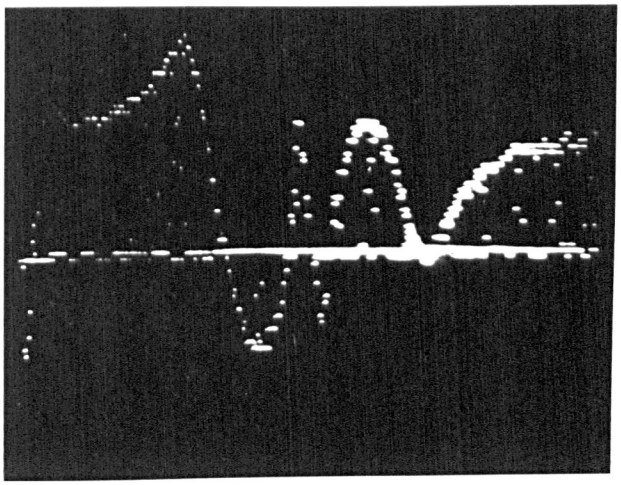

(ii)

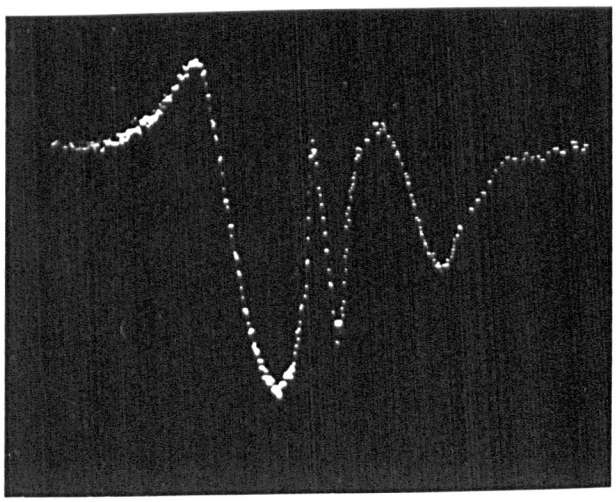

(iii)

It therefore follows that signals will only be stored permanently in the channels of the CAT if the time for which the gate is open is longer than the time for which it is closed and this, in turn, implies that $T_S > T_D$. This dependence of the stored signal on the ratio between T_S and T_D can be clearly seen in Fig. 4.11, which shows a signal from a stable free radical at g = 2. The data for Fig. 4.11 was obtained using the apparatus depicted in Fig. 4.12. Each photograph was taken after the same number of field sweeps had been completed but the traces do not change significantly however many sweeps are utilised.

The condition that $T_S > T_D$ imposed by this simple direct connection of the gate to the CAT inviolates the condition (ii) in Section 4.11.2 as the choice of a value for T_S and is quite unacceptable for signals which change with time. Only a very crude time resolution would then be possible and the system would not be suitable for detailed kinetic studies at all.

(b) Gate coupled to CAT via a pulse stretcher

One way of overcoming the destruction of information which occurs when $T_S < T_D$ is to stretch each sampling pulse for the period between successive sampling pulses. The CAT will then never be in the "no signal" condition and thus no destruction of information occurs. The great disadvantage of this method, however, besides those already mentioned in Section 4.11.4(a) is that poor spectral lineshape resolution will be obtained unless extremely slow field sweeps of duration $N\ T_D$ are used, N being the number of channels in the CAT. The provision of a long field

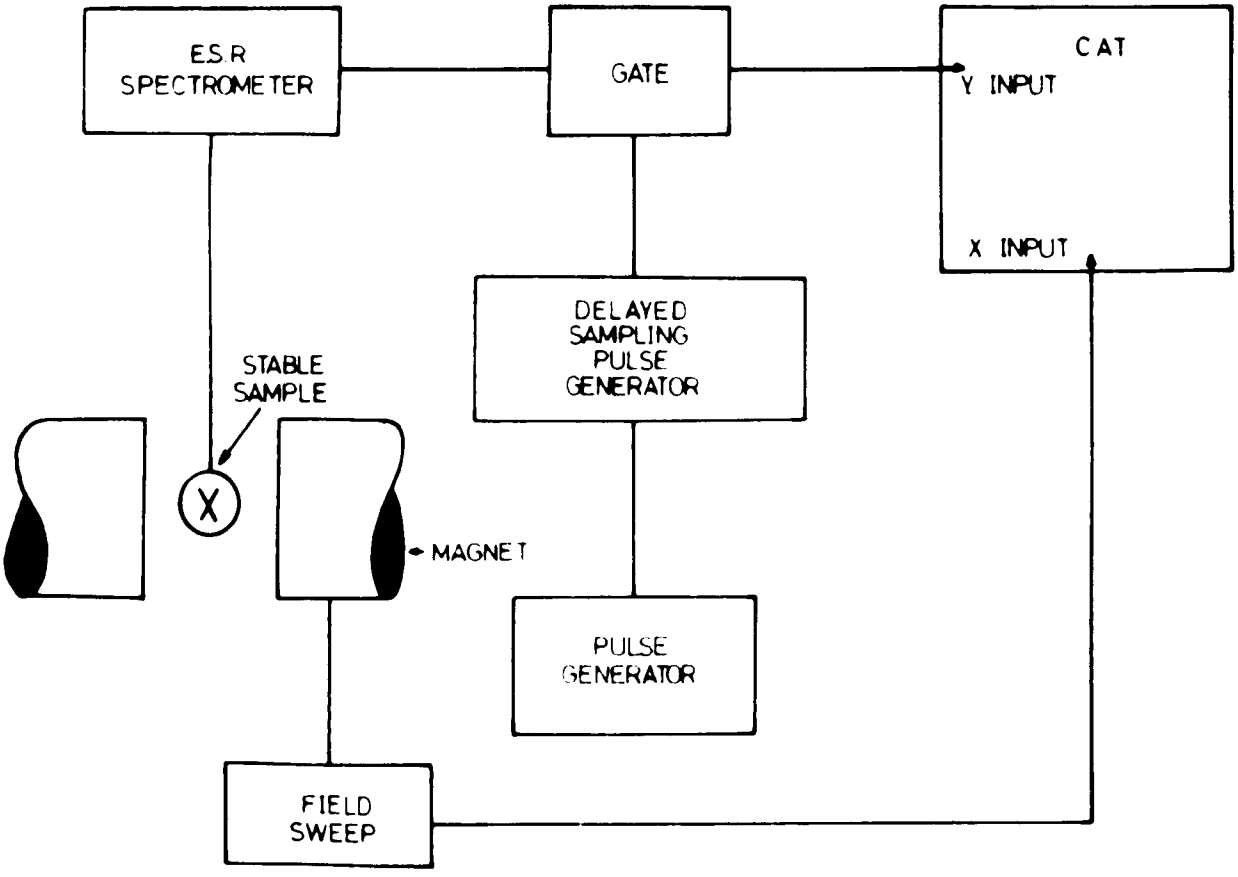

FIG. 4. 12. BLOCK DIAGRAM OF APPARATUS USED TO OBTAIN DATA SHOWN IN FIG. 4. 11.

sweep which must be of variable rate, so that it satisfies the above condition for different values of T_D, is very difficult. There are several other disadvantages in using long sweeps which will be discussed in a later part of the thesis.

(c) Gate coupling to CAT controlled by a memory inhibit

The direct connection of the gate to the CAT, as described in Section 4.11.4(A), is unsuitable because no distinction is made between the "signal" condition when the gate is open and the "no signal" condition when the gate is closed. The result being that, for the necessary conditions that $T_S \ll T_D$ (or τ - the lifetime of the sample) negligible information is stored and certainly not in usable form.

A distinction between the open and closed states of the gate, i.e. the "signal" and "no signal" conditions respectively, can be made. The two states of the gate are maintained by different electronic conditions in the output of the delayed sampling pulse generator. Thus by examining the electronic state of the delayed sampling pulse generator, e.g. measuring the gating voltage, it can be ascertained whether the "signal" or "no signal" condition prevails. The information obtained can be used to prevent the CAT from processing any information at its input unless sampling is taking place. Thus the CAT only accepts and processes data when the "signal" condition is present and does not accept information in the "no signal" condition but leaves unchanged any information previously stored in it. The input used to accomplish the discrimination is referred to as a memory NOT INHIBIT or $\overline{I}$ input. The circuitry details and principle of operation will be described in the following chapter.

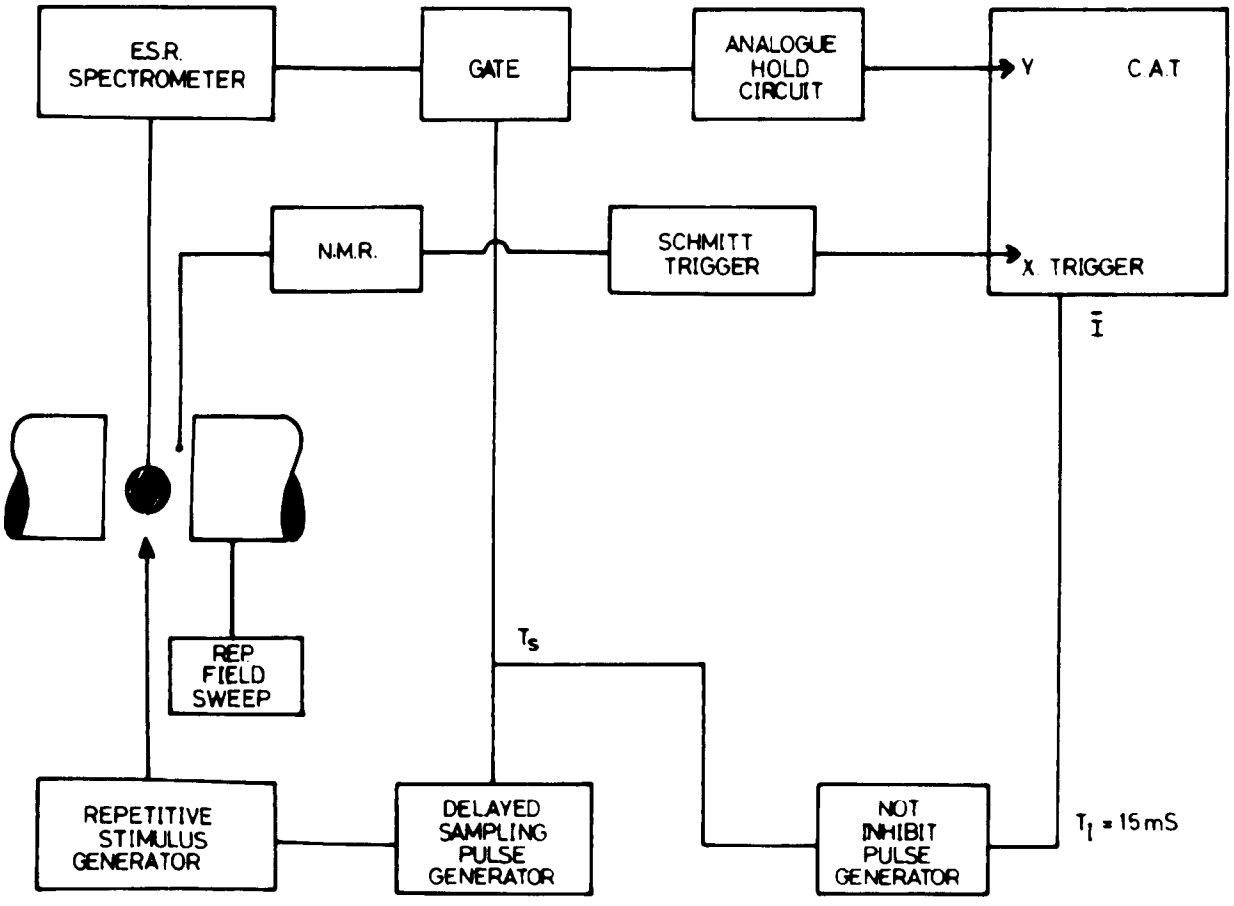

FIG. 4. 13. FINAL EXPERIMENTAL SET UP FOR C.S.S. USING PRINCIPLES DESCRIBED IN SECTION 4. 11.

Strictly speaking the gate is no longer required because the duration of the $\overline{I}$ pulse, T_I, = T_s. However in the following section a refinement of this technique is described in which the condition $T_I = T_s$ is no longer maintained and hence, for the sake of simplicity the use of the gate is retained.

(d) Gate coupled to CAT via an inhibited time limited analogue stretcher

During the course of preliminary experiments, conducted on r.f. generated atomic oxygen, a possible means of improving the apparatus was realised. A repetitive field sweep of 8 seconds is used and, as the sweep through the 512 memory channels of the CAT are synchronised with this, each channel is open for $\frac{8}{512}$ seconds, ~15msecs. Each time a sample of the decaying E.S.R. signal occurs, information is presented to the computer only for the duration, T_s, of the sampling pulse. In the previous discussion of the choice of a value for T_s (4.11.2) it was found that $T_s << T_D$ is a necessary condition. A sampling time, T_s, of 15msecs is only suitable for sample lifetimes of the order of seconds. The use of a T_s < 15msecs is necessary to improve the time resolution of the system; however no improvement in field resolution is obtained.

The ideal solution to this problem, corresponding to a hybrid version of methods (b) and (c) is to use very small values of T_s and to stretch the resulting narrow pulses of signal for the full time that the memory channel is open. Thus the memory channels will attain absolute values more rapidly while a good time resolution is maintained.

A block diagram of the final experimental set up is shown in Fig. 4.13. The design and development and practical details of the apparatus is described in Chapter V.

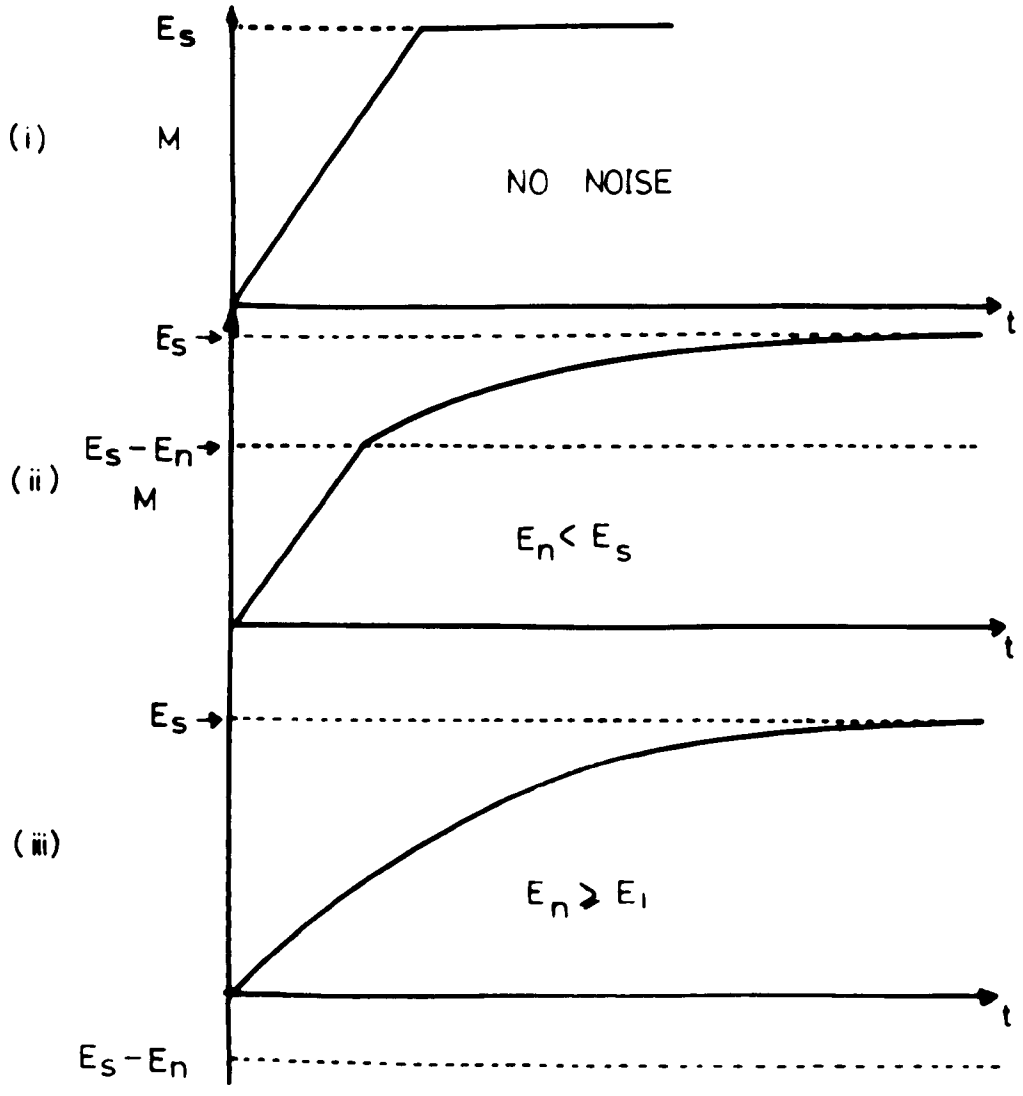

FIG. 4. 14. DIAGRAM SHOWING THE NUMBER OF COUNTS 'M' STORED IN A CHANNEL OF THE NS513 AS A FUNCTION OF TIME FOR VARIOUS NOISE LEVELS.

4.12 Signal Processing Properties of the System

4.12.1 Behaviour of an individual memory channel in the waveform comparison CAT

Each channel of the waveform comparison CAT can be regarded, from the point of view of signal processing, as an independent system. The behaviour of each individual channel of the CAT may be loosely considered as behaving as an R.C. time constant. The number of counts stored, as a function of time, in a channel of a CAT is shown under various noise conditions in Fig. 4.14. When a noiseless signal of voltage E_s is applied to the input during the interval that a particular channel is open, the number of counts stored in the part of the memory increases linearly with time and not exponentially. It is in this way that the CAT differs from a simple R.C. circuit. Comparisons between the input signal, E_s, and, M, the analogue equivalent of the number of counts stored in a particular channel is made at the rate of C/sec (25.6Kc/s for the device used). The number of comparisons occurring before a modification is made to M is controlled by the weighting factor, W, which can be varied by the experimenter. Thus for a signal input E_s, M will increase linearly with time, t, at a rate $\frac{C}{W}$ until it attains the value of E_s; and thus W/C can be considered as a type of time constant of the channel.

Under conditions of low noise as shown in Fig. 4.14(2) the increase in M is linear until the level $M = E_s - E_n$ is reached, where $2E_n$ is the peak to peak height of the noise. When M attains this condition the increase becomes an exponential increase $M = E_s(1 - e^{-Ct/W})$ because the probability of a favourable alteration in M becomes smaller as it approaches the value of E_s due to the noise.

When high noise conditions prevail such that $E_n \geq E_s$ the growth in M is of the form $M = E_s(1 - e^{-Ct/W})$ throughout the whole period that the channel is open.

The conditions under which the CAT operates with the system described in Chapter 4.11.4(d) is such that the growth of counts during any one period T_I is linear because the sample is held constant by the hold, or stretch, circuit, no fluctuations due to noise occurring. It must be realised however that the steady voltage held by the hold circuit is a representative of signal plus noise and thus a value of W must be chosen to suit the particular signal to noise ratio. The choice of W under experimental conditions is discussed in Chapter V.

4.12.2 The combined properties of the sample and hold system, CAT channels and inhibit pulse

The sample and hold system can be approximated to a Boxcar Generator when $T_s \ll T_I$; in the experimental set up T_s = 100μsec and T_I = 15msec and therefore this condition is satisfied. Each channel of the CAT can be approximately represented as an RC time constant with the reservations mentioned above. Thus, when a channel is open, the system behaves as an ideal boxcar integrator; at the end of the inhibit pulse duration, T_I, the system exhibits the properties of the Blume boxcar integrator by holding the stored signal constant until the channel is next presented with an input signal. Each channel is synchronised with a particular field increment and thus it will eventually store a signal representing the average value of the signal over the relevant field increment at the time

T_D after the cessation of the generating stimulus. The time required for the stored signal to achieve the absolute value depends on the factors C and W as indicated above. For noisier signals higher values of W are required in order to achieve a sufficient signal to noise ratio - a higher value of W being equivalent to a larger time constant. Although the time between samplings for a particular channel may be long there are in effect 512 Blume boxcars available for processing information. The "inefficiency factor" still applies, apart from the time wasting incurred by the use of sampling techniques, but the period is not wasted because with every sampling pulse one or other of the 512 "boxcar integrators" will assimilate more information.

REFERENCES

1. Fessenden, R.W., J. Phys. Chem. 68, 1508 (1964).

2. Parker, A.J., Ph.D. Thesis, University of Birmingham (1965).

3. Parker, A.J., Lainé, D.C. and Ingram, D.J.E., J. Sci. Inst. 43 688 (1966).

4. Edwards, D.B.G. and Aspinall, D., World Medical Electronics 3, 276 (1965).

5. Piette, L.H. and Landgraf, W.C., J. Chem. Phys. 32, 1107 (1960).

6. McQueen, J.G., Electr. Eng. 24, 436 (1956).

7. Buyle-Bodin, M. and Rosset, J., J. Phys. et Rad., S.4, 20, 32A (1959).

8. Mackey, R.C., Rev. Sci. Inst. 35, 859 (1964).

9. Robinson, J.D. and Yogi, T., Rev. Sci. Inst. 36, 517 (1965).

10. Lawson, J.L. and Uhlenbeck, G.E. "Threshold Signals" (McGraw-Hill (1950)).

11. Aubrun, J-N and Veillet, P., Compt. Rend. Acad. Sci. 256, 1696 (1963).

12. Aubrun, J-N, Veillet, P. and Van Hiep, T., p.534 Proc. XIIth Colloque Ampere Bordeaux 1963, (North Holland Publishing Co. Amsterdam 1964).

13. Aubrun, J-N, Van Hiep, T. and Veillet, P., C.R. Acad. Sci. (Paris) 256, 3430 (1963).

14. Blume, R.J., Rev. Sci. Inst. 32, 1016 (1961).

15. Robinson, F.N.H., "Noise in Electrical Circuits", p.94 (Oxford University Press (1962)).

16. Holcomb, D.F. and Norberg, R.E. Phys. Rev. 98, 1074 (1955).

17. Reichert, J. and Townsend, J, Rev. Sci. Inst. 35, 1692 (1964).

18. Ware, D. and Mansfield, P., Rev. Sci. Inst. 37, 1167 (1966).

19. Bennett, T.J., Ph.D. Thesis, University of Southampton (1966).

CHAPTER V

DETAILS AND DESIGN OF APPARATUS

5.1 Introduction

The apparatus designed to record transient paramagnetic species can be divided into two parts consisting of:-

(i) a standard E.S.R. spectrometer with certain modifications

(ii) a unit designed to extract and process the relevant information from the spectrometer output, store it and present it in a form suitable for either readout onto a pen recorder, or general observation on the screen of a C.R.O. The information system is designed so that it can easily be connected to the output of an E.S.R. spectrometer in which the necessary modification in response has been effected.

A general description of the spectrometer is given first. This is followed by a detailed description of the design and evaluation of the processing and storage circuitry, together with a discussion on the principles of operation.

The chapter concludes with a description of the gaseous flow system used to examine the kinetics of the formation and decay of oxygen atoms formed by an r.f. discharge.

5.2 Description of the E.S.R. Spectrometer

The general requirements for an E.S.R. spectrometer have been discussed in 2.3.2. The special requirements of an E.S.R. spectrometer suitable for the study of transient paramagnetic species are three in number:

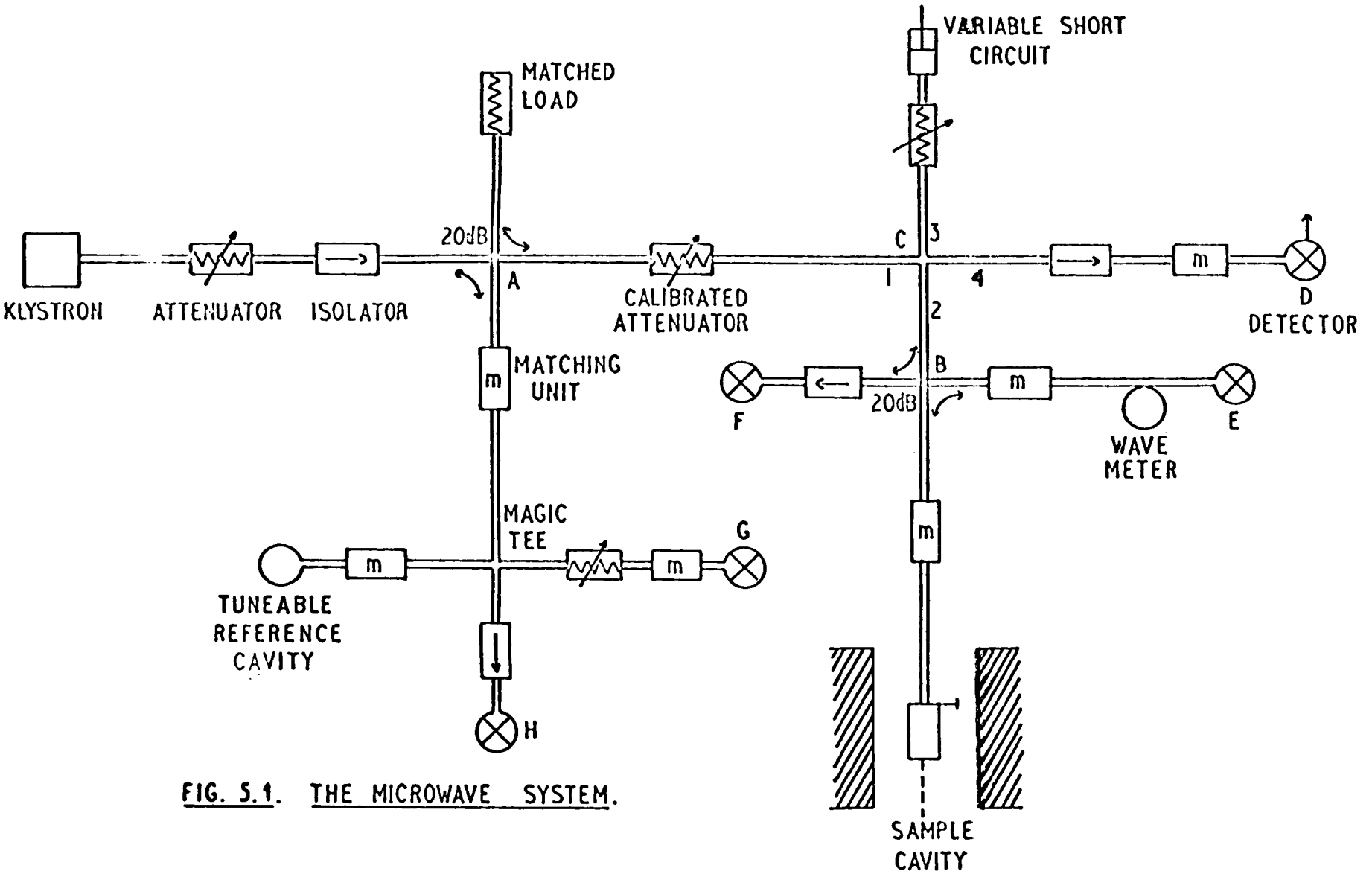

FIG. 5.1. THE MICROWAVE SYSTEM.

(i) A fast response time to enable the spectrometer to follow closely the amplitude of a decaying signal. This is usually achieved by employing a large bandwidth which is obtained by removing most of the output time constant from the P.S.D. The response time is then mainly limited by the bandwidth of the narrowband amplifier preceding the P.S.D.

(ii) Good stability is required so that long experiments can be performed without spectrometer adjustment. In order to extract all the relevant information using sampling techniques, long experimental times up to about 30 minutes are required.

(iii) High sensitivity is necessary because it is often difficult to generate paramagnetic species in large concentrations; and in the examination of any decay process the concentration at any time during the decay will be lower than the initial concentration.

In a conventional spectrometer required for the observation of stable paramagnetic species requirements (ii) and (iii) are highly desirable whereas (i) is not necessary, nor particularly desirable.

The spectrometer used in these studies can be broadly defined as an X-band, 100Kc/s field modulation, reflection cavity bridge spectrometer using phase sensitive detection.

The Klystron

The E.M.I. low voltage reflex klystron, type R9525, was used as an X band source for the spectrometer supplying approximately 150mW of microwave power. The klystron maintains adequate stability without the use of a cooling fan, although it is shielded from draughts.

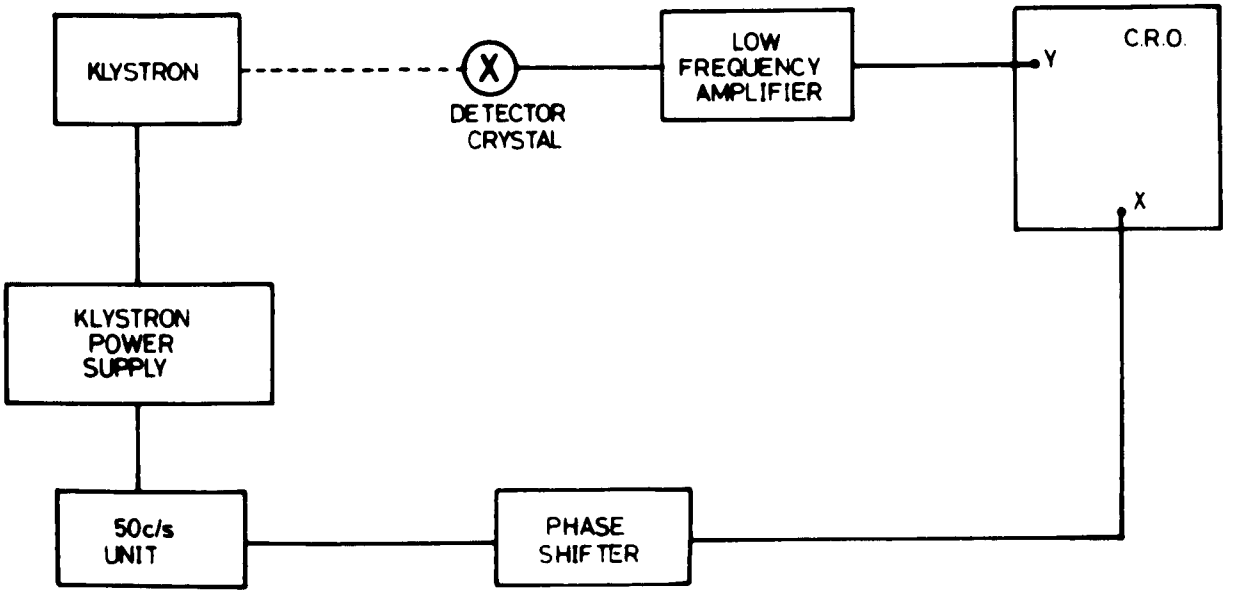

FIG. 5. 2. BLOCK DIAGRAM OF CRYSTAL VIDEO SYSTEM FOR TUNING KLYSTRON TO RESONANT CAVITY.

An A.P.T. low voltage klystron power supply Type 2763 is used to provide the stabilised D.C. voltages for the heater, resonator and reflector. A thermionic diode in the reflector circuit provides protection against the reflector becoming positive with respect to the cathode.

The klystron is mechanically tuneable over the range of 8 - 12kMc/s; adjustment of the reflector voltage provides a fine tuning over a range of approximately 500Mc/s. The initial tuning of the klystron to match the resonance frequency of the sample cavity is carried out by modulating the klystron reflector at 50c/s and observing the output of crystal E in Fig. 5.1. on an oscilloscope using the arrangement shown in Fig. 5.2. The crystal video technique employed enables the coupling of microwave power into the cavity to be adjusted to an optimum value for the sample under investigation.

Klystron Stabilisation

There are two possible methods of obtaining klystron automatic frequency control (A.F.C.). Either the klystron can be locked to the resonant frequency of an external high Q cavity, or to the resonant frequency of the sample cavity. In both cases any frequency difference is converted into an error voltage which is fed to the klystron reflector supply to compensate the klystron frequency drift.

The first type of A.F.C. is useful where high accuracy of g values are required as it maintains the klystron frequency constant.

If it is required that the spectrometer sensitivity remains constant and optimised so that lineshapes are accurately portrayed then the latter form of A.F.C. is most useful because the "cavity dip" is maintained in

FIG. 5.3.

PHOTOGRAPH SHOWING SIDE VIEW OF CAVITY USED

FOR OBSERVATIONS ON ATOMIC OXYGEN

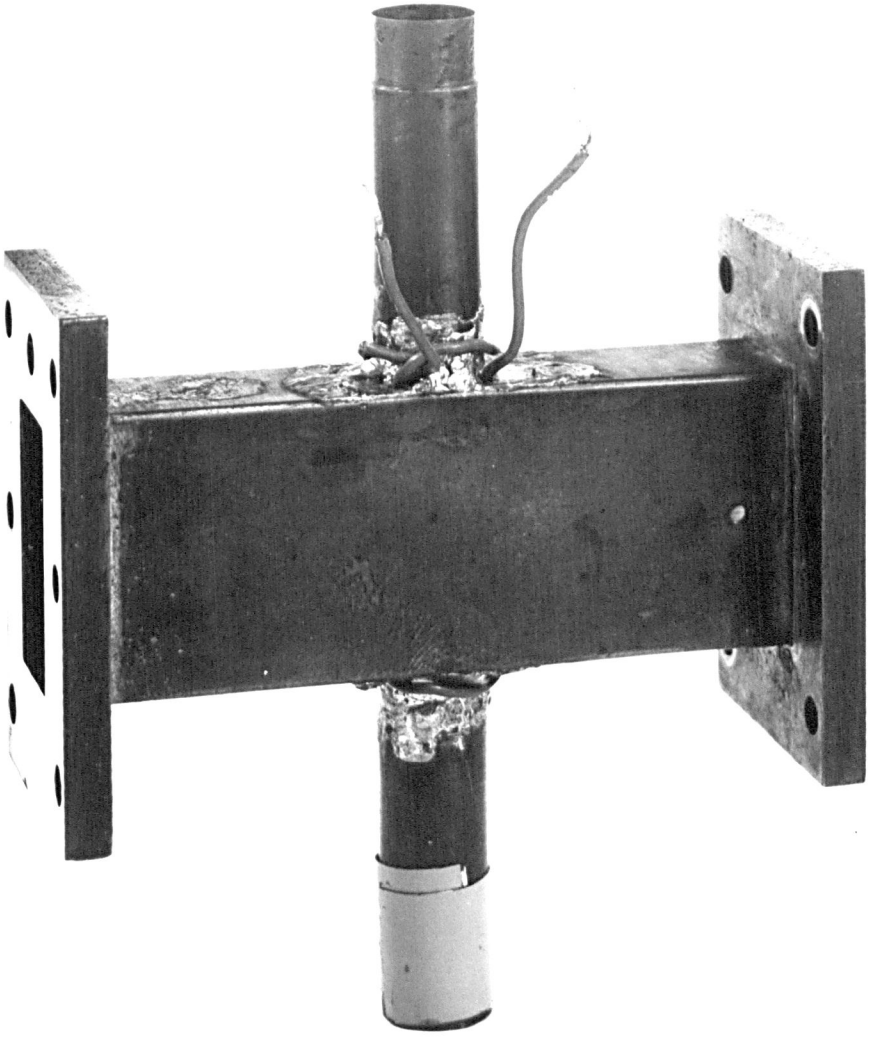

the centre of the klystron mode; the klystron frequency being locked to the resonant frequency of the sample cavity.

Thus although provision is made for both types of stabilisation, it is the latter form which was used. Power from a 13Kc/s oscillator is fed to crystal E in Fig. 5.1; any frequency drift causes the cavity to reflect microwave power, some of which passes through the 20dB directional coupler B to crystal E where it is modulated at 13Kc/s before passing to crystal F where after detection the 13Kc/s modulation is passed through a 13Kc/s P.S.D. and the resulting error voltage is passed via a D.C. amplifier to the reflector supply of the klystron to provide the necessary correction.

The Magnet

A Newport Instruments, Type D, 8" magnet was used in conjunction with a Newport Instruments C26 D.C. stabilised current supply fed from a motor generator.

The 8" pole-pieces are used at a separation of $3\frac{1}{2}$". Careful adjustment of the pole-pieces and screw shims enables the homogeneity of the magnet over the sample volume to be optimised. The optimisation process is carried out using a Newport Magnetometer type P; observation of the resonance absorption curve for protons in water under rapid passage conditions (50c/s modulation) enables the homogeneity to be adjusted to within 1 part in 10^5 by maximising the number of "squiggles" associated with the proton resonance signal. The magnetometer is also used for field calibration purposes and, in conjunction with a Schmitt trigger, to trigger the timebase of the CAT.

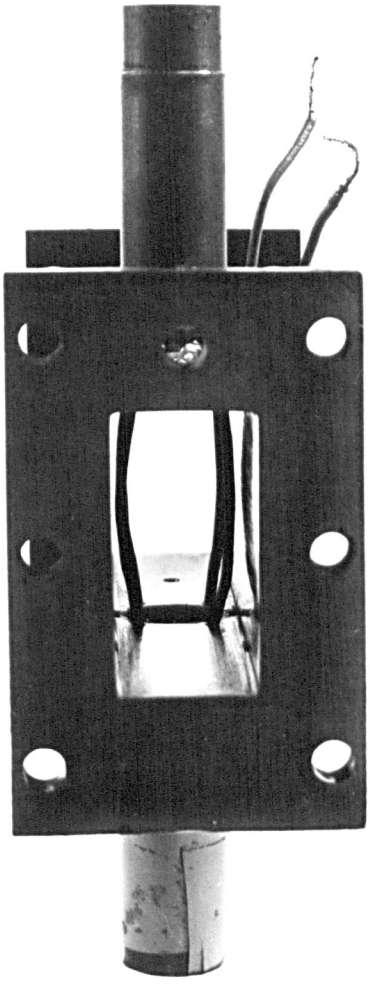

Application of a linear ramp voltage, supplied by a Newport Instruments Type A slow sweep unit to the C26 unit enables the magnetic field to be swept through the region of resonance; the sweep speeds and amplitudes being variable over a wide range by the operator.

50c/s field modulation is provided by supplying power to coils mounted on the inner cheeks of the main magnet coils, and is utilised for homogeneity adjustments in conjunction with the proton magnetometer and when the spectrometer is operated simply as a video system.

The Microwave System

The microwave system for the spectrometer is depicted in Fig. 5.1 and takes the form of a conventional balanced bridge system. Waveguide No. 16 is used with screw couplers, except at the cavity where bolted rectangular flanges are utilised.

The Resonance Cavity

The microwave resonant cavity, in which the paramagnetic sample is placed is a rectangular H_{014} cavity fashioned from brass waveguide No. 15. Two photographs of the cavity body and a cutaway diagram are shown in Figs. 5.3, 5.4 and 5.5 respectively. The microwave power is fed in at one end, the opposite end being terminated with a highly polished brass flat end plate bolted to it; brass shim is inserted to improve the electrical contact between the end plate and the cavity body. With careful polishing of all inner surfaces a loaded Q of 2000 - 3000 was obtained. The 100Kc/s field modulation loop is inserted, as shown in Fig.s 5.4 and 5.5, through the four holes in each narrow side of the cavity. The sample modulation loop is fed from a 100Kc/s crystal

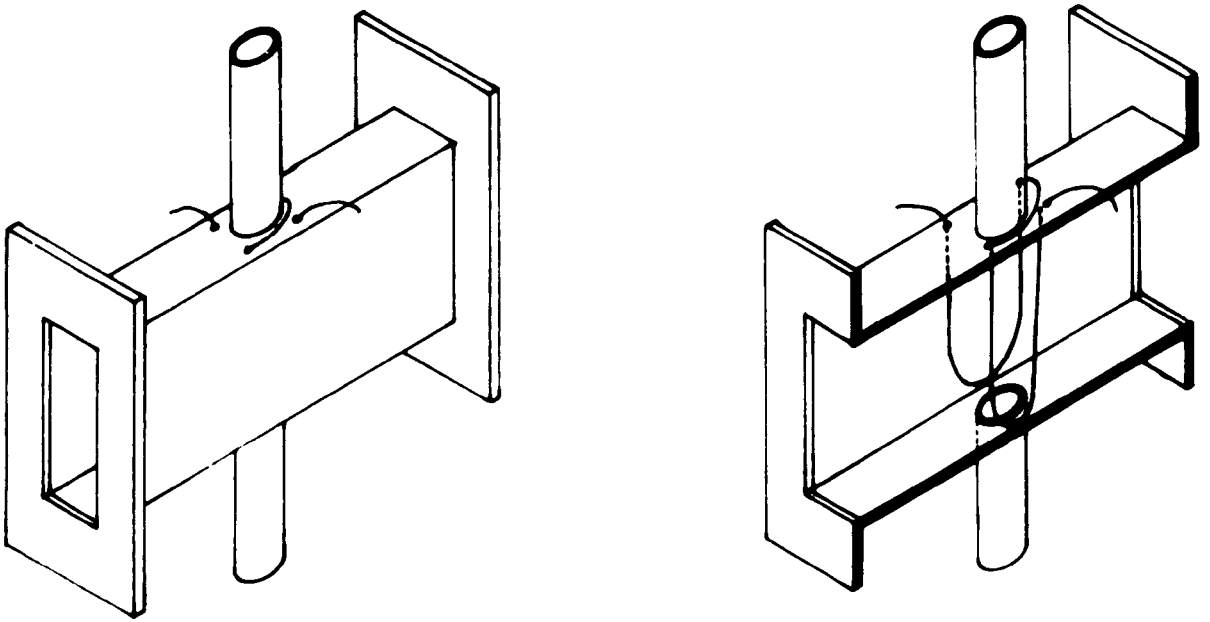

FIG. 5. 5. CUTAWAY DIAGRAM OF RESONANT MICROWAVE CAVITY USED FOR OBSERVATION OF GASEOUS SAMPLES.

controlled power oscillator of conventional design; field modulation of up to 10 gauss peak to peak is possible with this system although the modulation is usually maintained at a lower level than this to avoid lineshape distortion.

The coupling of microwave power in and out of the cavity is made via a 0.4" diameter coupling hole in the brass plate at the cavity entrance. A P.T.F.E. disc is placed in the hole to optimise coupling and fine adjustment is effected by screwing a O.B.A. brass bolt in or out of the coupling hole.

Electronic Detection System

The detector crystal is an A.E.I. C.S.10B silicon device with a tungsten point contact, individually selected for optimum signal to noise ratio. The D.C. output of the detector is fed to a moving coil milliammeter so that the initial tuning of the klystron and cavity can be adjusted and the optimum crystal bias set for the crystal by unbalancing the microwave bridge. The 100Kc/s crystal output is fed to a Hilger and Watts Type FA911 100Kc/s low noise preamplifier having a gain of ~70dB and a bandwidth of ~2.5Kc/s. The preamplifier output is fed into a Hilger and Watts Type FA206 100Kc/s narrowband amplifier and phase sensitive detector. The overall gain and bandwidth of the 100Kc/s is ~130dB and ~2Kc/s respectively. The phase sensitive detector is based on Schuster's original design (1); the reference voltage for this device is supplied from an output of the 100Kc/s oscillator passed through a limiting stage to maintain a constant reference amplitude. The limited

output is passed, via a 100Kc/s phase shifter, to the reference input of the P.S.D.

Pen Recorder

For the observation of stable samples the output of the P.S.D. is fed into a Varian Model G10 servomechanism pen recorder. The permanent recording of transient spectra is effected by feeding the pen recorder output of the CAT into the Varian recorder.

Provision of a Rapid Response Time for the Spectrometer

As discussed in an earlier part of this section, besides such factors as long term stability and high sensitivity which are necessary for a spectrometer suitable for the study of transient species and are desirable in any form of E.S.R. spectrometer, there is also the necessity for a short response time.

It has been shown that the response time of a P.S.D. is defined mainly by the response time of the circuitry connected to its output (Equation 3.11). Thus by the removal of the R.C. time constant circuitry of the FA 206 P.S.D., the response time of the spectrometer was reduced to ~500μsecs. This was measured using the method described by Parker et al. (5). The overall bandwidth of the 100Kc/s preamplifier and amplifier is ~2Kc/s and because the condition $B_D << B_A$ (see pages 46 and 48) is no longer maintained this bandwidth must be taken into consideration. The 100Kc/s system thus provides ~125μsecs ($\sim\frac{1}{4B_A}$secs) response time, the remaining ~375μsecs is due to the intrinsic time constant of the P.S.D. circuit.

5.3 Description and Design of the Information Processing Equipment

5.3.1 The Computer of Average Transients

For reasons discussed in Chapters 3.5 and 4.11.3, the 'waveform comparison' CAT is more suitable than a totalising type of instrument.

The actual instrument utilised in the work described in this thesis is a Northern Scientific NS513 instrument. The NS513 possesses 512 coordinate points or channels supported by a magnetic core memory with a capacity for storing 512 twenty bit words. The instrument makes comparisons between the memory and input at the rate of 25,600 samples per second; with the 15 - 16ms not inhibit pulse utilised, approximately 400 comparisons are made. The use of the "weighting factor" setting and its bearing on the time required to obtain the complete recording of a transient spectrum are now discussed.

The "quick approximation" setting of the weighting factor is used when measurements are made at a high signal to noise ratio, e.g. for measurements of transient spectra made a short time after the cessation of the stimulus, and thus for 400 comparisons, each advancing the memory by 8 counts, it is possible to arrive at a digital equivalent of the value of the largest signals within a small fraction of this time.

When the input signals have poorer signal to noise ratios, a correspondingly larger weighting factor is used. Thus with the weighting factor set at the position where each comparison modifies the number of counts by one, two 15ms periods are needed for each channel, thus increasing the experimental time required to obtain a complete spectrum.

However, by initially setting the baseline at the halfway position, i.e. + 500 counts/channel corresponding to zero volts, absolute values will usually be obtained during one 15ms period. With lower signal to noise ratios correspondingly higher settings of the weighting factor switch are required and thus proportionally longer periods are required to obtain a complete spectrum with the absolute values which are essential for kinetic studies.

The additional apparatus, utilised with the CAT, to complete the rapid recording section of the equipment can be broadly categorised into three sub-sections:-

(i) Equipment for triggering the timebase sweep through the channels from the magnetic field.

(ii) Analogue equipment for presenting the correct signal to the Y input of the NS513.

(iii) Logic and timing equipment, necessary to ensure that the CAT will only accept and process the relevant information in its memory.

These three portions of the apparatus will be discussed in the following sections.

5.3.2 Equipment used to trigger the CAT timebase

With each sweep of the repetitive field scan, it is required that the CAT sweeps through its channels in synchronism, so that each channel corresponds to the same small field increment for each successive sweep. The method utilised, to synchronise the field sweep and channel sweep, is to provide a trigger pulse each time the magnetic field passes through a

certain value. The trigger pulse initiates a single shot sweep in the CAT; no further sweep is initiated until the advent of the next pulse and thus the start of the timebase sweep occurs at the same field value each time.

A proton resonance probe is used to provide an output at a definite field value. For initial experiments the Newport Instruments Type P magnetometer, described previously in Section 5.2, was used. In later experiments a transistorised 1Kc/s field modulation proton resonance unit, based on a design by Robinson, was employed; the output was fed to a 1Kc/s P.S.D. using a design by Faulkner and Harding (2). The field modulations for the vaseline sample was provided by two miniature modulation coils mounted on either side of the probe with their axes parallel to the D.C. magnetic field.

Due to the fact that the sweep triggering field is traversed twice during each sweep, once during the experimental sweep and again during the flyback, a distinction must be made between them. The proton resonance signal produced during flyback was selected by passing the output of the probe through a differentiating circuit which acts as a high pass filter; the signal on flyback is traversed rapidly and is, hence, richer in higher harmonics than the signal produced during the larger, experimental sweep. There is thus a larger resultant output, after passing through the differentiating circuit, for the flyback signal. The differentiated pulses are fed via a differential amplifier to a variable threshold Schmitt trigger. The Schmitt circuit's trigger voltage is adjusted so that only

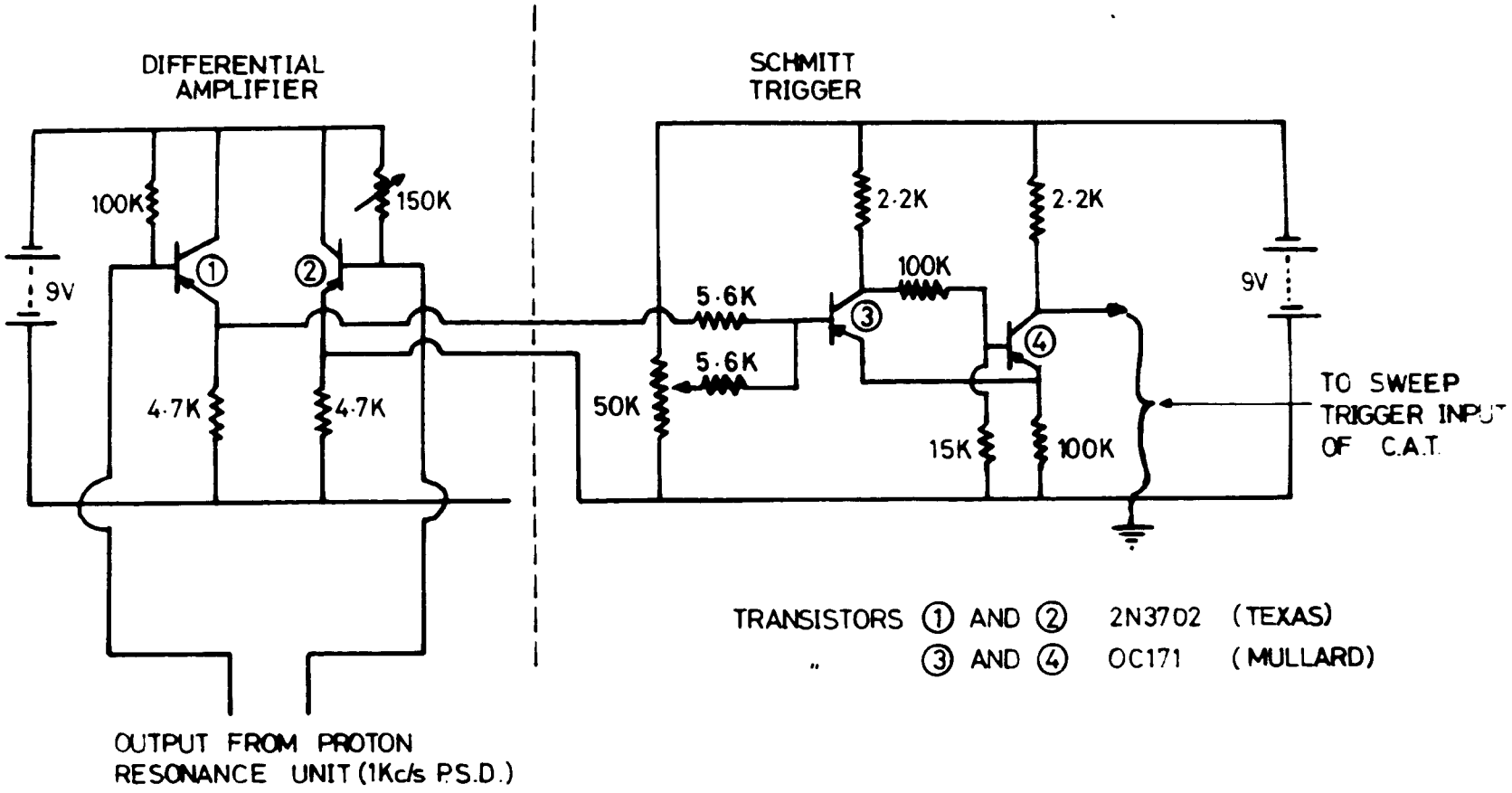

FIG.5. 6. DIFFERENTIAL AMPLIFIER AND SCHMITT TRIGGER CIRCUIT TRIGGERING C.A.T. SWEEP FROM PROTON RESONANCE CIRCUIT.

the proton resonance signal produced on flyback is sufficient to trigger it. The circuit for the differential amplifier and Schmitt trigger is shown in Fig. 5.6. The transistors used in the differential amplifier are epoxy encapsulated silicon devices each in common emitter mode; thus the circuit possesses high input impedance, good isolation between input and output and negligible thermal drift. The OC171 transistors used in the Schmitt trigger section of the circuit were chosen for their fast operation in order to supply a sufficiently fast risetime pulse for the CAT.

5.3.3 Analogue signal processing equipment

The analogue equipment for feeding the relevant signal to the Y input of the CAT is shown in Fig. 5.7 and can be divided into two main parts:-

(1) D.C. Amplifier

(2) Sample and Hold Circuit

5.3.3.1 The D.C. Amplifier

The D.C. Amplifier is used mainly as a buffer between the P.S.D. output and the input to the D.C. coupled analogue gate. The type used was a Northern Scientific NS301 D.C. amplifier with an adjustable voltage gain of 2 - 100, an input impedance of 1MΩ and an output impedance of 20kΩ. The minimum rise and fall times of 20μsec do not add any significant contribution to the overall response time of the spectrometer and the low output impedance provides a good current drive to charge the storage capacitor in the hold circuit.

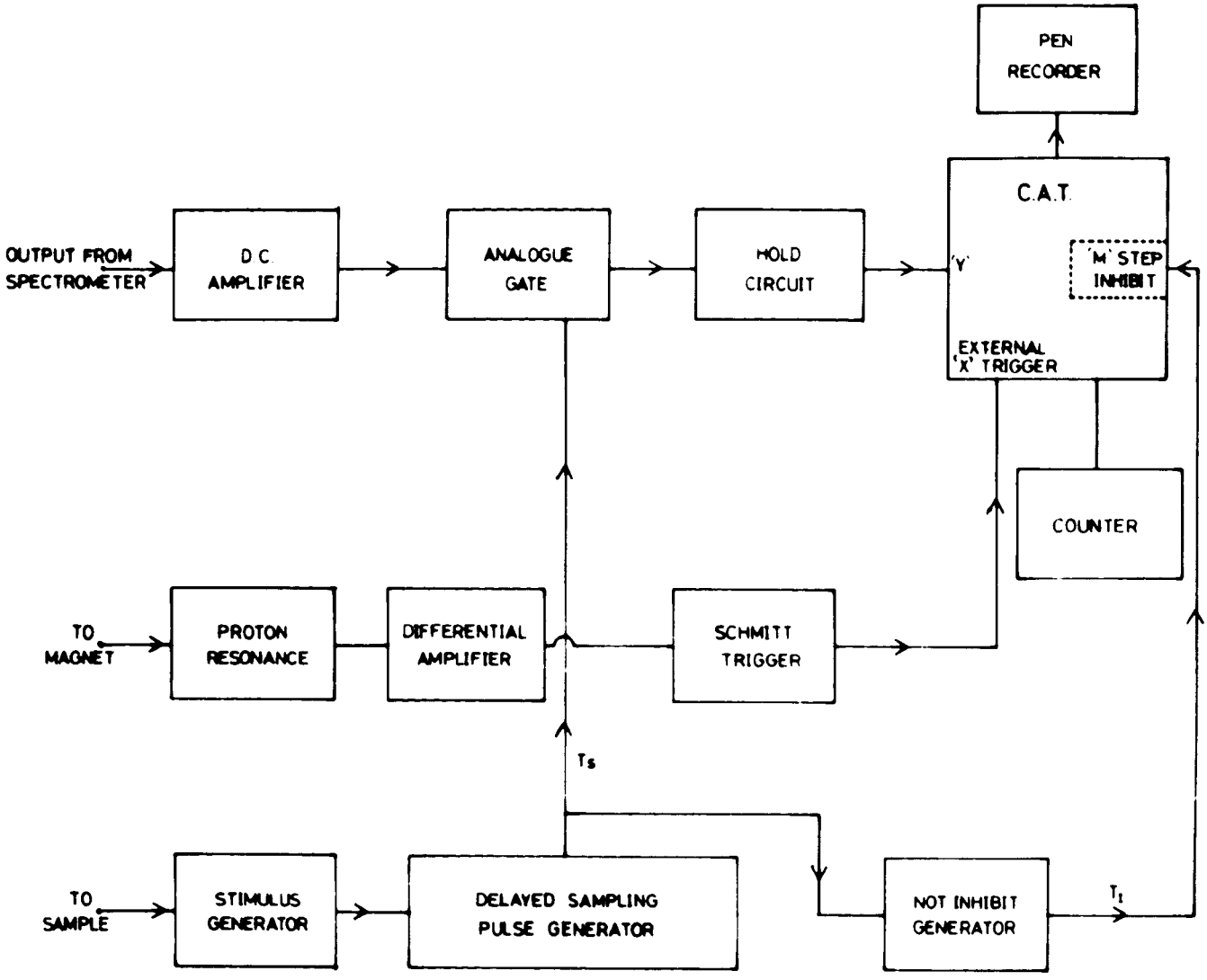

FIG. 5. 7 BLOCK DIAGRAM OF THE RAPID RECORDING SECTION OF THE APPARATUS

5.3.3.2 Sample and Hold Circuit

The sample and hold circuitry consists of two main parts:-

(i) A D.C. coupled analogue gate, the output of which is fed to:-

(ii) a clamping circuit which maintains its output at the same voltage level as that of the sampling pulse from the gate. The short pulse of signal given at the gate output is "stretched" in time until the gate is next opened when the clamping, or holding, circuit quickly readjusts and clamps its output to the new signal pulse level.

5.3.3.2(i) The Analogue Gate

(i) The features to be considered when designing an analogue gate may be categorised under four main headings:-

(A) Signal passage through the gate

(B) Switching properties of the gate

(C) Interaction of signal and switching waveforms

(D) Thermal stability

The gate forms a very critical and important part of the recording apparatus and although the final circuit appears uncomplicated, a detailed analysis of the design and construction is described.

For ease of explanation the gate input and output concerned with the signal will be referred to as signal input and signal output respectively; similarly the inputs at which the gating commands are inserted will be known as the gating inputs.

An ideal gate possesses properties which will be discussed under the four main headings mentioned above.

A Signal Passage through an Ideal Gate

An ideal gate possesses the following properties regarding the passage of a signal from the signal input to the signal output:

(i) The gate offers easy passage of the signal between signal input and output only during the time that the correct command signal is present at the gating inputs. The gate is then said to be in the ON or open mode.

(ii) At all other times any signal at the signal input is prevented from passing to the signal output. The signal output during these intervals remains at zero. Under these conditions the gate is in the OFF or closed mode.

(iii) During the periods when the gate is ON it possesses good amplitude and frequency linearity, for D.C. and A.C. signals, between signal input and output. An extension of the principle of amplitude linearity is that the gate is capable of processing signals of either polarity equally well: this property is referred to as bidirectionality.

B Switching Properties of an Ideal Switch

(i) In the OFF mode an ideal gate's signal output is well isolated, electrically, from all circuits excepting those connected to the signal output.

(ii) For a zero risetime gating command there is no transition time in switching from OFF to ON or vice-versa.

(iii) The ideal gate operates precisely at the onset and only for the duration of the gating signal. Failure to exhibit this property will be referred to as "switching jitter".

C Interactions between Gating Signal and Analogue Signal in an Ideal Gate

(i) There is no 'pedestal' at the output of an ideal gate, i.e. for zero volts at the signal input the signal output voltage is zero regardless of whether the gate is ON or OFF.

(ii) At the gating transition points (ON to OFF and vice-versa) there are no spurious outputs or switching transients.

D Thermal Stability

(i) Any of the properties mentioned in the above sections (A, B and C) remain invariant under temperature change.

Practical Designs for an Analogue Gate

Any practical design attempts to approach the ideal conditions, listed above, as closely as possible. Many possible systems were considered, several designs being immediately rejected as obviously unsuitable. Some of the initial circuits will be discussed including the reasons for their rejection in order to illustrate how the final design was chosen.

Mechanical devices, such as a simple, mechanically operated, on-off switch, are obviously unsuitable because they completely fail to satisfy conditions B(ii), B(iii) and C(ii) mentioned above. Similarly electromechanical devices, such as the electromagnetic relay, is unable to satisfy similar conditions and suffers particularly seriously from contact bounce giving rise to serious switching transients. The advantage of both mechanical and electromechanical devices is that they rely on mechanically opening and closing contacts, and, for this reason, perform

exceedingly well with reference to conditions A(i), (ii), (iii), B(i) and C(i). However, mechanical devices are unsuitable because they are incapable of operating sufficiently rapidly.

In order to achieve the necessary speed and precision the obvious solution is to find a purely electronic means of gating. In the design of an electronic gating system one additional condition is considered besides the ones considered above:-

E(i) The gating and signal sources are not required to dissipate excessively high power in order to secure the correct operation of the gate.

Condition E(i), while not being absolutely essential, is highly desirable in order that the gating and signal equipment, associated with the gate, is not unduly complicated.

The first device considered for use in a gating circuit was the bipolar transistor. A small change in voltage between the base and emitter electrodes can result in a vast change in the conductivity between collector and emitter terminals. There are several disadvantages in using the bipolar transistor as an accurate analogue switch. A particular shortcoming, particularly at low signal voltages, is the offset voltage, V_{CES}, which occurs between signal input and output when the device is switched on. V_{CES} is virtually independent of the current through the device and thus the transfer impedance does not obey Ohm's law. This makes the device difficult to use as a bidirectional gate; also the device fails to satisfy conditions A(iii), B(i), C(i), C(ii), D(i) and it only partially fulfils conditions A(i), A(ii) and B(ii).

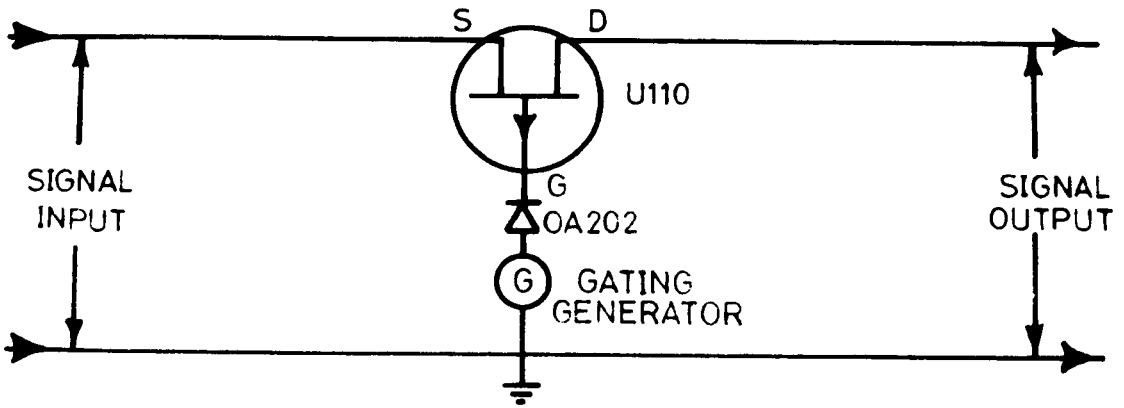

FIG. 5.8. CIRCUIT USED TO EVALUATE THE PERFORMANCE OF A F.E.T. AS AN ANALOGUE GATING DEVICE.

Transistors are often utilised in chopper circuits for D.C. amplifiers where the conditions imposed on the circuit performance are not as rigorous as those required for the gating circuit used in the equipment described. Three terminal devices, such as the transistor, require that there is an isolation between the source of the gating voltage and the devices connected at the gate's signal input and output. The necessary isolation is usually provided by a transformer which is far from suitable for fast pulse work.

In an attempt to eliminate the offset voltage the use of a unipolar device, called a field effect transistor (F.E.T.) was investigated. This device behaves as a voltage controlled resistor when a control voltage is applied at its gate terminal. The circuit on which the gating performance of this device was assessed is shown in Fig. 5.8. Application of a positive gating pulse turns the gate OFF by making the resistance between drain (D) and source (S) terminals very large. The resistance during conduction, between the drain and source terminals, r_{DS} is dependent on the voltage, V_{GS}, between gate and source; thus r_{DS} varies depending on the signal input voltage. A gate circuit of this type was found to exhibit little improvement on the bipolar transistor gate.

In order to achieve a definite gating, over a wide range of time intervals, it is essential that the gating voltages are directly coupled to the gating inputs. To ensure that the gating voltage does not interact with the signal in any way, some form of bridge circuit was decided upon; such an arrangement can also be used to minimise any offset effects.

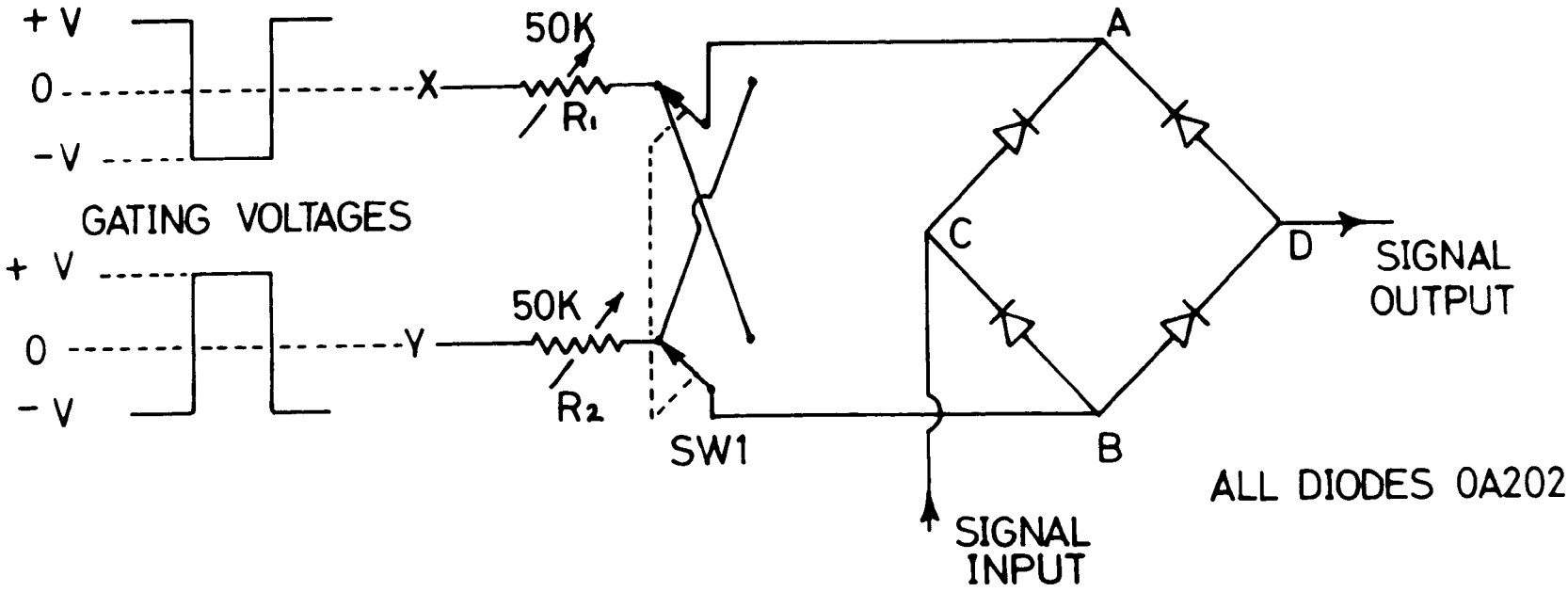

FIG. 5. 9. CIRCUIT DIAGRAM OF D.C. COUPLED ANALOGUE GATE SHOWING GATING VOLTAGE LEVELS.

For the gate circuit to operate satisfactorily with the hold circuit to be described, the circuit must satisfy conditions A(ii) and B(i) exceptionally well. Silicon junction diodes are available which exhibit an extremely high resistance when reverse biased $\sim 10^{10}\Omega$ and an extremely low resistance when forward biased. Devices of this type exhibit a small offset voltage but by the use of bridge techniques, this voltage is cancelled out. The thermal drift is very low at normal laboratory temperatures. The devices can make the transition from fully OFF to fully ON in times << 1μsec.

The circuit utilised was a 4 diode gate which is essentially the type described by Millman and Puckett (3) and Millman and Taub (4). A schematic diagram is shown in Fig. 5.9 with the gating voltage levels required for the operation of the device.

The impedance of the input and output to earth and the transfer impedance are all functions of the gating voltages at A and B, the values of R_1 and R_2 and the signal input (under large signal conditions). These factors will be discussed in the following paragraphs.

The gate is ON or open when the gating voltage at points A and B in Fig. 5.9 are such that diodes 1 → 4 are forward biased (A - negative and B - positive). Point D (signal output) is then free to "follow" point C (signal input) by normal bridge action. The gate will remain ON provided the signal at point C does not exceed the voltage at A (negative) and B (positive). In the ON state the impedance 'seen' by the signal input between C and earth is approximately $\frac{R_1R_2}{R_1+R_2}$ paralleled with any load at D. The transfer impedance is very low providing the gating

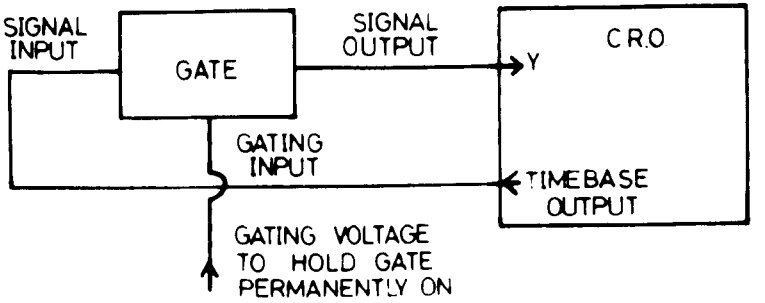

FIG. 5. 10. BLOCK DIAGRAM OF APPARATUS USED FOR AN AMPLITUDE LINEARITY CHECK OF ANALOGUE GATE.

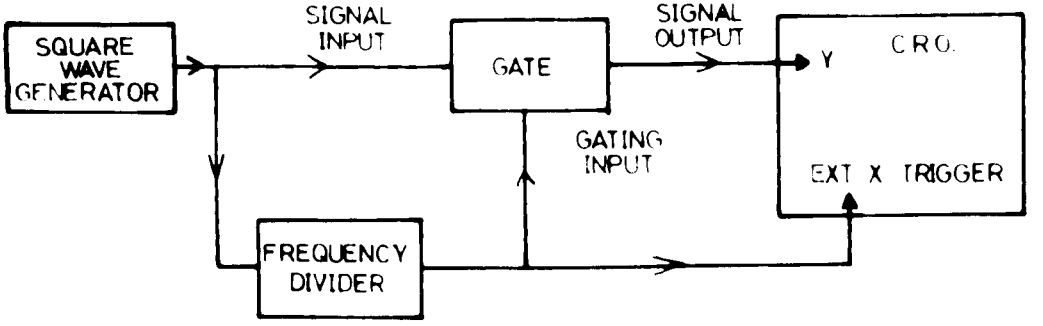

FIG. 5. 12. CIRCUIT USED FOR OBSERVATION OF GATING CHARACTERISTICS AND FREQUENCY LINEARITY OF ANALOGUE GATE.

voltages are adequate to bias all the diodes well forward.

The gate is OFF (closed) when the diodes are reverse biased, thus isolating points C and D, by application of gating voltages of positive and negative polarity at points A and B respectively. The gate will remain in the OFF mode providing the signal voltage at C does not become sufficiently large to forward bias the diodes. In the OFF mode the only connection between points C and D is approximately equal to the back resistance, R_B, of one diode; the impedance of the signal input or output to earth is approximately $R_B/2$. The Mullard OA202's used in the gate circuit have a minimum R_B of $10^{10}\Omega$.

By using gating voltages well in excess of the highest signal voltages encountered, it is ensured that the diodes are always biased firmly ON or OFF when the gate is held in the ON or OFF modes respectively. Minimum gating voltages of ±8 volts are used with a maximum signal excursion of ±0.3 volts.

Several tests were carried out on the circuit to determine how closely it approached the performance of the ideal gate.

A display of the gate amplitude linearity was obtained, using the apparatus depicted in Fig. 5.10, by applying the free running time-base ramp voltage to the signal input and monitoring the signal output using the Y amplifier of the same oscilloscope, the gate being held in the ON mode. Thus a continuous trace of $V_{IN} = V_C$ (X direction) versus $V_{OUT} = V_D$ (Y direction) is obtained; a typical example is shown in Fig. 5.11. Regions $\alpha \rightarrow \beta$ and $\gamma \rightarrow \nabla$ are the negative and positive saturation regions respectively; saturation occurring when the signal

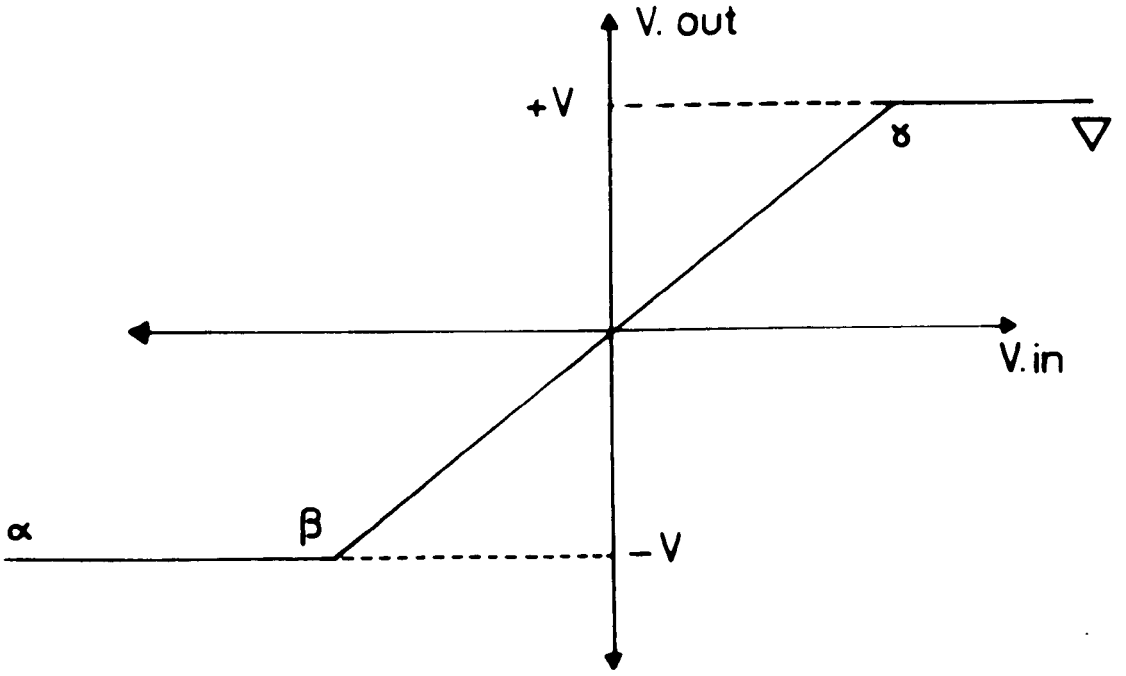

FIG. 5.11 ANALOGUE GATE AMPLITUDE CHARACTERISTIC

input voltage exceeds either the positive or negative gating voltages. The linear transfer region is between β and γ in Fig. 5.11. A graphical plot of V_{IN} versus V_{OUT} in the linear transfer region indicates that the transfer ratio, $\frac{V_{OUT}}{V_{IN}}$, is independent of signal amplitude to within the 1% accuracy of the moving coil voltmeter used, being indistinguishably different from unity.

The gating characteristics and frequency linearity were checked using the circuit depicted in Fig. 5.12. Photographs of the traces of typical waveforms are shown in Fig. 5.13 for a 2Kc/s square wave input.

The gate is set up for use by adjusting R_1 and R_2, shown in Fig. 5.9, in conjunction with the gating voltage levels for zero pedestal with no input. To maintain thermal stability the diodes are mounted together in a shaped copper block; application of a hot soldering iron to the assembly did not produce any observable effects in the performance of the gate. A photograph of the gate assembly, Fig. 5.14, clearly shows the copper block heat sink.

5.3.5.2(ii) The Hold Circuit

The output of the analogue gate consists of a series of narrow pulses of signal of duration T_s. Due to the fact that the CAT cannot deal effectively with narrow pulses of signal it is of considerable advantage to stretch the narrow pulses so that they are present for the total 15msecs that a channel is open. The method used to carry out the stretching for a controlled time, T_I (= 15msecs) is to stretch the signal pulse of duration, T_s, for a much greater period than T_I and artificially to limit

FIG. 5.13.

WAVEFORMS ILLUSTRATING GATING ACTION OF D.C. COUPLED ANALOGUE GATE

(i) Gated 2Kc/s square-wave

(ii) 2Kc/s square-wave signal input

(iii) Gating waveform at point B in Fig. 5.9.

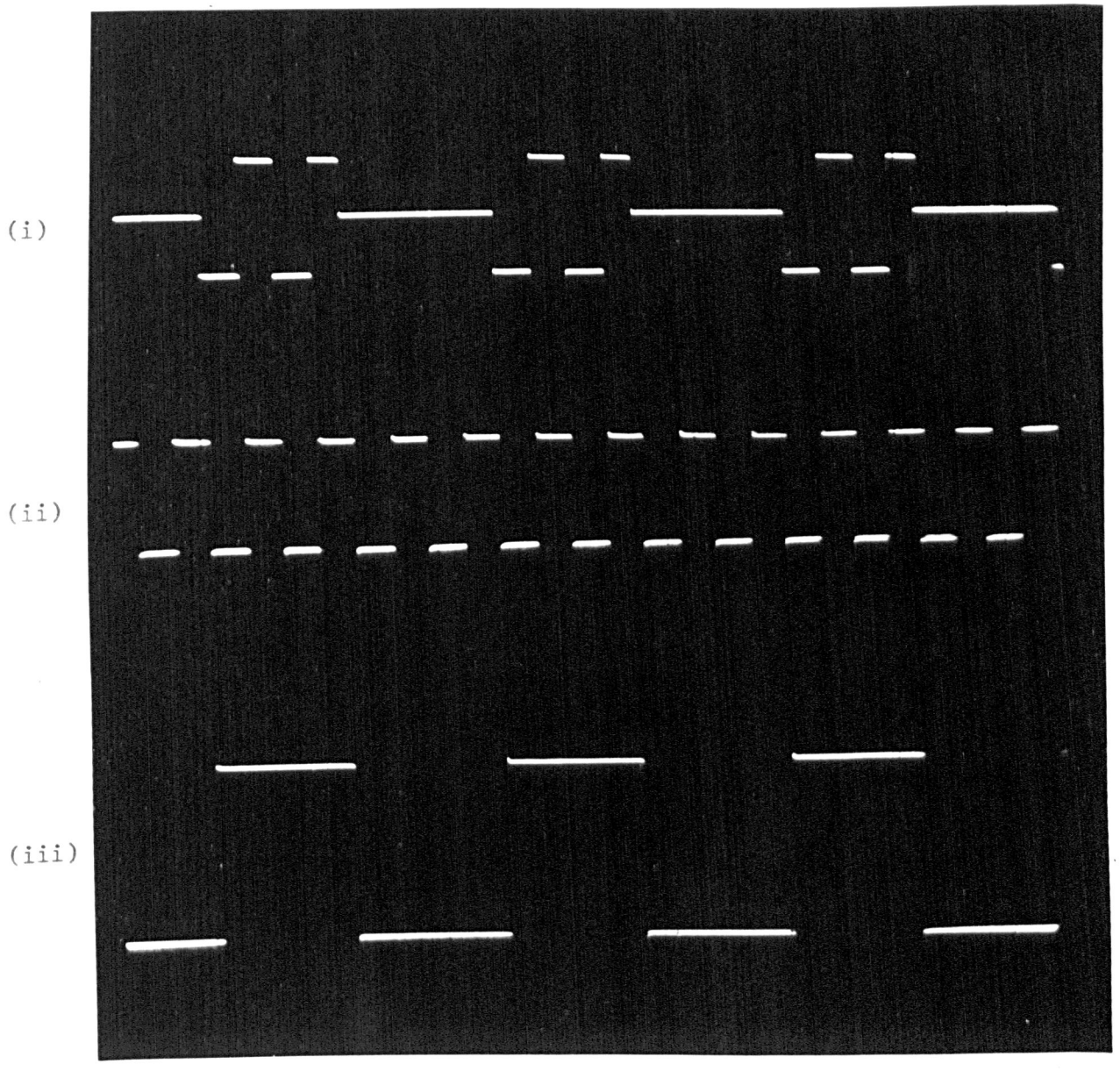
(i)
(ii)
(iii)

FIG. 5.14.

PHOTOGRAPH SHOWING D.C. COUPLED ANALOGUE GATE ASSEMBLY MOUNTED IN THE COPPER-BLOCK

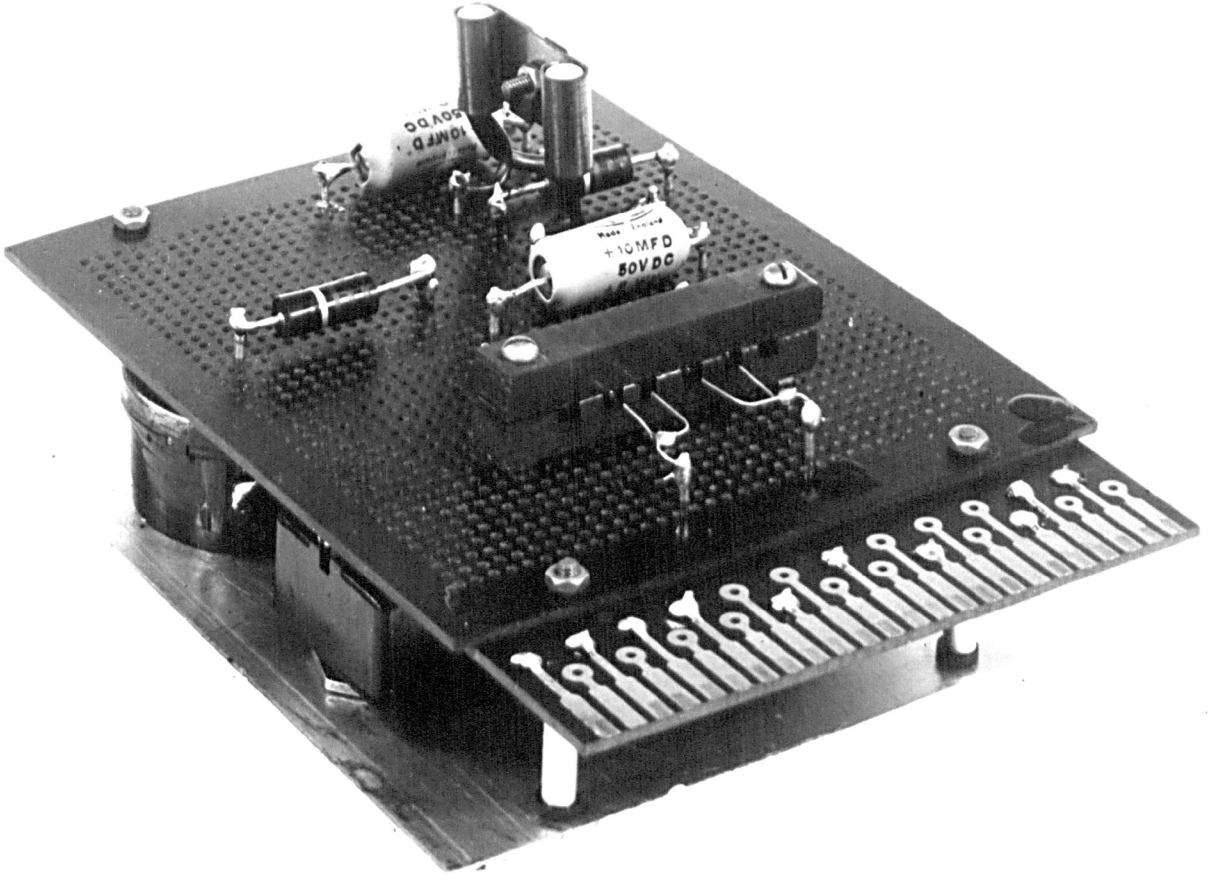
+10MFD
50VDC

by application of a pulse of duration T_I to the NOT INHIBIT input of the CAT, the time for which the stretched output is accepted and processed in the memory. The design and performance of the hold circuit is discussed below; the NOT INHIBIT input to the CAT and the NOT INHIBIT pulse generator are described in a later part of this thesis.

The hold circuit consists, basically, of a capacitor on which a voltage, corresponding to the height of the sampled pulse of signal, is stored. The voltage across the capacitor is monitored by means of an extremely high impedance circuit. When the analogue gate is ON the low output impedance of the NS 301 D.C. amplifier, preceding the gate, is effectively connected across the storage capacitor enabling the voltage of the capacitor quickly to adjust to the output of the D.C. amplifier. However, when the gate is OFF there is a negligible discharge path for the capacitor, and, thus, the capacitor voltage remains essentially constant at the voltage of the previous sampling pulse. Hence, the resulting output of the high impedance monitor represents a time stretched version of the short duration signal pulse.

A circuit diagram of the hold circuit is shown in Fig. 5.15 showing the method of connection to the gate signal output. The U110 is a p channel field effect, or unipolar, transistor (F.E.T.) manufactured by Silconix and forms the high impedance capacitor voltage monitor circuit. The circuit configuration is known as a source follower and extends the inherent high input impedance of the F.E.T. to the full. The circuit is analogous to the emitter follower arrangement using a bipolar transistor and exhibits similar properties; possessing a voltage gain of approximately

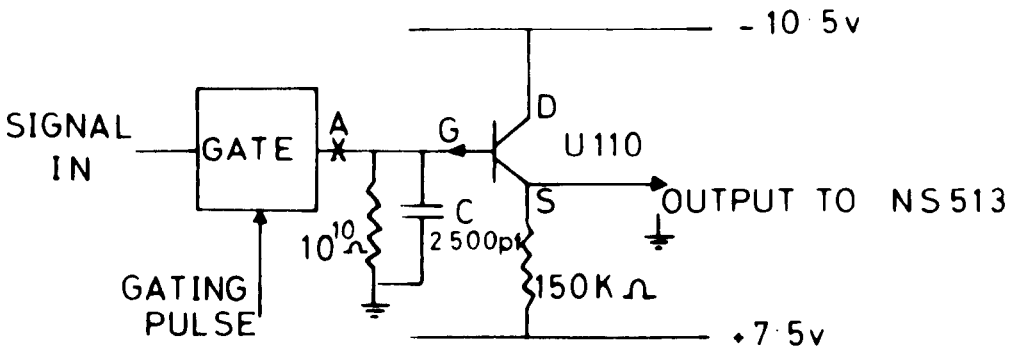

FIG.5.15. DETAILS OF SAMPLE AND HOLD CIRCUIT

unity while exhibiting a much greater input impedance. The total impedance from point A to earth (Fig. 5.15) was calculated as $2 \times 10^9 \Omega$ by observing the rate of decay of the voltage stored on the 2,500pf capacitor with the gate held in the permanently OFF position. The holding time, rather severely defined by Blume as RC/100, is 50msecs and is the time required for the voltage to decay to 0.990 of its initial value.

When the gate is ON, the $10^{10}\Omega$ resistor in the input is effectively shunted by 10KΩ - a combination of the ON impedance of the gate to earth and the output impedance of the D.C. amplifier - so that the risetime is at worst 25μsecs; a sampling time, T_s, of 100μsecs being used. If a shorter sampling time is required, the value of C in Fig. 5.15 can easily be reduced to as low as 750pf before the Blume holding time approaches T_I = 15msecs.

The combined properties of the sample and hold circuit were investigated using the circuit portrayed in Fig. 5.16. Typical appearances of the waveforms at points (2) and (3) are shown for a ramp input at point (1) for long (1msec) and short (50μsec) values of T_s respectively in Figs. 5.17 and 5.18.

With short values of T_s the sample and hold circuit forms a very close approximation to a Boxcar generator of the Lawson and Uhlenbeck type described earlier.

5.3.4 Design of the logic and timing equipment

The logic and timing circuits consist of four main sections:

(1) The stimulus generator

(2) Delayed sampling pulse generator

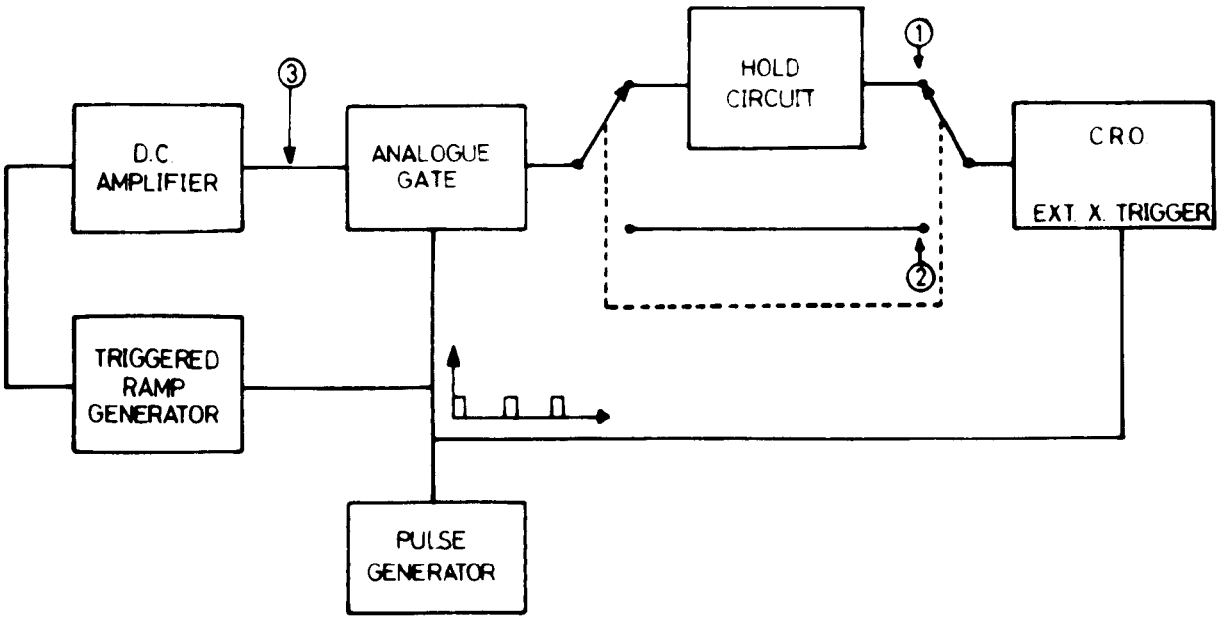

FIG.5. 16. BLOCK DIAGRAM OF EQUIPMENT USE TO OBSERVE FUNCTIONING OF SAMPLE AND HOLD CIRCUIT.

(3) N-step inhibit circuitry

(4) NOT INHIBIT generator

5.3.4.1 The stimulus generator

The type of stimulus required to generate transient paramagnetic species in a sample obviously depends on the type of samples under investigation.

In the experimental work described in this thesis, an investigation on the formation and decay of oxygen atoms, produced by the r.f. dissociation of oxygen gas, was carried out. The stimulus system used for this investigation is depicted in Fig. 5.19. A purely electronic system was used instead of the relay multivibrator used by Parker (5) which was considered imprecise. The lowest frequency square wave available from the square wave generator (Farnell L.F.1) is 1c/s and as the stimulus repetition rate, needed for the experiments was -$\frac{1}{2}$c/s, this frequency was divided by four by using two bistable multivibrator circuits in cascade. This arrangement gave equal ON and OFF times for the stimulus; in later experiments on oxygen shorter ON times (~150msec) than OFF times (~1sec) were used, as a time saving measure, and these were provided by an unsymmetrical free-running astable multivibrator which replaced the square wave generator and divide by four circuit in Fig. 5.19. The electronic keying circuit for the transmitter consisted of an emitter follower, using a Texas 2N3702 silicon transistor, with a variable emitter load R_1, R_1 being adjusted so that the transmitter is just off with no gating voltage at the emitter follower input. A negative going pulse turned the transmitter on, a positive pulse switching it off.

FIG. 5.17

TYPICAL WAVEFORMS OBTAINED USING CIRCUIT DEPICTED IN FIG. 5.16. WITH LONG GATE ON TIME

(i) Sample and hold output

(ii) Signal output of gate

(iii) Signal input to gate

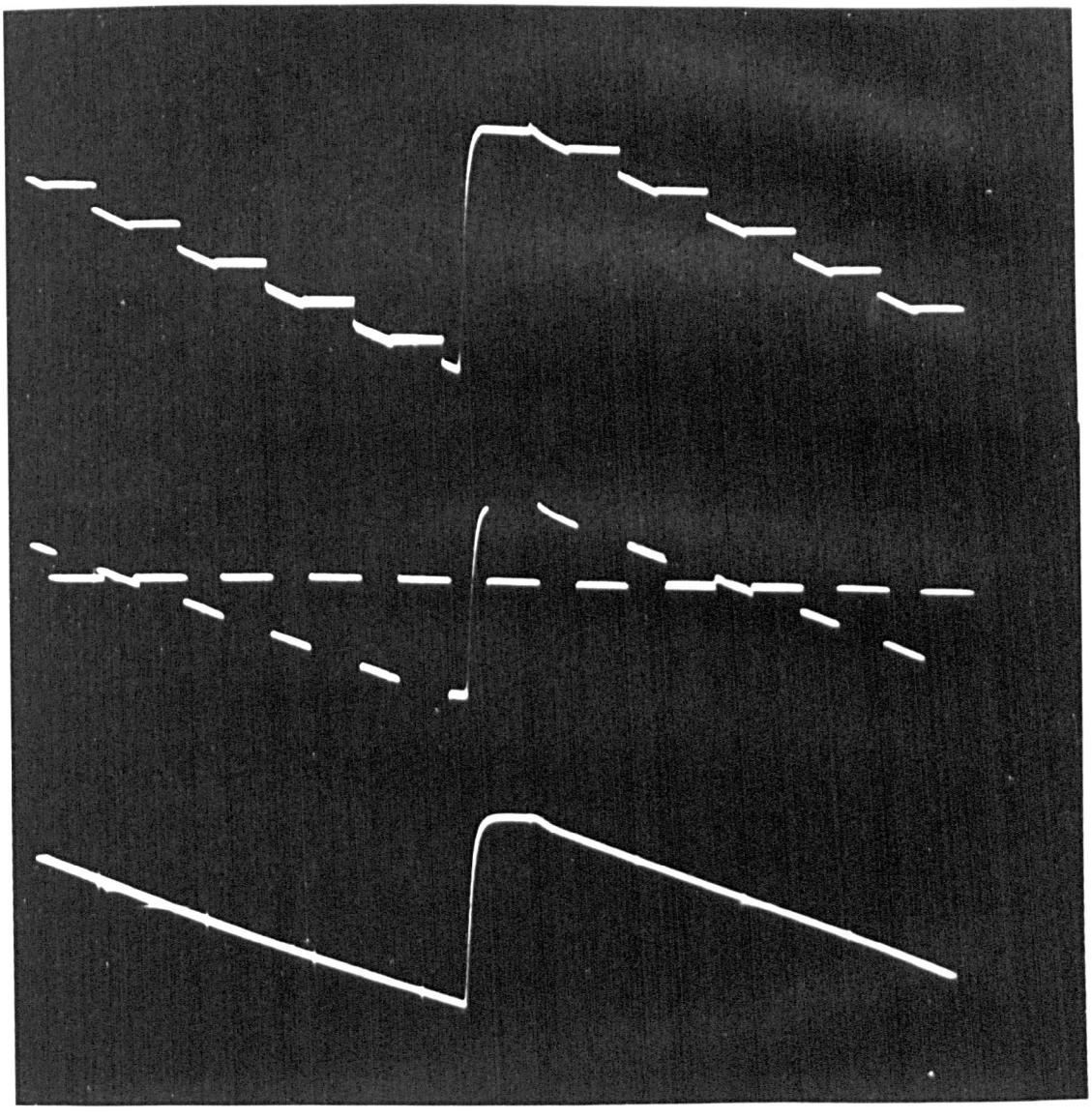
(i)
(ii)
(iii)

FIG. 5.18.

TYPICAL WAVEFORMS OBTAINED USING CIRCUIT DEPICTED IN FIG. 5.16 WITH A SHORT GATE ON TIME

(i) Sample and hold output

(ii) Signal output of gate

(iii) Signal input to gate

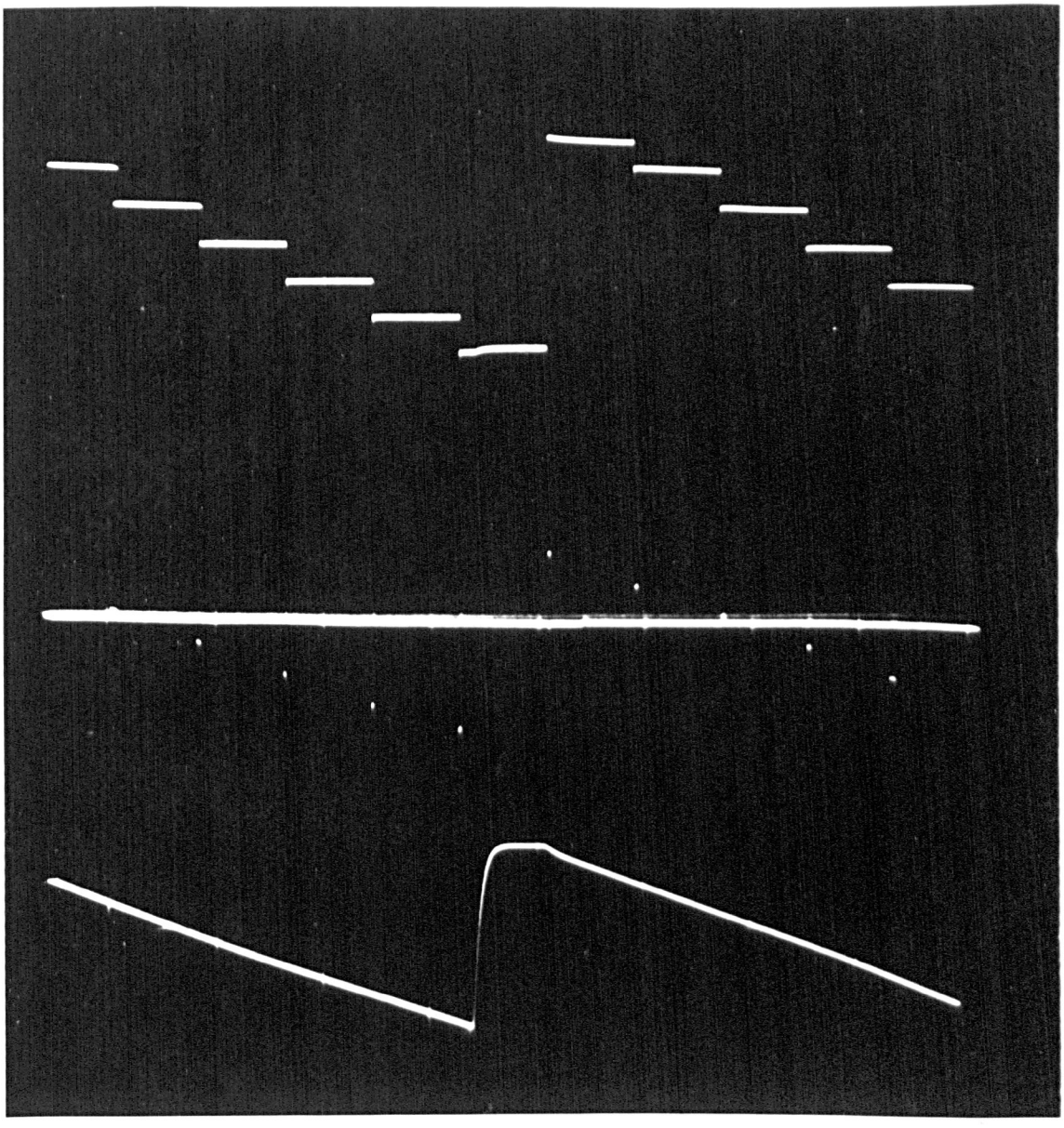
(i)
(ii)
(iii)

5.3.4.2 The delayed sampling pulse generator

The function of the delayed sampling pulse generator is to provide gating pulses, suitable for turning the analogue gate from the OFF to the ON mode, for a duration T_s. The timing and duration of the sampling pulses must be extremely precise and accurately controllable over a wide range. In order that the hold circuit functions correctly, the gate transition times from OFF to ON, or vice-versa, must be executed extremely rapidly, and the gate held in whichever mode is intended. In order to minimise the sources of inaccuracy digital timing techniques, in binary code, are used throughout because of their independence of amplitude. A block diagram of the timing system is shown in Fig. 5.20 together with the typical appearance of the pulses at various points. A complete circuit diagram is shown in Fig. 5.21, the transistors being numbered 1 to 12 from top to bottom. The design procedures and properties of the various sections will be discussed below.

(i) Trigger pulse amplifier

The pulse obtained at the cessation (for observations of decay) or onset (for formation process observations) of the stimulus is differentiated and greatly amplified by transistor 1. By means of polarity dependent feedback it is possible selectively to amplify either the negative or positive 'spike' by selection with a switch, (S.W.2). Transistor 2 accepts outputs from the first stage and acts as a unity gain phase inverter and is also switched in and out of operation by S.W.2. It is thus possible to produce a sharp negative going pulse from the leading edge of either negative or positive going trigger pulses by

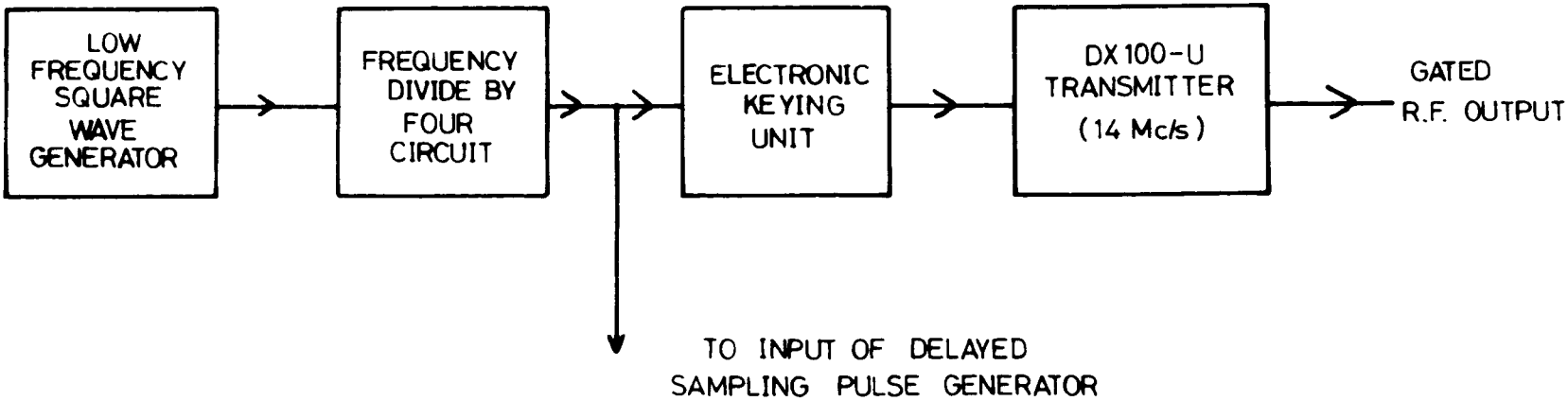

FIG. 5. 19. BLOCK DIAGRAM OF STIMULUS GENERATOR SYSTEM USED IN THE OBSERVATION OF OXYGEN ATOMS.

selection with S.W.2. The selection is necessary as the following stage, a Schmitt trigger, requires a negative pulse to operate it.

(ii) Schmitt trigger S1

A Schmitt trigger has the property of changing states extremely rapidly when a certain threshold voltage, V_t, is present at its input. Thus if the input voltage $V_{IN} < V_t$, the Schmitt trigger will remain in its quiescent state (with the input transistor, 3, non-conducting and the output transistor, 4, conducting); when V_{IN} exceeds V_t the Schmitt circuit changes extremely rapidly to its triggered state (the inverse of the quiescent state). In the triggered state the collector of the first transistor (3 in S1) is more positive than in its quiescent state the collector of the second transistor (4 in S1) being more negative. When V_{IN} falls below V_t the Schmitt trigger rapidly returns to its quiescent state. Thus the Schmitt trigger can be used to sharpen up slow rise and fall pulses providing the pulse amplitudes are greater than V_t, producing a sharpened inverted pulse at the first collector and a sharpened non-inverted pulse at the second collector. The Schmitt trigger used in the circuitry described operates from a negative going pulse when in its quiescent state. The negative pulse output from the pulse amplifier is passed, via a trigger level potentiometer, to the Schmitt trigger; the positive going output pulse (from the first collector) is coupled to the input of the following circuit which is a monostable multivibrator and is described below.

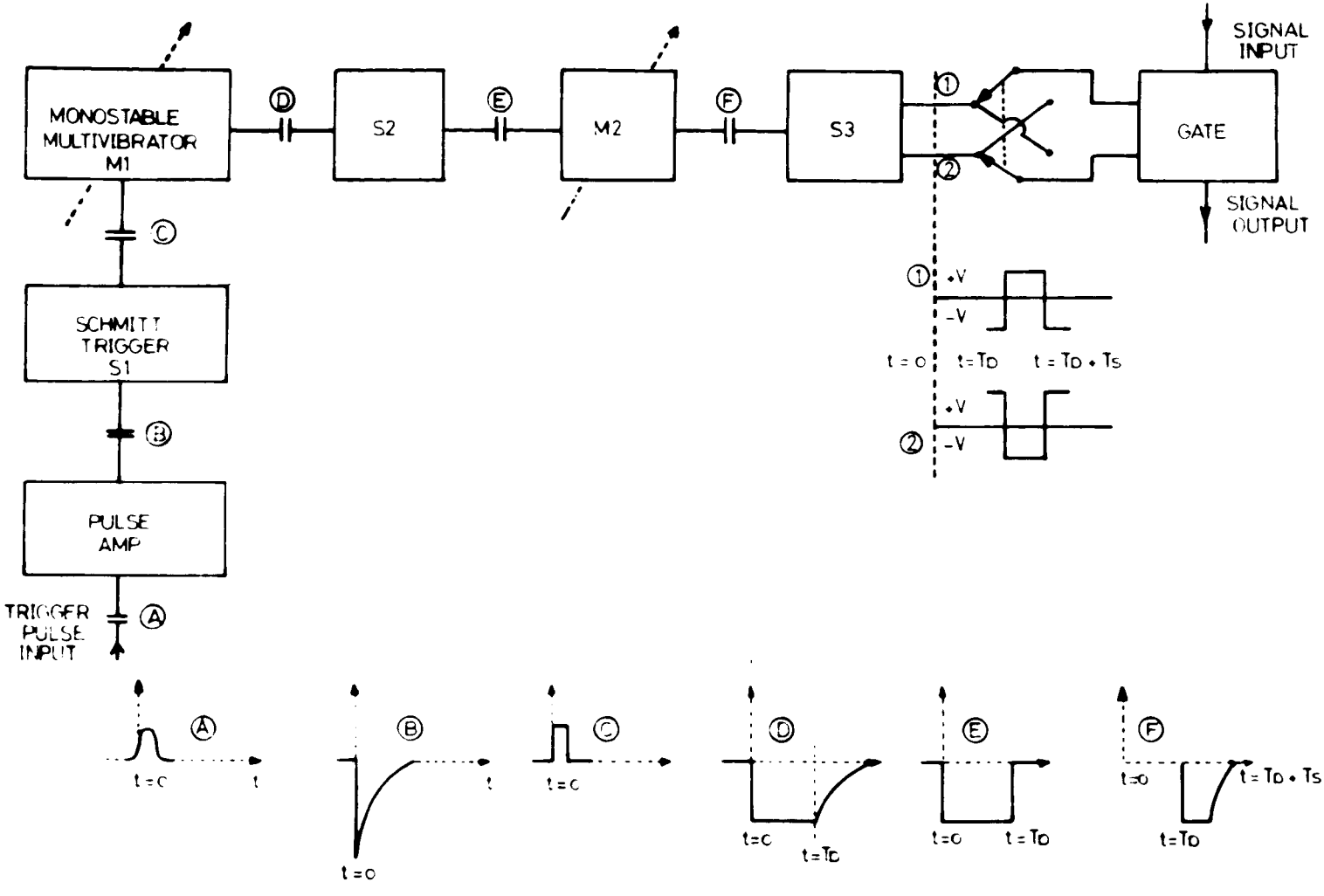

FIG.5. 20. BLOCK DIAGRAM OF DELAYED SAMPLING SYSTEM.

(iii) Generation of the delay time, T_D

The delay time, T_D, required between the trigger pulse at the pulse amplifier input and the gating pulses for the analogue gate is provided by a monostable multivibrator, M1. The monostable multivibrator, like the Schmitt circuit, possesses two states. The monostable circuit remains in its quiescent state until a positive going pulse is applied at its input whereupon it changes over to a quasistable state. The time for which the circuit remains in the quasistable state is dependent entirely on certain circuit parameters within the circuit; in the case of M1 the relevant components are C_D and R_D, and the quasistable duration, T_D, is approximately $C_D R_D$ seconds (C_D in farads, R_D in ohms). The output from the second collector of the monostable (collector 6) is a positive going pulse of duration T_D and this is directly coupled to a Schmitt circuit (S2) working in the inverted mode because of the steady state negative voltage at the second collector of M1. The direct coupling is a necessary feature in order to cope adequately with large values of T_D.

(iv) Generation of the sampling and gating pulses

The positive going trailing edge of the pulse from the collector of transistor 7 (S2) is A.C. coupled to a second monostable multivibrator M2, with a quasistable duration T_S. The output at the collector of transistor 9 (M2) is thus a negative going pulse of duration T_S delayed by a time T_D from the trigger pulse applied at the pulse amplifier input. The output from collector 9 is A.C. coupled to the input of a balanced Schmitt circuit, S3, which is so arranged that in its quiescent state the

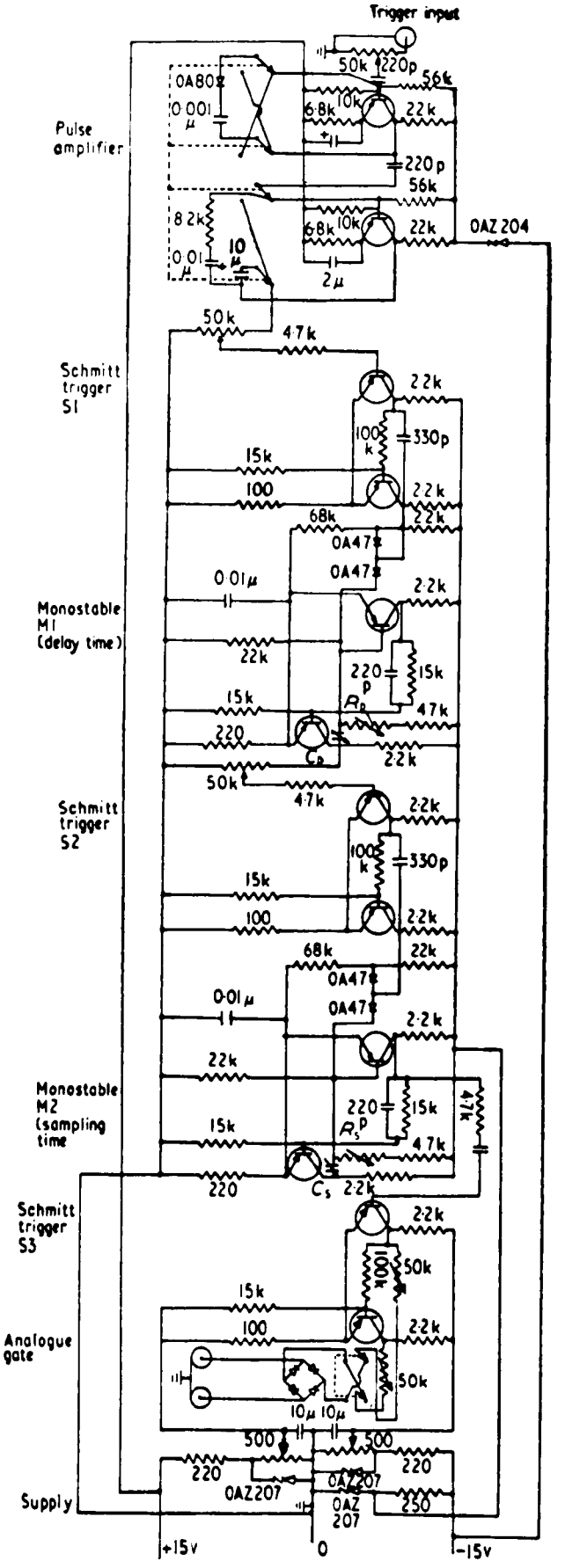

Fig. 21. Circuit of delay and sampling pulse generator showing connection to gate. (All transistors OC171).

collectors of transistors 11 and 12 are at ~ + 8v and - 8v with respect to earth and in its triggered state the position is reversed. The outputs of the Schmitt S3 are fed, via a reversing switch, SW1, to the gating inputs of the 4 diode analogue gate described in Section 5.3.3.2(i). SW1 is set so that the analogue gate is normally OFF (only being turned ON when a delayed sampling pulse triggers S3); the outputs of S3 are of the balanced form required to drive the gate.

(v) Switching speeds

The overall transition times for the analogue gate and switching system are minimised by the use of fast switching diodes and transistors. The inclusion of low valued collector loads in the switching transistors ensures that there are no large time constants due to stray capacitances. The pulse amplifier at the input of the timing circuitry is operated in the active region during its risetime, thus eliminating saturation and turn off effects. The trigger levels for the various digital devices (Schmitt triggers and monostable multivibrators) are made as low as possible consistent with good noise immunity and reliable operation. The transition times for the analogue gate are further reduced because gating overdrive is ensured by the use of adequate gating pulse amplitudes.

The use of the above techniques results in transition times of the order of 0.5μsec and these can be considered negligible. The main contributions towards the, albeit negligible, switching times arise from the charge storage occurring in the semiconductor diodes (OA202s) of the analogue gate. Reverse biased semiconductor diodes behave as voltage dependent capacitors obeying an approximate inverse square root voltage

FIG. 5.22.

PHOTOGRAPH OF DELAYED SAMPLING PULSE GENERATOR CIRCUIT BOARD SHOWING COPPER BLOCK MOUNTING ASSEMBLIES FOR DELAY AND SAMPLING MONOSTABLE MULTIVIBRATOR INPUT TRANSISTORS.

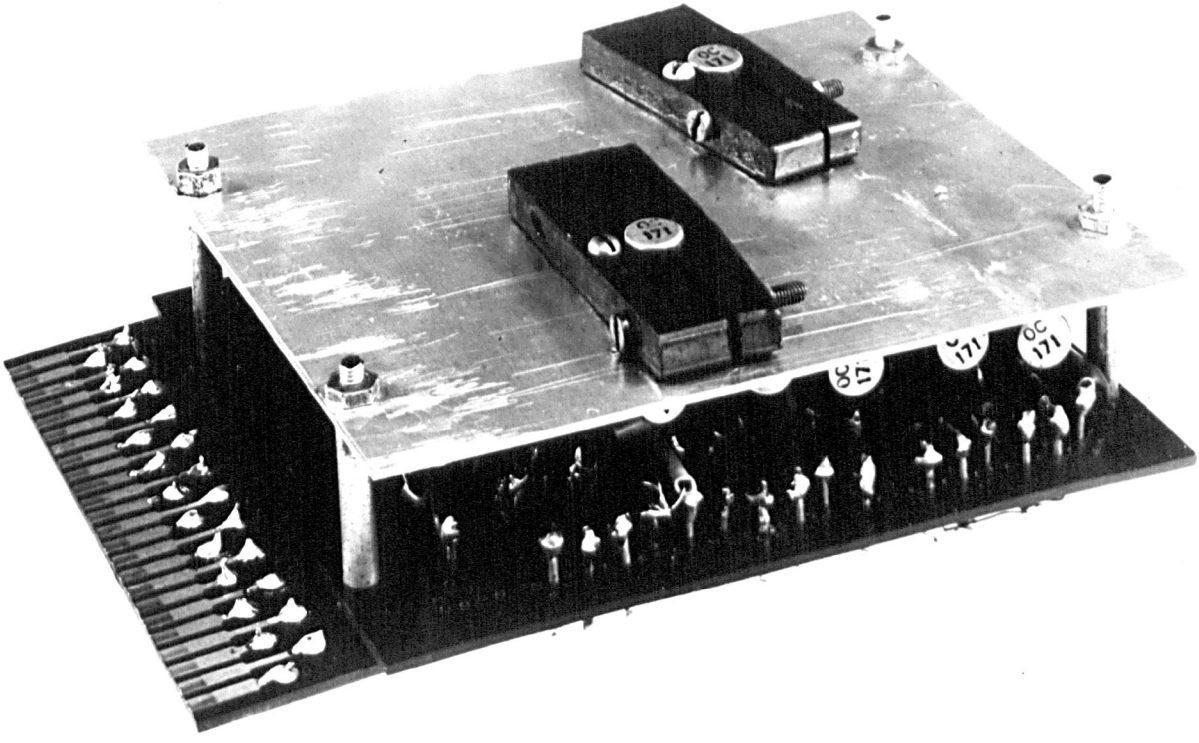
OC
171
OC
171
OC
171
OC
171

relationship. Thus in the transition from reverse to forward bias the charge stored in this depletion layer capacitance must be dissipated giving rise to a non-zero switching time and switching transients.

A forward biased semiconductor diode stores charge, in the form of minority carriers, and when the transition from forward to reverse bias occurs a reverse current continues to flow, i.e. under reverse bias conditions, for a finite time until the carriers have been removed.

A small contribution towards the switching time results from the fact that the balanced Schmitt circuit is operated in saturation but little improvement is to be gained by operation in the active region. The input transistors in the delay and sampling time monostables, normally conducting, are prevented from saturating by diode clamping of their bases; this measure ensures that the monostable trigger input remains sensitive by maintaining the input transistors in the active region where they exhibit a large gain. The disadvantage of operation in the active region is that the transistors tend to be more temperature sensitive than their saturated or cut off counterparts and, for this reason, transistors 5 and 9 are bolted to substantial copper heat sinks as shown in Fig. 5.22 to maintain their thermal stability. The timing instability caused by thermal effects is thus minimised; if desired the stability could be further improved by the use of silicon transistors and clamping diodes, but the timing is accurate to, at least, 0.1% over the period of one hour, after a five minute stabilisation period, which is perfectly adequate for its required use.

FIG. 5.23.

TYPICAL WAVEFORMS AT VARIOUS POINTS IN DELAYED SAMPLING PULSE GENERATOR:-

(i) Output of S1

(ii) Output of M1 (delay generator)

(iii) Output of S2

(iv) Output of M2 (sampling generator)

(v) Output of collector l1 } S3 Gating pulses

(vi) Output of collector l2 }

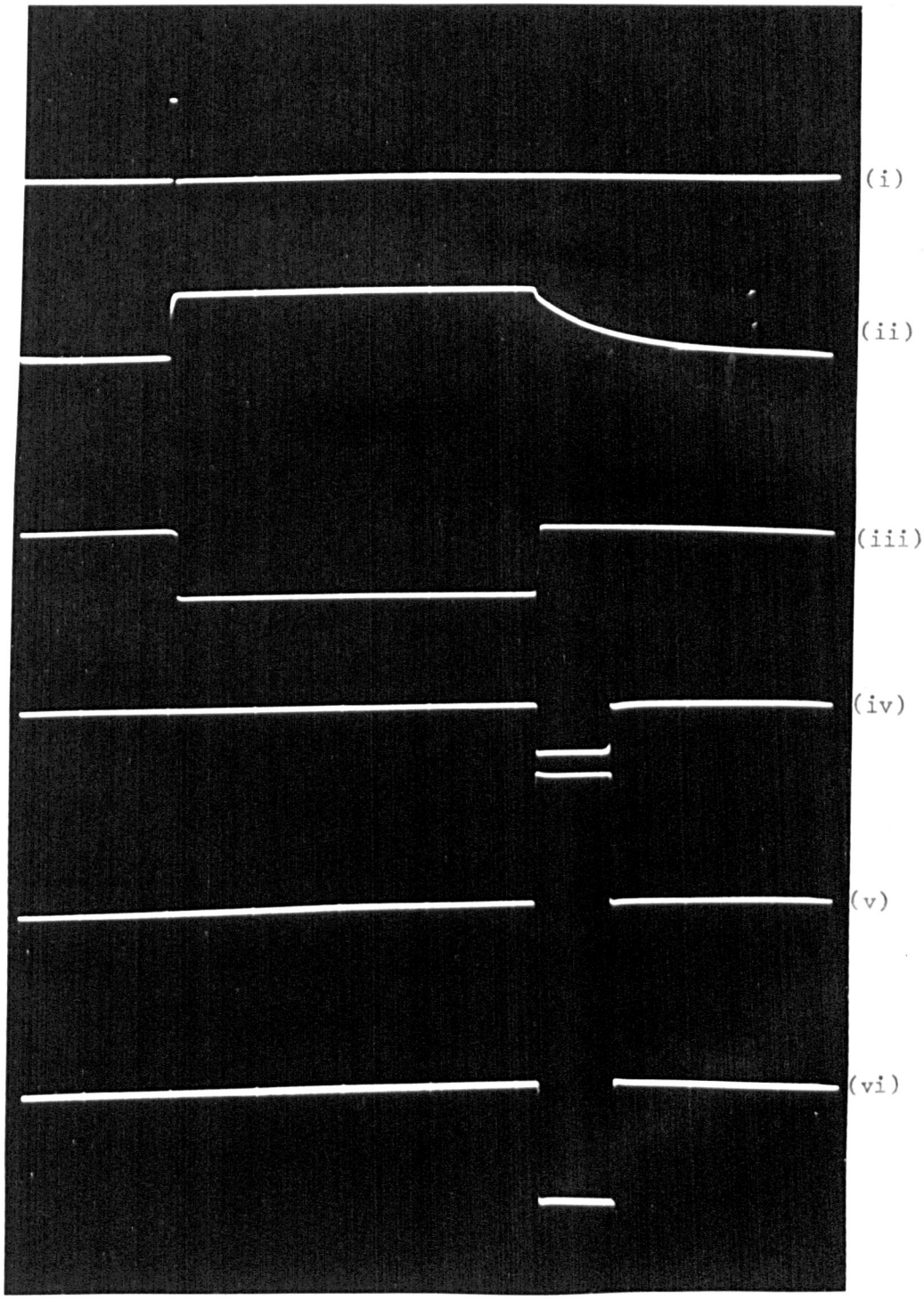
(i)
(ii)
(iii)
(iv)
(v)
(vi)

(vi) Performance of the complete circuit

The duration, T, of the quasistable state for the monostable circuit utilised in the timing circuit is given by T = 30 C msecs, where C is the capacitance of the timing capacitor in microfarads. T is variable by ±15% about this value by varying R between its limits. R_D and R_S, in the delay and sampling monostables respectively, take the form of 10 turn helipots for the fine control of the delay and sampling times respectively. The coarse control for T_D and T_S is provided by switched sets of capacitors C_D and C_S. Delay and sampling times variable over the range 25μsecs - 13.5secs and 25μsecs - 155msecs respectively can be selected.

The recovery time of the monostables used in the timing circuitry form a very important consideration particularly with regard to the delay time monostable. When a monostable multivibrator has been triggered into its quasistable state and reverted to its quiescent state a certain amount of time, called the recovery time, must elapse before the circuit can be triggered again if timings are to remain precise. The recovery time is usually some fraction of the quasistable time; in the monostable circuits used a duty cycle of 80% can be achieved before a measurable change occurs in the timing. The performance of the sampling time monostable is not as important in this respect because a time of at least T_D elapses between each of its T_s sec. duration quasistable states and it has already been established that $T_s << T_D$ (4.11.2).

The stabilised voltages for the delayed sampling pulse generator are provided by a Coutant KD100 transistorised supply. The values of T_D and T_s are monitored using a Marconi Instruments Frequency Counter TF1417/2.

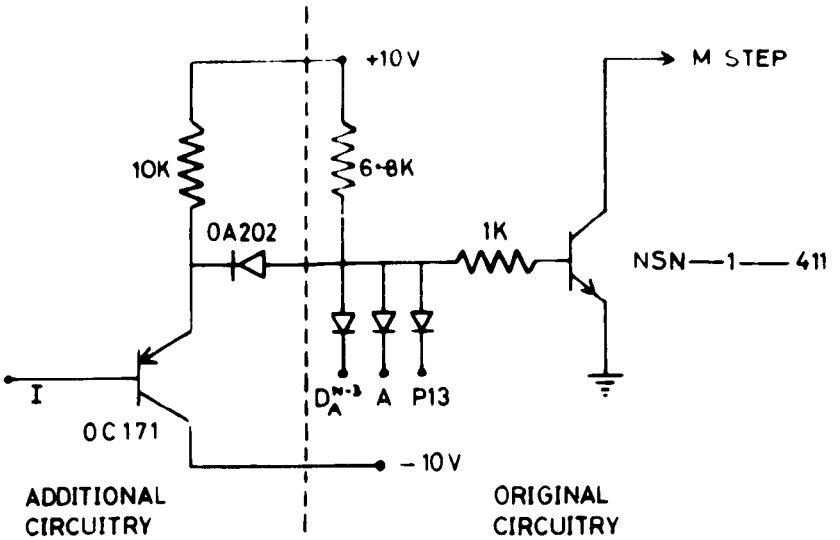

FIG. 5. 24. DETAILS OF M. STEP INHIBIT MODIFICATION TO NS513.

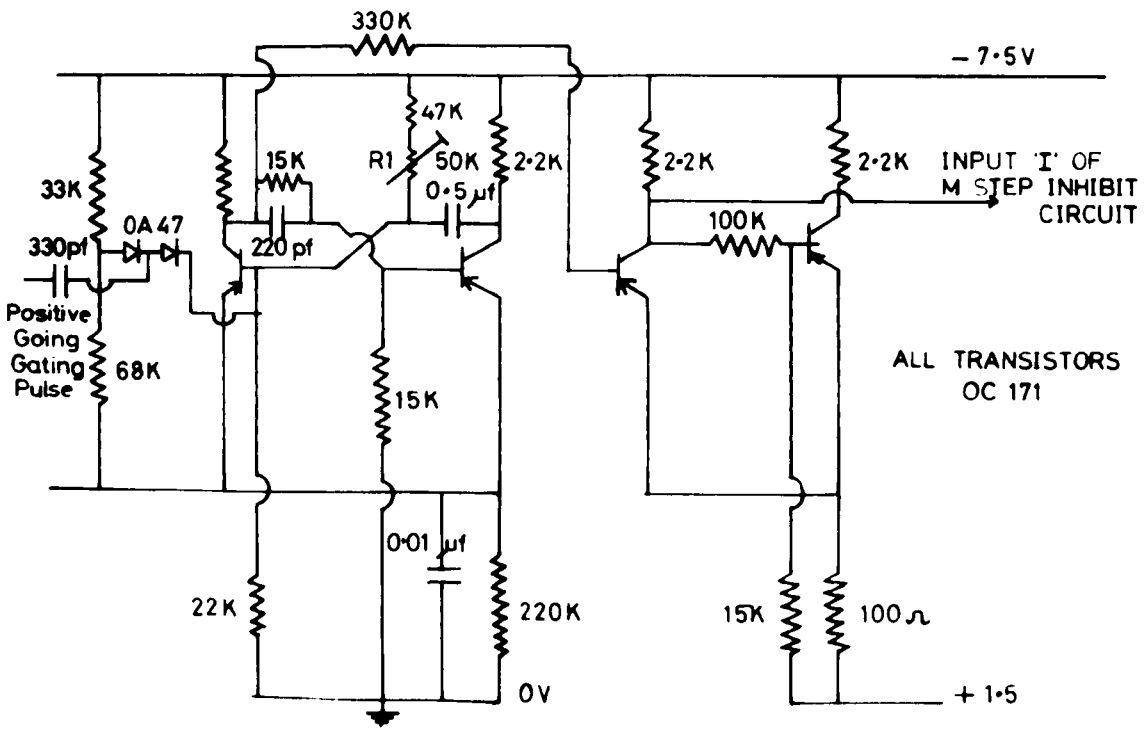

FIG. 5. 25. CIRCUIT DIAGRAM OF NOT INHIBIT PULSE GENERATOR

Photographs of the typical appearance of waveforms at the various points in the timing circuit are shown in Fig. 5.23.

5.3.4.3 The M step inhibit circuitry

It will be recalled, from the description of the principles of the C.S.S. method, that some form of distinction must be made between the "signal" and "no signal" conditions in order that only the relevant information is processed by the CAT. The method used will be referred to as a memory inhibit and ensures that information stored in the memory is only modified by input signals when instructed to do so.

A comparison of information stored in the memory with a signal at the input of the CAT is made at the rate of 25,600 times a second. Each comparison is preceded by an M step pulse provided by an AND gate and transistor within the CAT. In order to prevent a comparison with, and modifications of, the memory being made in the "no signal" condition, the M step is inhibited by the use of an additional diode in the AND gate at all times except when the "signal" condition prevails. Under the " "signal" condition a NOT INHIBIT, $\overline{I}$, pulse of 15msec duration is then presented at the inhibit input and thus the CAT accepts and processes information from the output of the hold circuit for this period. The M step inhibit circuit used to modify the NS513 Northern Scientific digital memory oscilloscope is shown in Fig. 5.24. If point "I" is positive operation is normal; i.e. the memory accepts information in the normal way. With "I" negative, the OA202 diode becomes conducting and the M step is inhibited and thus the memory will not accept information, but leaves unchanged any information previously stored in it.

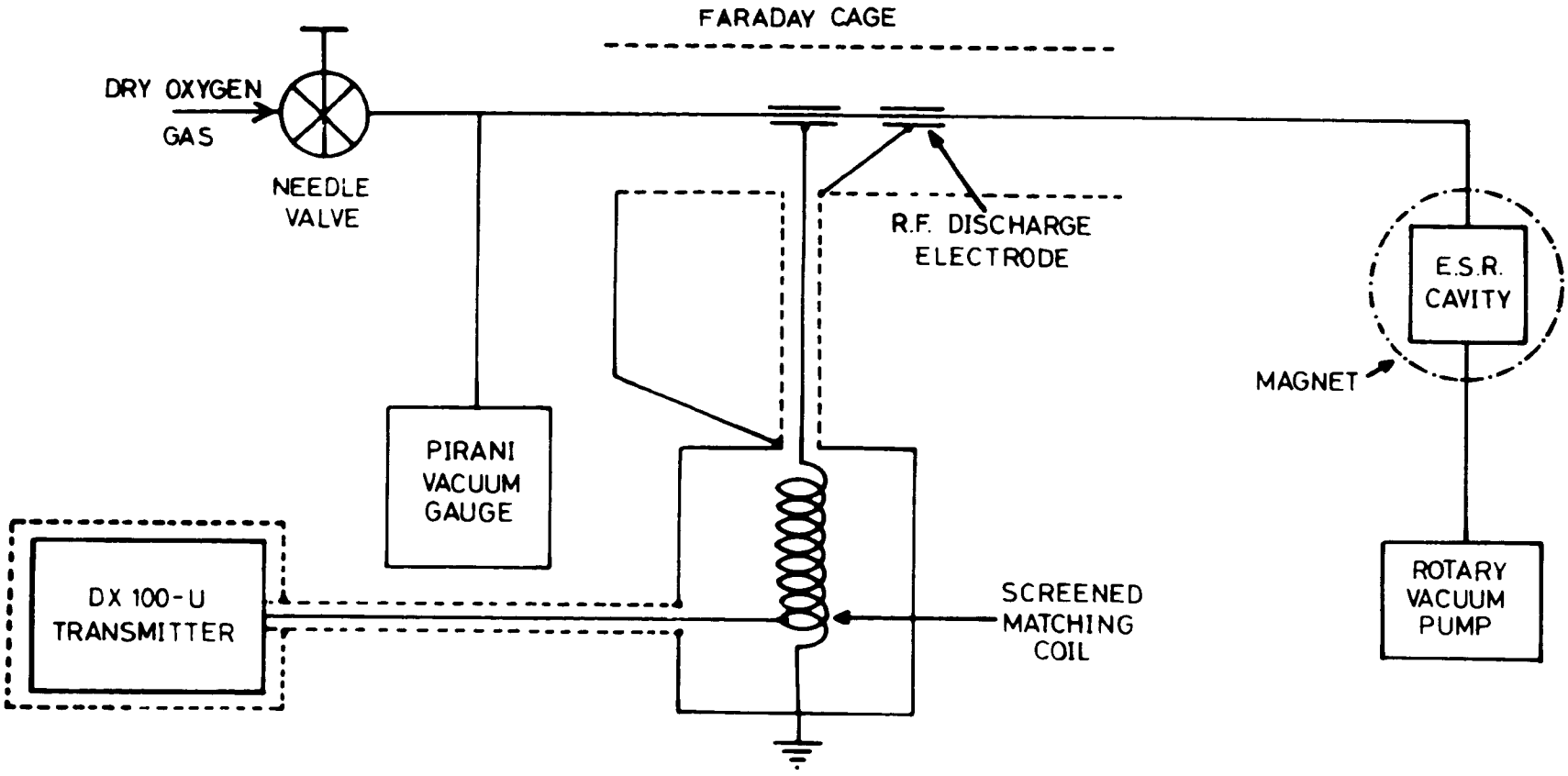

FIG.5. 26. SCHEMATIC DIAGRAM OF GASEOUS FLOW SYSTEM

5.3.4.4 The NOT INHIBIT pulse generator

The circuit of the M step NOT INHIBIT pulse generator is shown in Fig. 5.25. The circuit consists of a monostable multivibrator, of the type previously described, with a quasistable state of 15msecs duration, which is finely adjusted using R_I. The negative 15msec pulse, $\overline{I}$, is fed to a Schmitt circuit, the output of which is normally negative with respect to earth thus ensuring that the M step is inhibited. When the Schmitt circuit is triggered the output is made to swing positive with respect to earth by the use of a positive supply rail; this ensures that the OC171 transistor in the NOT INHIBIT circuit (Fig. 5.25) is firmly turned off and thus the operation of the CAT is normal for the duration, T_I, of the NOT INHIBIT, $\overline{I}$, pulse.

5.4 Description of the Gaseous Flow System

In order to evaluate the performance of the C.S. spectrometer, described in this thesis, a system capable of producing transient paramagnetic species was devised. An observation of the formation and decay of oxygen atoms, produced by the r.f. dissociation of oxygen gas, was carried out using the experimental set up depicted in Fig. 5.26.

The stimulus generator, already described, consisted of a Heathkit DX100-U transmitter operating at 14.2Mc/s. The transmitter was matched to the discharge using a matching coil consisting of 30 evenly spaced turns of 18S.W.G. enamel covered copper wire wound on a $3\frac{1}{2}$" diameter former 5" in length. The power from the transmitter was fed onto the first two turns of the coil and the power take-off for the discharge electrodes was

taken from the whole coil. The whole matching assembly was mounted in a screened metal box. The transmitter was mounted in a screened steel and wire netting cage. Earthing points were kept to a minimum. The purpose of the matching-coil was two-fold; first, it provided a step up in r.f. voltage thus facilitating an easy and definite start to the discharge; secondly, it provided a buffer between the transmitter and discharge, so that there was a minimum change in the load as "seen" by the transmitter between the "discharge off" and "discharge on" conditions.

The r.f. electrodes consisted of 1" strips of brass shim wrapped and clamped around the outside of the gas flow tube; the advantage of this arrangement is that the electrodes do not contaminate the sample. The discharge was shielded using a Faraday cage consisting of parallel copper wires joined electrically at one end and set in a cylindrical form around the discharge.

The discharge tube consisted of high purity quartz tube, outer diameter ~1cm and inner diameter 0.8cm. The discharge was situated well outside the D.C. magnetic field of the E.S.R. spectrometer and, in this way, any interaction between the discharge and the field was avoided. Operating the discharge in the field could be effected, by minimising the interaction, by positioning the discharge parallel to the magnetic field.

Dry oxygen gas from a British Oxygen cylinder was fed, to the quartz flow tube, via a pressure reducing valve and a needle valve which provided the fine pressure control.

A Pirani Vacuum Gauge (Speedivac Model 8/1) was used to measure the oxygen pressure in the discharge tube. After passing the pressure measuring head and r.f. electrodes the gas moved along the quartz tube which made a right angle bend and passed through the sample cavity. The end of the quartz tube was connected to a rotary vacuum pump which maintained the flow of oxygen through the tube at the pressure adjusted by the needle valve.

The system contained many variable and interdependent parameters and was essentially a qualitative system intended to demonstrate that the rapid recording spectrometer worked satisfactorily. Reliable turn on of the discharge could only be ensured between 0.55 and 0.8 torr.

A description and analysis of the results obtained with this system is given in the following chapter.

REFERENCES

1. Schuster, N.A., Rev. Sci. Inst. 22, 254 (1951).

2. Faulkner, E.A. and Harding, D.W., J. Sci. Inst. 43, 97 (1966).

3. Millman, J. and Puckett, T.H., Proc. I.R.E. 43, 29 (1955).

4. Millman, J, and Taub, H., 'Pulse and Digital Circuits' Ch. 14 (McGraw-Hill (1956)).

5. Parker, A.J., Lainé, D.C. and Ingram, D.J.E., J. Sci. Inst., 43, 688 (1966).

CHAPTER VI

EXPERIMENTALLY DERIVED SPECTRA

6.1 Introduction

With the completion of the construction and testing of the information processing section of the apparatus, the next step was to assess the performance of the complete system with a transient paramagnetic specimen.

6.2 The Choice of a Suitable Sample

Several systems were considered for use in testing the complete rapid recording spectrometer, including samples which produced transient paramagnetic centres on the application of U.V. irradiation. For example:

(i) Phosphorescent States

Paramagnetism of the metastable triplet (phosphorescent) state of molecules such as napthalene and quinoxaline in durene has been observed by many workers (1, 2, 3). Samples with Lucite as a host medium have been used by Thomson (4). The spectra obtained when $\Delta m = 1$ transitions occur between adjacent sublevels are highly anisotropic so that the resonance lines for polycrystalline samples are very broad and thus difficult to detect. Spectra involving the $\Delta m = 2$ transitions are comparatively isotropic but have a much lower transition probability. Difficulty was experienced in growing crystals of napthalene in durene and the few successful samples did not give detectable signals even in the steady state, when irradiated with a Phillips low pressure mercury arc lamp as a

u.v. source. Failure of these experiments was probably due to insufficient u.v. output from the lamp.

(ii) Paraquat

Paraquat or dimethyl 4 - 4' bipyridyl is a member of a group of compounds known as the Viologens. When irradiated with u.v. in an ethanol-water solution, the blue dipyridyl radical, called "Tony Blue" is formed. This radical gives a multiline E.S.R. spectrum as observed by Bruin et al. (5) and Johnson and Gutowsky (6). The lifetime of "Tony Blue" depends on its chemical environment being particularly sensitive to oxygen. Deoxygenated samples of paraquat dichloride in an aqueous ethyl alcohol solution were prepared by freeze-pump cycling and, on u.v. irradiation, they exhibited the characteristic blue colour and gave strong E.S.R. signals. No means was found whereby a reversible reaction could be produced; both the blue colour and the E.S.R. signal disappearing very rapidly on breaking the sample tube seal thereby admitting oxygen. Unfortunately insufficient quantities of paraquat dichloride were available to justify the use of a flow system.

6.3 Gaseous Free Radicals

Paramagnetic resonance of a gaseous free radical was first observed by Rawson and Beringer (7) in atomic oxygen produced by a micro-wave discharge in gaseous oxygen. Later observations were also made on atomic hydrogen (8) and atomic nitrogen (9). Krongelb and Strandberg (10) used paramagnetic resonance techniques to estimate the recombination times of atomic oxygen. Ultee (11) observed the paramagnetic resonance

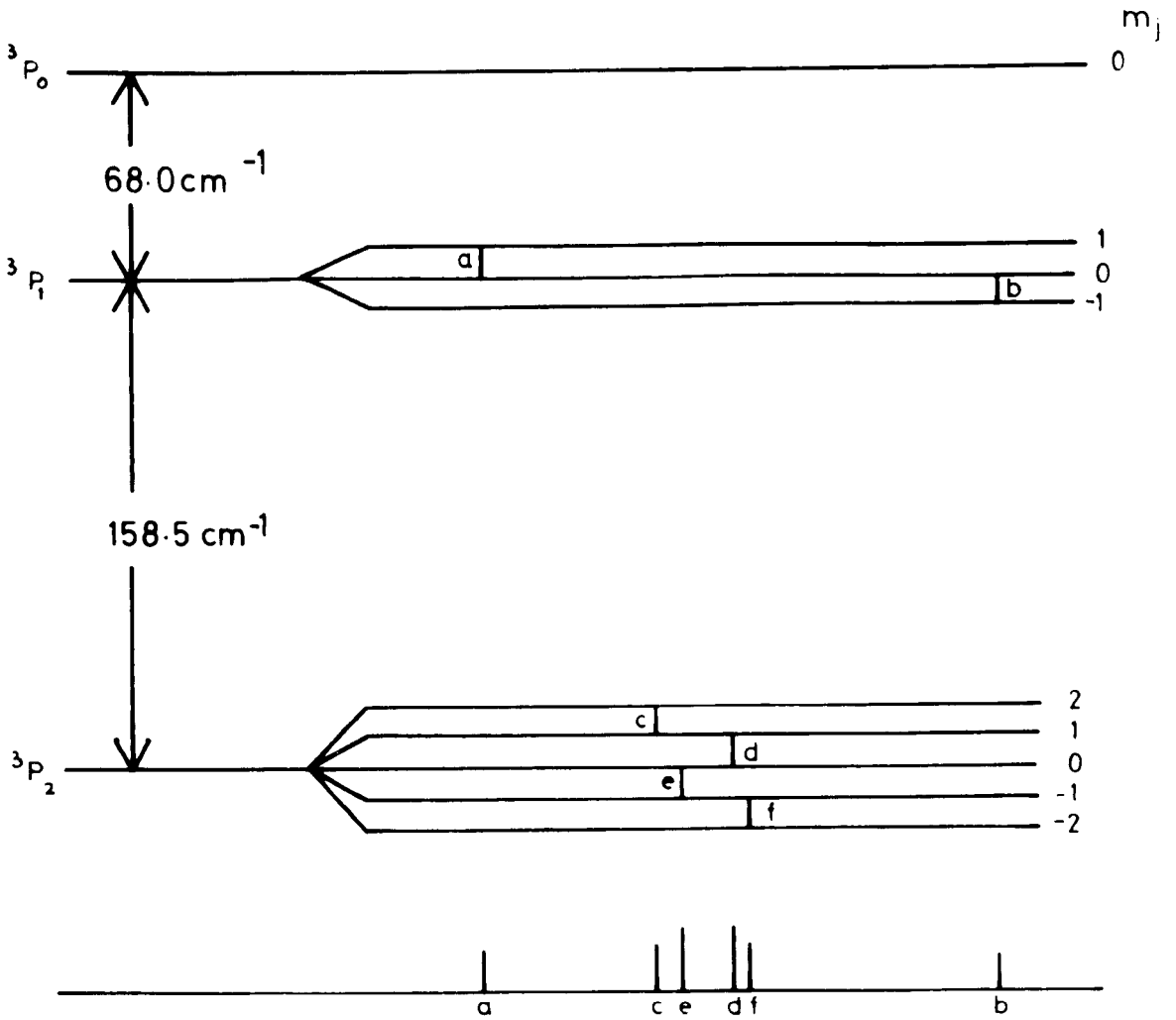

FIG. 6.1. ENERGY LEVELS AND ALLOWED E.S.R. TRANSITIONS OF ATOMIC OXYGEN IN A MAGNETIC FIELD

absorption of atomic nitrogen, hydrogen and oxygen over wide pressure ranges and has also observed the effect on the spectrum of atomic nitrogen of the addition of varying amounts of molecular oxygen.

Unsuccessful attempts were made to observed the spectra of atomic nitrogen and hydrogen produced by passing the respective gases through an r.f. discharge. During the observations on atomic nitrogen, its presence was definitely established as shown by the characteristic greenish yellow afterglow as described by Ultee (11); the inability to observe the spectra was probably due to saturation of the transitions with the microwave power.

Observations on atomic oxygen, produced in the gas handling system described in Chapter V, gave spectra which agreed well with those described by Ultee (11). Atomic oxygen undergoes recombination to form molecular oxygen and thus proves a suitable transient species.

6.4 The E.S.R. Spectrum of Atomic Oxygen

6.4.1 The expected spectrum

The energy level configuration of atomic oxygen in a magnetic field is shown in Fig. 6.1. The only significant states that undergo splitting in a magnetic field are the $^3P_1$ and $^3P_2$ levels to give 3 and 5 levels respectively. Far above the $^3P_0$ level there also exists a $^1D_2$ and $^1S_0$ state but, although the $^1D_2$ state will split into 3 levels in a magnetic field, the level has a low population due to the Boltzman factor; the absorption is proportional to the population difference between split levels which is proportional to the total population of the unsplit level and thus the $^1D_2$ state gives a very weak paramagnetic resonant absorption.

If Russell-Saunders or LS coupling holds, to form the total angular momentum vector J, a single line would be expected. Assuming LS coupling then the g value is given by:-

$$g = 1 + \frac{J(J+1) + S(S+1) - L(L+1)}{2J(J+1)} \qquad 6.1$$

Thus for a $^3P_2$ level (J = 2, S = 1, L = 1) and thus g = 1.5.

Similarly for a $^3P_1$ level (J = 1, S = 1, L = 1), g = 1.5.

Thus a single line at g = 1.5 would be expected from the ^3P levels with transitions a, b, c, d, e and f all contributing.

6.4.2 Observed spectra of atomic oxygen

The experimentally observed spectrum of atomic oxygen departs considerably from the simple single line expected. At pressures in the region of 0.1 torr and below the spectrum consists of four central lines, due to the $^3P_2$ transitions, and two outer lines, due to $^3P_1$ transitions, symmetric about these. The transition energies of the six lines are slightly different due to a phenomenon known as the Paschen-Bach effect.

The normal situation of Russell-Saunders or LS coupling occurs under weak field conditions when the orbital angular momentum $\underline{L}$ and the spin momentum $\underline{S}$ add vectorially to give a resultant angular momentum $\underline{J} = \underline{L} + \underline{S}$ giving rise to 2J+1 equispaced energy levels in a magnetic field. Under high field conditions the coupling between $\underline{L}$ and $\underline{S}$ is destroyed and the contributions of $\underline{L}$ and $\underline{S}$ must be considered separately. The magnetic field still splits the level into 2J+1 energy levels but they are no longer equispaced. Between these two extremes of LS coupling and L and S separate there is a transition from the weak to the strong field case;

this is known as the Paschen-Bach region. Thus in the case of atomic oxygen, the Paschen-Bach effect results in 6 lines at slightly different frequencies due to the different spacings of the 7 energy levels as shown in Fig. 6.1.

The difference in the overall population between the $^3P_1$ and $^3P_2$ levels is determined by the Maxwell-Boltzman distribution and thus the relative intensities of the $^3P_1$ and $^3P_2$ transitions gives a measure of the temperature of the oxygen atoms. Krongelb and Strandberg (10) used this technique to show that the oxygen atoms were at room temperature just beyond the discharge and this was later corroborated by Westenberg and de Haas (15).

The author's observations were concentrated on the spectra resulting from the $^3P_2$ transitions; as originally observed by Ultee (11) the four lines are pressure broadened into a single line at pressures above 0.2 torr. Experiments were conducted in the range 0.55 and 0.8 torr as the gated r.f. discharge became unstable outside this pressure range. The $^3P_2$ line was observed to have a width of approximately 3 gauss at these pressures.

6.5 Experimental Procedures

The experimental details peculiar to the observations on atomic oxygen are discussed below.

6.5.1 Preparation of quartz flow tube

The quartz tube was cleaned in order to present a pure and uniform surface to the atomic oxygen to prevent "recombination centres" forming at highly localised positions on the inner wall of the quartz tube.

The cleaning process consisted of soaking the whole inner surface of the tube in a mixture of concentrated hydrochloric and nitric acids for a period of twelve hours followed by alternate rinsings with absolute alcohol and deionised distilled water. At the beginning of each experimental run the system was flushed with oxygen gas and then pumped down to a pressure well below 0.05 torr and held at this pressure for at least two hours before oxygen was again admitted and any experiments carried out.

6.5.2 Adjustment of the gas flow system

The essential features of the gas handling system have already been outlined in Chapter 5.4 and Fig. 5.25. Flexible connections between the oxygen cylinder, needle-valve and experimental tube and to the rotary pump and Pirani gauge were provided by thick walled rubber pressure tubing, silicon vacuum grease being used to provide seals at the various junctions. The oxygen cylinder pressure was lowered to approximately 2lb/sq. in. using a British Oxygen pressure reducing head screwed to the cylinder; the pressure in the experimental tube was adjusted to the desired value by using the needle valve as a controlled leak. After an initial adjustment period of ~5 minutes the pressure remained constant throughout the total experimental period.

6.6 Estimation of Relative Concentrations of Atomic Oxygen

A field modulation spectrometer using phase sensitive detection gives a first derivative of the resonance absorption curve at its output, as shown in Chapter 2.4.3 and Equations 2.34 and 2.35.

Lifetime broadened absorption lines tend to be Lorentzian in shape,

whereas inhomogeneous broadening gives rise to a Gaussian line. The majority of E.S.R. lineshapes encountered in practice thus approximate to a Gaussian or Lorentzian shape although notable exceptions are the Dysonian line shape for samples such as sodium and unsymmetrical lineshapes for certain powder samples with anisotropic g factors.

The paramagnetic concentration of samples exhibiting Gaussian or Lorentzian lineshapes may be estimated by measuring the peak-to-peak height, h, of the derivative providing certain conditions are satisfied and these are briefly discussed below.

6.6.1 Gaussian line

A Gaussian line has the form:-

$$g(H) = g(H_o)\, e^{-k(H-H_o)^2} \qquad 6.2$$

The concentration, C, of a paramagnetic sample with lineshape g(H) is represented by the area under this curve.

$$\text{i.e.} \qquad C = \int_0^\infty g(H)dH \qquad 6.3$$

$\therefore$ from Equations 6.2 and 6.3:-

$$C = g(H_o)\sqrt{\pi/k} \qquad 6.4$$

The first derivative of the absorption is given by differentiation of Equation 6.2:-

$$g'(H) = \frac{d(g(H))}{dt} = -g(H_o)2k(H-H_o)e^{-k(H-H_o)^2} \qquad 6.5$$

FIG. 6. 2. APPEARANCE OF E.S.R. SPECTRUM OF $^3P_2$ OXYGEN ATOMS AT VARIOUS STAGES DURING THEIR FORMATION. ($g = 1.5$) ($p = 0.65$ torr.)

The maximum and minimum points of the derivative occur at fields H_{max} and H_{min} given by:

$$g'(H_{\substack{max \\ min}}) = 0 \qquad 6.6$$

$$g''(H) = -2kg(H_o)\ e^{-k(H-H_o)^2}\left[1 - 2k(H - H_o)^2\right] \qquad 6.7$$

$$\therefore\ H_{max} - H_o = H_o - H_{min} = \sqrt{1/2k} \qquad 6.8$$

The peak to peak height, h, of the derivative curve is given by:

$$h = \left|g'(H_{max}) - g'(H_{min})\right| = 2g(H_o)\sqrt{2k}\ e^{-\frac{1}{2}} = 2Ck\sqrt{2/\pi e} \qquad 6.9$$

If b is the "width" of the line defined as $H_{max} - H_{min}$, then:-

$$b = \sqrt{2/k} \qquad 6.10$$

$\therefore$ from Equations 6.9 and 6.10:-

$$h = \frac{4}{b^2}\, C\, \sqrt{2/\pi e} \qquad 6.11$$

6.6.2 Lorentzian line

The equation for a Lorentzian line is:-

$$g(H) = \frac{g(H_o)}{1+A^2(H-H_o)^2} \qquad 6.12$$

The use of a similar procedure to the one outlined above for the Gaussian line yields:-

$$h = \frac{C\sqrt{3}}{b^2\pi} \qquad 6.13$$

6.6.3 Time dependent concentration measurements

Thus for both Gaussian and Lorentzian lines the "height", h, of the first derivative is directly proportional to the concentration, C,

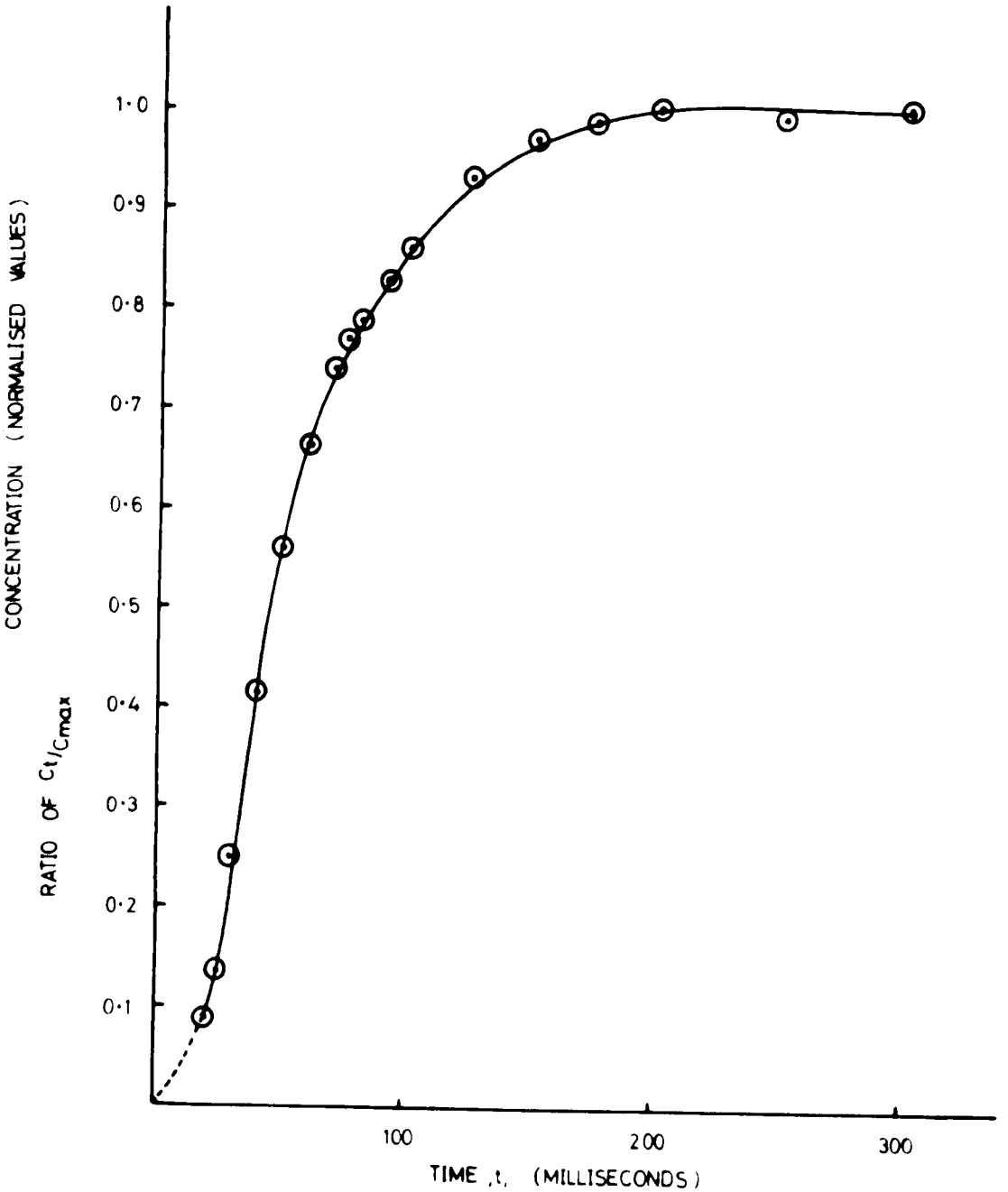

FIG. 6. 3. GRAPH OF CONCENTRATION OF OXYGEN ATOMS AGAINST TIME DURING FORMATION. (NORMALISED VALUES) (p=0·65 torr.)

providing the "width", b, of the derivative remains constant.

The results outlined below, for the formation and decay curves of oxygen atoms, are derived by measuring the peak to peak height, h, of the derivative of the absorption. In all cases b appeared constant and h was used as an estimate of the concentration C. It was assumed that the pressure broadened $^3P_2$ lines approximated to a Lorentzian line so that the above method of estimating the concentration is justified; in fact, the use of the 1st derivative in estimating the concentration of gaseous free radicals has been used by many authors (13, 14, 15).

6.7 Formation Times of Oxygen Atoms in a Gaseous Discharge

The $^3P_2$ line of atomic oxygen was recorded at various times after the onset of the 14.2Mc/s discharge. The appearance of the spectrum at various times during its formation is shown in Fig. 6.2. A plot of C_t/C_{max} is shown in Fig. 6.3 where C_t = the concentration at time t after the onset of the discharge and C_{max} is the maximum concentration achieved by the atomic oxygen.

Making the assumption that the formation is of the form:-

$$C_t = C_{max}(1 - e^{-t/\tau_f}) \qquad 6.14$$

where τ_f is the formation time of the process then:-

$$\log (1 - C_t/C_{max}) = - \frac{t}{\tau_f} \qquad 6.15$$

Thus if the time dependence of C_t is of the form of Equation 6.14 a log plot of $(1 - C_t/C_{max})$ against time t (linear) will give a slope $- \frac{1}{\tau_f}$ intercepting the $(1 - C_t/C_{max})$ axis (t = 0) at 1. A log plot of Equation 6.15 is shown in Fig. 6.4 and, as predicted, is a straight line.

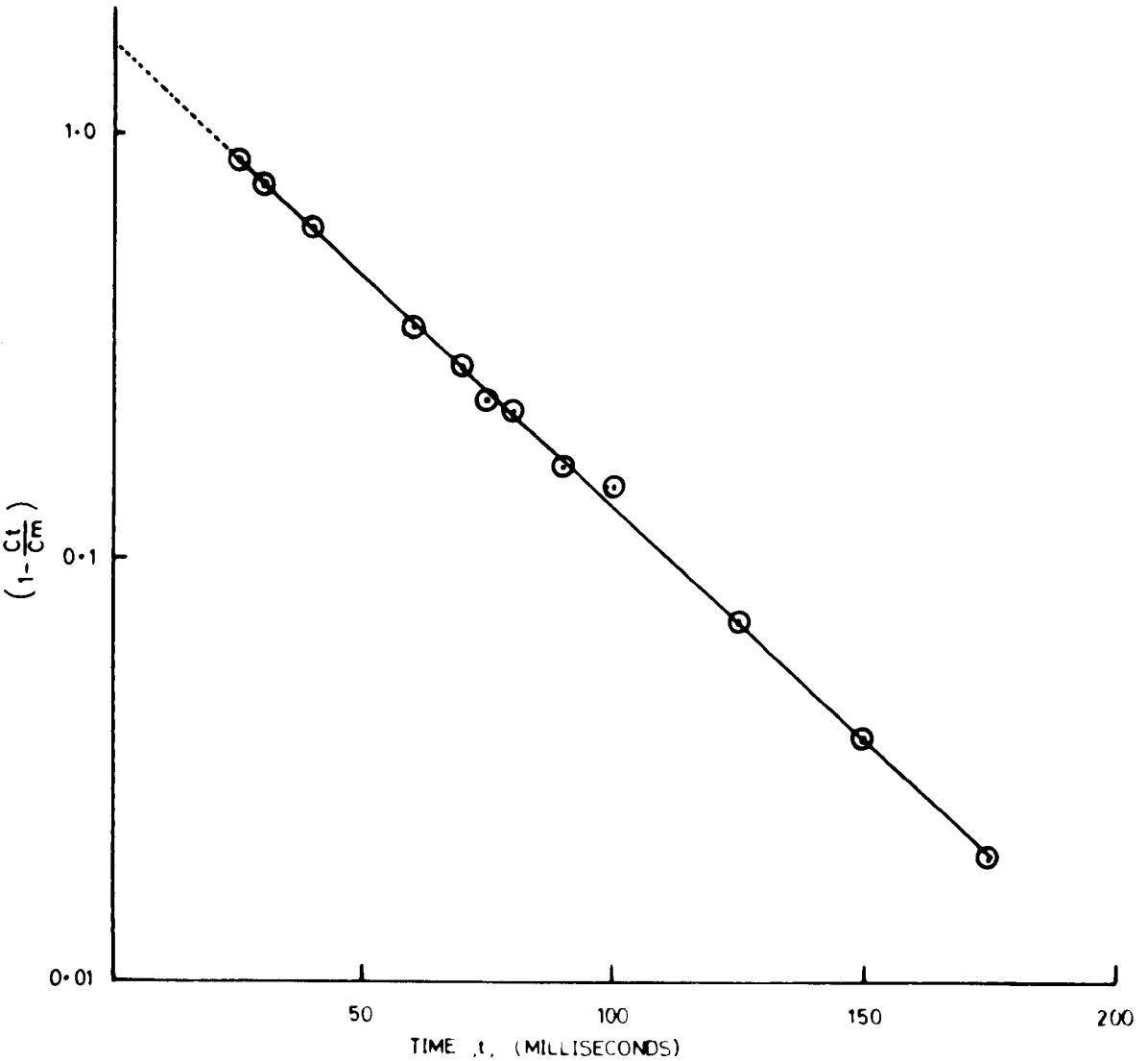

FIG. 6. 4. LOG GRAPH OF $(1-\frac{Ct}{Cm})$ AGAINST TIME FOR THE FORMATION OF OXYGEN ATOMS. (p = 0·65 torr.)

However it intercepts the logarithmic $(1 - C_t/C_{max})$ axis at 1.6 and thus a more accurate formulation would be of the form:

$$C_t = C_{max}(1 - e^{(-t/\tau_f - K)}) \qquad 6.16$$

where $e^K = 1.6 = 1 - C_o/C_{max}$.

There thus appears to be an initial concentration with a negative value and it may be concluded that during the initial stages, the formation, where the signal was too small to measure accurately, is not of the form of Equation 6.14, but a somewhat slower process. Thus extrapolation back to t = 0 gives an apparent negative initial concentration.

The initial slow formation rate may possibly be due to a certain time requirement for the discharge to form in the gas. The risetime of the r.f. oscillator was measured to be ~2μsecs and this is negligible compared with the period over which the slower formation process extends indicating that the initial slow rise was probably governed by physical rather than electrical factors.

The formation time, τ_f, deduced from the slope of the straight line graph in Fig. 6.4 is $\tau_f \simeq 40$msecs.

6.8 Decay Times of Atomic Oxygen

The experiments conducted on the formation and decay times of atomic oxygen were primarily of a qualitative nature and the parameters affecting the decay processes were not varied in any controlled way but were maintained as steady as possible throughout the series of experiments.

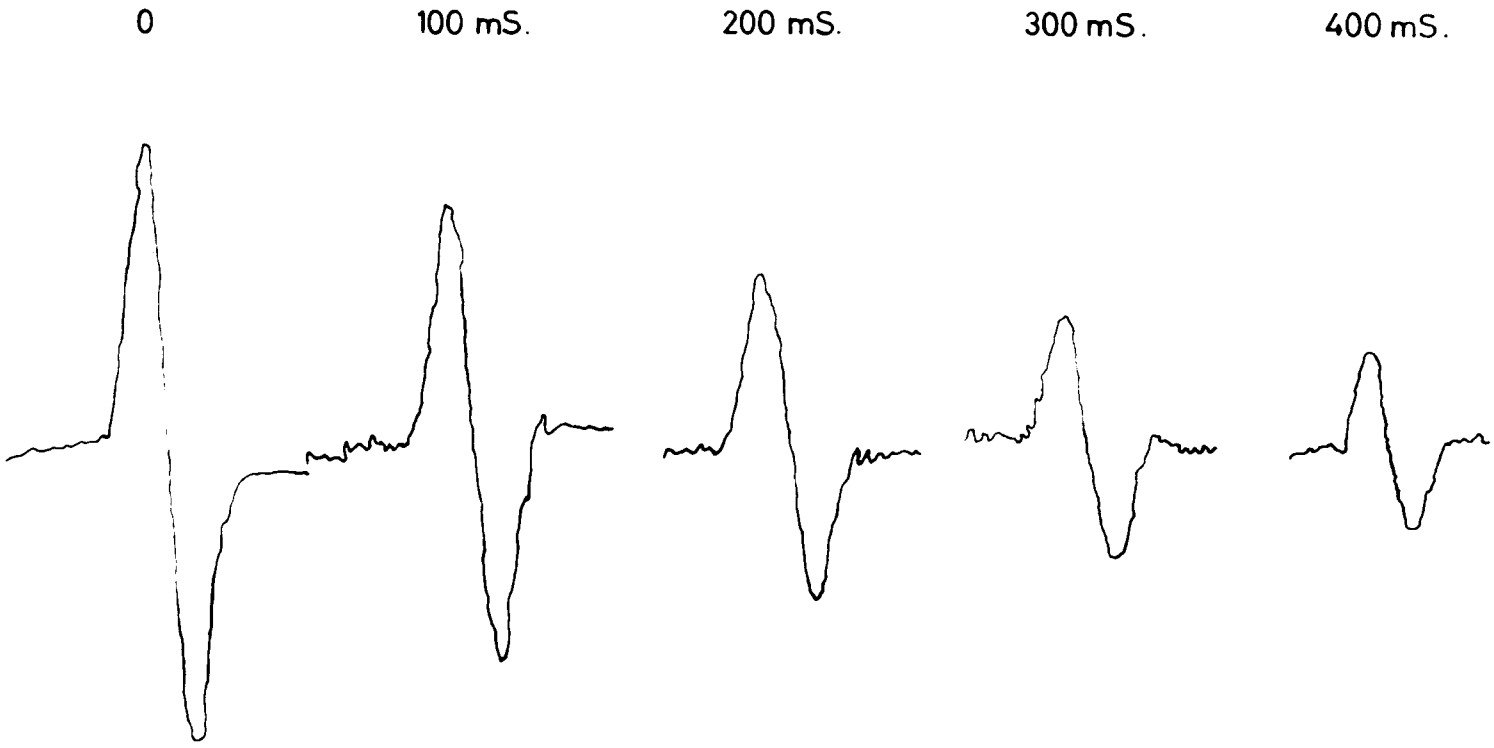

FIG. 6. 5. APPEARANCE OF E.S.R. SPECTRA OF $^3P_2$ OXYGEN ATOMS AT VARIOUS STAGES DURING THEIR DECAY. (g=1·5)(p=0·65torr.)

Krongelb and Strandberg (10) and recently, in more detail, Kaufman (12) have studied the possible recombination process of atomic oxygen.

There is a possibility of three main recombination processes occurring:-

(i) A first order recombination process occurring at the walls of the quartz discharge tube, $O + O + 3rd\ body \rightarrow O_2$.

(ii) A second order wall recombination process.

(iii) A second order process involving molecular oxygen as the "third body" - volume recombination. A first order process is described by the equation:-

$$\frac{dC}{dt} = - k_1 C \qquad 6.17$$

where C is the concentration and k_1 is known as the first order rate constant. The solution to Equation 6.17 is:-

$$C_t = C_o\, e^{-k_1 t} \qquad 6.18$$

where C_o and C_t are the initial concentration and the concentration at time t respectively.

Equation 6.18 may be rewritten as:

$$\frac{C_t}{C_o} = \text{normalised concentration} = e^{-t/\tau_D} \qquad 6.19$$

where $\tau_D = \frac{1}{k_1}$ = decay time of the recombination process.

Thus a log plot of normalised concentration, C_t/C_o, against time, t, will give a straight line of slope $-\frac{1}{\tau_D}$ for a first order decay process.

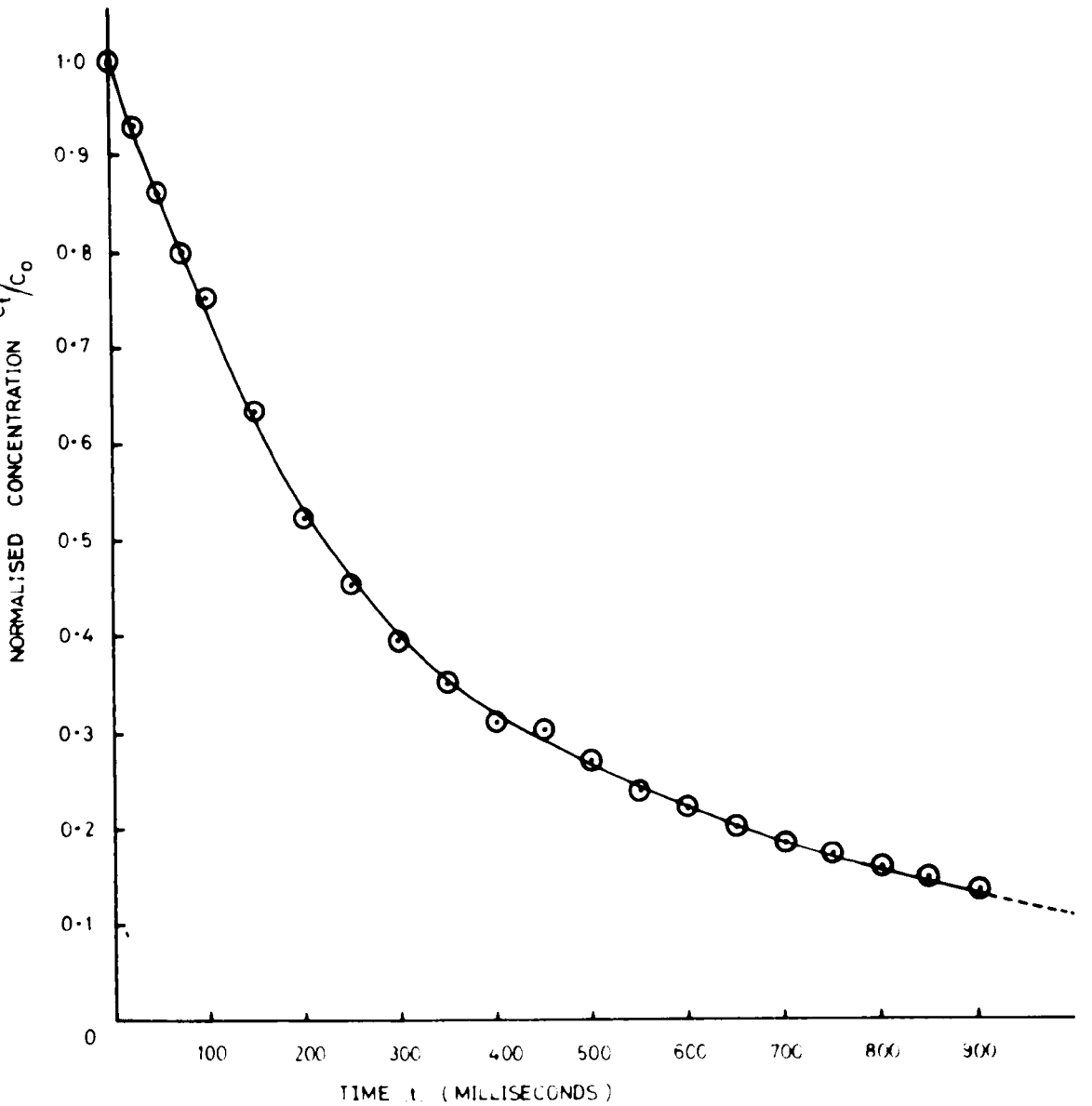

FIG. 6. 6.

LINEAR PLOT OF NORMALISED CONCENTRATION C_t/C_o AGAINST TIME, t, FOR THE DECAY OF $^3P_2$ OXYGEN ATOMS. (p = 0·65 torr.)

A second order process is of the form:-

$$\frac{dC}{dt} = - k_2 C^2 \qquad 6.20$$

where k_2 is the 2nd order rate constant.

The solution to Equation 6.20 is:-

$$\frac{1}{C_t} = k_2 t + \frac{1}{C_o} \qquad 6.21$$

and thus a plot of $\frac{1}{C_t}$ vs. time t will give a straight line of slope + k_2 with an intercept of $\frac{1}{C_o}$ on the $\frac{1}{C_t}$ axis.

Typical appearances of the spectra at various times after the cessation of the r.f. discharge are shown in Fig. 6.5; a plot of normalised concentration C_t/C_o v. time is shown in Fig. 6.6 and a log plot of C_t/C_o against time is drawn in Fig. 6.7. A reciprocal plot of the process was also drawn, but it did not give a straight line. The graph in Fig. 6.7 consists of two straight lines which probably indicates the admixture of one or more second order processes with the dominant first order process. Kaufman (12) indicates that with the type of experimental tube used volume recombination only becomes noticeable at pressures of 1 torr, being negligible at pressures of 0.1 torr. Sets of measurements were made in the region 0.5 → 0.8 torr where the volume recombination will only form a very small part of the decay process and thus the 1st and 2nd order wall or surface recombinations are probably the dominant mechanisms in the decay process. Reference to Kaufman's paper (12) suggests that the error in k_1 due to the use of a flow system is negligible for the pressures and tube dimensions used.

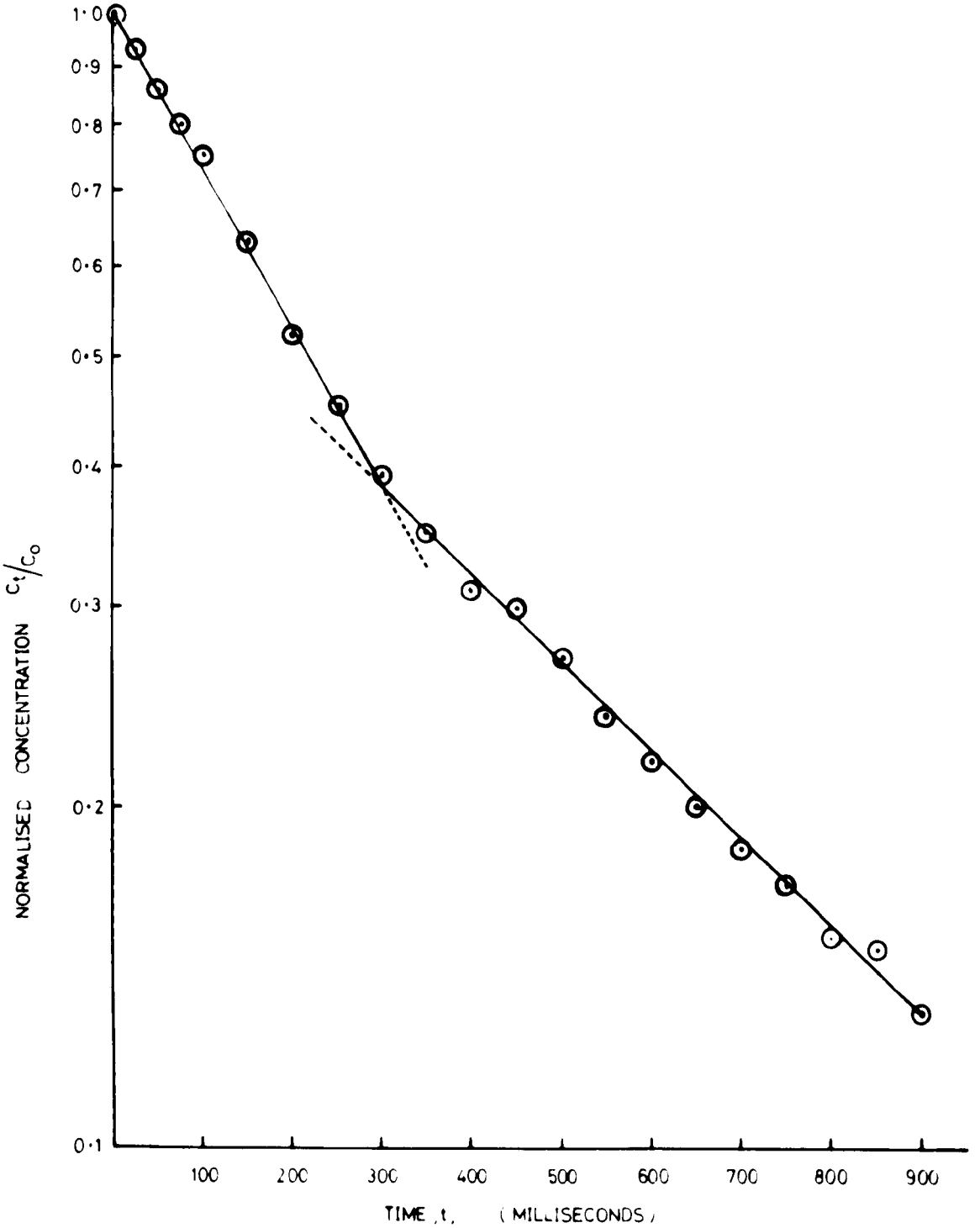

FIG. 6. 7

LOG PLOT OF NORMALISED CONCENTRATION C_t/C_o AGAINST TIME, t, FOR THE DECAY OF $^3P_2$ OXYGEN ATOMS. (p = 0·65 torr)

As an approximate indication, the slopes of the two straight lines in the graph shown in Fig. 6.7 were calculated and separate lifetimes assigned to each, i.e.

$$\frac{C_t}{C_o} = e^{-t/\tau_{id}} \qquad \text{for the initial (low t) process} \qquad 6.22$$

and $$\frac{C_t}{C_o} = e^{-t/\tau_{fd}} \qquad \text{for the final process} \qquad 6.23$$

Based on Equations 6.22 and 6.23, values of τ_{id} = 313msecs and τ_{fd} = 554msecs were obtained from the graph in Fig. 6.7. Kaufman (12) quotes a value for $\tau = \frac{1}{k_1}$ of between 200msecs and 1 second. A mean value $\tau_m = \frac{\tau_{id} + \tau_{fd}}{2}$ was calculated as ~430msecs and this forms a fairly good agreement with Parker's (16) value obtained with a similar tube.

REFERENCES

1. Vincent, J.S. and Maki, A.H., J. Chem. Phys. 39, 3088 (1963).

2. Van der Waals, J.H. and de Groot, M.S., Mol. Phys. 2, 339 (1959).

3. Hutchinson, C.A. and Mangum, B.W., J. Chem. Phys. 34, 908 (1961).

4. Thomson, C., J. Chem. Phys. 41, 1 (1964).

5. Bruin, F., Heinken, F.W., Bruin, M. and Zahlan, A., J. Chem. Phys. 36, 2783 (1962).

6. Johnson, C.S. and Gutowsky, H.S., J. Chem. Phys. 39, 58 (1963).

7. Rawson, E.B. and Beringer, R., Phys. Rev. (Letters) 88, 677 (1952).

8. Beringer, R. and Heald, M.A., Phys. Rev. 95, 1474 (1954).

9. Heald, M.A. and Beringer, R., Phys. Rev. 96, 645 (1954).

10. Krongelb, S. and Strandberg, M.W.P., J. Chem. Phys. 11, 1196 (1959).

11. Ultee, C.J., J. Phys. Chem. 64, 1873 (1960).

12. Kaufman, F., "Reactions of Oxygen Atoms", Ch. 1 of 'Progress in Reaction Kinetics' Vol. 1. Ed. by Porter, G. (Pergamon Press Ltd., 1961).

13. Thrush, B.A., "Reactions of Hydrogen Atoms in the Gaseous Phase", Ch. II of 'Progress in Reaction Kinetics', Vol. III. Ed. by Porter, G. (Pergamon Press Ltd., 1965).

14. Barth, C.A., Hildebrandt, A.F. and Papatoff, M., Disc. Farad. Soc. 33, 162 (1962).

15. Westenberg, A.A. and de Haas, N., J. Chem. Phys. 40, 3087 (1964).

16. Parker, A.J., Ph.D. Thesis, University of Birmingham (1965).

CHAPTER VII

CONCLUSIONS AND PROPOSALS FOR FURTHER DEVELOPMENTS

7.1 Performance of the System

A Computer of Average Transients has been successfully employed in conjunction with an E.S.R. spectrometer to display the spectra of transient paramagnetic species. The performance of the system was tested with atomic oxygen possessing a formation lifetime of 40msecs; there is every indication that the apparatus will record the full spectrum of a sample with a process lifetime as low as 5msecs. The equipment was also satisfactorily operated with sample lifetimes as long as ~500msecs.

The apparatus proved trouble free and easy to use; any difficulty experienced in obtaining the transient spectra of atomic oxygen arose from peripheral equipment such as the r.f. generator. The rapid recording system also possesses the advantage that the whole spectrum is available for readout at the end of an experiment rather than the readout occurring as the experiment progresses.

7.2 Limitations of the System

Before discussing any limitations of the system, it is necessary to consider the performance expected of an ideal system. It will be assumed that the ideal system utilises a repetitive stimulus to generate paramagnetic species which decay reversibly and will be referred to as "reversible species". Samples which do not behave as reversible species will be discussed later.

An ideal system would utilise all the information presented with the application and removal of each stimulus. The results can be regarded in terms of a 3 dimensional array assumed to be a right angled array for simplicity. The vertical z axis represents the amplitude (A) of a signal and extends in both positive and negative directions; the x and y directions, in the horizontal plane, represent the magnetic field (H) and time (T_D) axes respectively. As an example we will assume that the decay of a transient paramagnetic specimen is being studied. The magnetic field is repetitively swept through the region in which the spectrum occurs; this may be regarded as a movement of the amplitude time (AT_D) plane of interest in a normal direction (i.e. in a direction parallel to the H axis). Similarly at the cessation of each stimulus, the AH plane of interest can be considered as moving in a normal direction (parallel to the T_D axis). The instantaneous region of interest is the line which occurs where the two planes intersect and is parallel to the A axis.

Thus in order to record and display a complete set of transient spectra a three dimensional memory is required and ideally all the available information should be utilised, thus overcoming the "inefficiency factor".

The system described in this thesis falls short of the ideal in that the CAT only possesses a two dimensional memory. For a particular experimental run data is only selected from a particular AH plane situated at a particular position along the T_D axis. The AH plane has a finite thickness, T_s, but this is made extremely small (c.f. T_D as discussed in Chapter IV). A rough picture of the complete decay is built

up by carrying out several experiments, each with the AH plane chosen at a different value of T_D. This method gives a well resolved spectrum but information on the decay process itself relies on interpolation between discrete values of T_D. Information could be accumulated continuously in the A T_S plane at discrete values of H corresponding to the peak observation systems described in Chapter IV, but this would lead to poor field resolution.

To summarise:

The peak observation system is continuous in the A T_D plane at discrete values of H.

The complete spectrum system is continuous in the AH plane at discrete values of T_D.

The ideal system is continuous throughout all relevant AHT_D space and makes full use of the available information.

Of the three processes the C.S.S. system is the most wasteful in time; the use of sampling implies the rejection of a large amount of information. However, the results are presented, in a more useful way than the P.O.S. system, as well resolved spectra.

Sampling techniques may have to be used with P.O.S. systems because of bandwidth considerations discussed in Chapter IV.

7.3 Suggestions for a Practical Ideal System

With the advent of fast computing techniques, the use of an on-line computer programmed to act as a 3-dimensional digital memory is suggested as a possible solution. The bandwidth problems, associated with

short lifetimes, could be overcome by the use of fast record slow playback (FRSP) techniques utilised in the interfacial equipment between the E.S.R. spectrometer and the on-line computer. The FRSP techniques would ensure that data would be presented to the computer at a sufficiently slow rate for accurate processing. The C.S.S. system described by the author could be utilised as a visual progress check. The use of modern high stability techniques in the design of the E.S.R. spectrometer, as described in Chapter II, would mean that data could be collected over much longer periods than possible with the spectrometer used by the author. A large signal-to-noise enhancement would be possible bringing the recording of very weak transient signals within the bounds of possibility.

7.4 Time Saving Methods with Present Systems

The large inefficiency of the present system with regard to time means that any method of reducing the time required to record a spectrum will prove extremely useful. There are two main ways in which time saving may be effected:-

(1) Tailoring of the stimulus on time, T_1, and the stimulus off time, T_2, to suit the formation and decay times of the sample under investigation. For example, the initial investigations of atomic oxygen used values of $T_1 = T_2 \sim 3\tau_d = 1\text{sec}$ ($\tau_d > \tau_f$). Examination of Fig. 6.3 shows that atomic oxygen reaches its maximum concentration after 200msecs and thus 800msecs of stimulus on time were unnecessary. In later experiments the condition $T_1 = T_2$ was no longer obeyed; an unsymmetrical astable multivibrator, feeding the electronic key of the r.f. generator, was used to gate the

discharge on and off. In the case of the observations on atomic oxygen this should and did lead to a reduction in data acquisition time by a factor of $\frac{1,200}{2,000}$ = 0.6. Thus spectra which originally took 18 minutes to record were recorded, with the later arrangement, in ~11 minutes.

(2) The use of a bidirectional field sweep. The field sweep used in the experiments described above was unidirectional with a fairly rapid flyback; even so, under these conditions, the flyback time is wasted as no data is acquired in its duration. The NS513 is equipped with a bidirectional sweep mode and synchronisation of this with a bidirectional field sweep would lead to a reduction in the required experimental time.

7.5 Alternative "Channel Skipping" Version of a C.S.S. System using a CAT

Fig. 7.1 shows a suggested alternative for using a CAT in a C.S.S. system. The use of the signal sample and hold system, feeding the Y input of the CAT, is retained but the use of the NOT INHIBIT pulse is dispensed with. The NS513 CAT can be used in an XY mode when the magnitude of a signal, between 0 and 512mV, determines which of the 512 channels is open to accept information. A 0 - 512mV ramp is obtained from the field sweep voltage and is fed to the second sample and hold circuit as shown in Fig. 7.1. When the signal gate is opened by a sampling pulse the sample and hold circuit, feeding the H input, samples and holds the value of the ramp voltage at its value at the time at which the sampling pulse occurred; in this way the channel relevant to the field at which the sampling pulse occurred is held open and the stretched signal pulse is fed continuously into the open channel until the next sampling pulse occurs. When the

next sampling pulse occurs, the H input sample and hold circuit immediately readjusts to the new value of the sampled ramp voltage, thus causing a 'skip' to a new channel corresponding to the field at which the new sample was taken. The behaviour of each channel is a closer approximation to an Ideal Boxcar integrator and a much larger weighting factor can be used. However, the same number of samples/channel is required for a given enhancement and thus a spectrum will take the same time to accumulate with either system. The possible advantage of this system, over the method used, is that the inhibit circuitry is not required. The disadvantages are that a complex form of field stabilisation would be necessary and the hold circuits would require hold times ~100 seconds.

7.6 General Limitations on Types of Sample

With repetitive systems of the type described it is necessary that the production and decay reactions of the transient species be reversible; i.e.

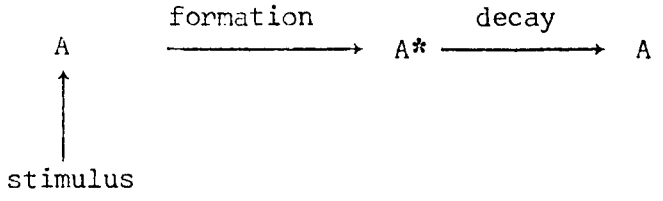

where A* is the transient paramagnetic species.

For the study of irreversible reactions the use of variable flow techniques has been shown to be inaccurate, but a reversible reaction, in the liquid and/or gaseous phase, can be approximated by the use of large reservoirs supplying the necessary reagents; the reaction products

being withdrawn from the cavity before the reaction is repeated. This system presupposes the availability of large quantities of reagents and would be very complex in execution. The limitations mentioned are common to any transient recording system utilising many observations to build up a complete picture of a time dependent process; i.e. this is not a disadvantage confined to the author's system.